Exploring Factors Affecting Reactor Performance and Microbial Community of Purple Non-Sulfur Bacteria

Ananya Mohanty

Department of Civil Engineering
McGill University, Montreal

December 2023

A thesis submitted to McGill University in partial fulfillment of the requirements of the degree of

Masters of Civil Engineering

Abstract

The excessive presence of phosphorus in municipal wastewater streams is a critical concern, contributing to environmental issues, including eutrophication. The potential solution lies in harnessing the capabilities of Purple Non-Sulfur Bacteria (PNSB) to remove and recover phosphorus from municipal wastewater, transforming it into a valuable resource for agriculture as P-fertilizer. PNSB, with their unique ability to accumulate phosphorus as polyphosphate (polyP) within their cells, offer a promising avenue for sustainable resource recovery.

This thesis is part of a multifaceted research endeavor aimed at advancing our understanding of PNSB-driven bioresource recovery in municipal wastewater treatment. The research is structured around three interrelated objectives: (1) investigating the impact of decoupling Solid Retention Time (SRT) and Hydraulic Retention Time (HRT) on phosphorus uptake by PNSB, (2) exploring the consequences of varying phosphorus concentrations in the influent on PNSB-mediated phosphorus uptake (3) employing 16s rRNA gene analysis to unravel the intricate microbial community dynamics within the

reactors, shedding light on the population diversity and shifts in response to changing operational conditions.

The methodology involved the operation of steady-state batch reactors over a period of 230 days, with PNSBs cultivated in synthetic wastewater. Reactor operation was monitored by measuring TSS, VSS, COD, and inorganic orthophosphate (Pi), or (PO_4^{3-}-P) periodically. The microbial communities were assessed using 16s DNA sequencing, and visualized using the fluorescent stain DAPI and the chromatic stain LP2.

The results revealed that decoupling SRT-HRT parameters led to the formation of distinct PPB communities with genera from *Rhodobacteraceae* and *Xanthobacteraceae* forming the PNSB guild. The emergence of fermenters in the system underlines the challenges of reactor stability in wastewater treatment, particularly in the presence of high organic loads.

This research offers valuable insights into the potential of PNSBs for phosphorus recovery and highlights the need for robust systems to maximize resource valorization while addressing challenges associated with reactor stability and phosphorus measurement accuracy. The study's findings contribute to the broader goal of sustainable wastewater treatment and resource management, paving the way for future advancements in this critical field.

Résumé

La présence excessive de phosphore dans les flux d'eaux usées est une préoccupation majeure qui contribue à des problèmes environnementaux tels que l'eutrophisation. La solution potentielle consiste à exploiter les capacités des bactéries pourpres non sulfureuses (PNSB) pour éliminer et récupérer le phosphore et le transformer en une ressource précieuse pour l'agriculture sous forme d'engrais. Les PNSB, avec leur capacité unique à accumuler le phosphore sous forme de polyphosphate (polyP) à l'intérieur de leurs cellules, offrent une voie prometteuse pour la récupération durable des ressources.

Cette thèse porte sur un projet de recherche à multiples facettes visant à améliorer notre compréhension de la récupération des bioressources par les PNSB dans le cadre du traitement des eaux usées. La recherche s'articule autour de trois objectifs interdépendants : (1) étudier l'impact du découplage du temps de rétention solide (SRT) et du temps de rétention hydraulique (HRT) sur l'absorption du phosphore par le PNSB, (2) explorer les conséquences de la variation des concentrations de phosphore dans l'influent sur l'absorption du phosphore par le PNSB (3) utiliser l'analyse des gènes de l'ARNr 16s pour

démêler la dynamique complexe de la communauté microbienne au sein des réacteurs, en mettant en lumière la diversité et les changements en réponse à des conditions opérationnelles changeantes.

La méthodologie a consisté à faire fonctionner des réacteurs discontinus en régime permanent sur une période de 230 jours, avec des PNSB cultivés dans des eaux usées synthétiques. Le fonctionnement du réacteur a été contrôlé en mesurant périodiquement les MES, les MESV, la DCO et le PO_4^{3-}-P. La communauté microbienne a été évaluée par séquençage de l'ADN 16s.

Les résultats ont révélé que le découplage des paramètres SRT-HRT a conduit à la formation de communautés PPB distinctes avec des genres de *Rhodobacteraceae* et *Xanthobacteraceae* formant la guilde PNSB. L'émergence de fermenteurs dans le système souligne les défis de la stabilité des réacteurs dans le traitement des eaux usées, en particulier en présence de charges organiques élevées.

Cette recherche offre des indications précieuses sur le potentiel des PNSB pour la récupération du phosphore et souligne la nécessité de systèmes robustes pour maximiser la valorisation des ressources tout en relevant les défis associés à la stabilité du réacteur et à la précision de la mesure du phosphore. Les résultats de l'étude contribuent à l'objectif plus large du traitement durable des eaux usées et de la gestion des ressources, ouvrant la voie à de futures avancées dans ce domaine essentiel.

Acknowledgements

The culmination of a three-year-long research project in a thesis is not possible by a lone person. Although I worked day and night to bring this piece of writing to fruition, it has been made possible by the consistent guidance, support, and resources of several people to whom I am eternally grateful.

I dedicate this thesis to my mother, father, Anshu, and Adithya G, who have been the pillars of my life in all the joys and sorrows and showered their blessings and unconditional love.

I convey my deepest gratitude to Dr. Dominic Frigon, my supervisor, for giving me this opportunity, and for his patience, and kindness. Thank you, Dr. Sidney Omelon, my co-supervisor, who provided troubleshooting support, and encouragement. I express my highest appreciation to all the lab members of Prof. Frigon's, Loeb's, Liu's, Ghoshal's, Omelon's, Chemistry, and ABIF labs, for their expertise, concern, and assistance without inhibition. Special thanks to Natalia, Pinar, Anindya, Catherine, Medinah, Estefania, Aditya & Tian.

Arriving and completing a project in a new country became a reality with the support of new friends. I want to thank Sneha, Subodh, Fathima and friends, Austine, Medinah, my amazing roommates, Caro & Fer, and landlords. I am in Montréal because of my old friend Nikhil.

Last, but not the least, all the people who helped me through Ethiopia during COVID-19.

Contents

List of Figures

List of Tables

List of Abbreviations

ADF	Aerobic Dynamic Feeding.
AF	Anaerobic Filter.
ATP	Adenosine Triphosphate.
BOD	Biological Oxygen Demand.
CBB	Calvin-Benson cycle.
COD	Chemical Oxygen Demand.
DAPI	4'6-Diamidino-2-Phenylindol.
EBPR	Enhanced Biological Phosphorus Removal.
EBR	expanded bed.
EMP	Embden-Meyerhof- Parnas pathway.

GAC	Glyoxylic Acid cycle.
HRT	Hydraulic Retention Time.
LP2	LipidGreen2.
MBRs	Membrane bioreactors.
MMCs	Mixed Microbial Communities.
NADH	nicotinamide adenine dinucleotide (NAD) + hydrogen (H).
NADPH	Nicotinamide Adenine Dinucleotide Phosphate Hydrogen.
OD	optical density.
OLR	Organic Loading Rate.
PAOs	Phosphate Accumulating Organisms.
PB	packed bed.
PBR	Photobioreactor.
PBS	phosphate buffer saline.
PEP	phosphoenolpyruvate.
PHAs	polyhydroxyalkanoates.

PHBs	Polyhydroxybutyrate.
PMCs	Phototrophic Mixed Consortia.
PNSBs	Purple Non-Sulfur Bacteria.
polyphosphates	polyP.
PPB	Purple Phototrophic Bacteria.
PPDK	pyruvate-phosphate dikinase.
PPK	Polyphosphate Kinase.
PPS	PEP Synthetase.
PSI	photosystem I.
RAS	Return Activated Sludge.
sCOD	soluble Chemical Oxygen Demand.
SRT	Solid Retention Time.
TCA	Tricarboxylic Acid Cycle.
VFAs	Volatile Fatty Acids.

Chapter 1

Introduction

1.1 Municipal Wastewater as a Resource

Municipal wastewater consists of organic, inorganic, and biological pollutants that can cause harm to humans and the environment if the water is directly discharged into natural water bodies. Among all the nutrients present in wastewater, phosphorous is important because it contributes to the excessive growth of cyanobacteria and other photosynthetic aquatic organisms leading to the eutrophication of lakes (Jenkins and Wanner, 2014). Therefore, processes have been developed that employ open microbial communities to achieve phosphorus removal and recovery, such as the Enhanced Biological Phosphorus Removal (EBPR) process. Once recovered from the wastewater, phosphorus has traditionally been applied on agricultural and reforested land as biofertilizer (Burn et al., 2014; Schaum, 2018).

Carbon, nitrogen, phosphorus, and other elements present in wastewater are essential for the

metabolic functions of the microorganisms in wastewater (Madigan et al., 2018). The microbiota of domestic wastewater that originates in part from human waste and greywater, and that grows in the sewer system itself, has the capacity to accumulate these nutrients within their cell bodies.

The nutrient-accumulating property of microorganisms is utilized in an activated sludge process where the process of cell formation transfers part of the soluble nutrients from the wastewater to the solids that can settle in the secondary clarifier. Such filamentous (e.g., Microthrix spp.) and floc-forming (e.g., Zoogloea) organisms growing in appropriate balance provide the matrix in which other bacteria thrive. They form a structure that is called a floc, which is readily separated from the treated water by gravity (Grady et al., 2011). However, cell synthesis alone is insufficient to remove the phosphorus for adequate protection of the natural environment. A special activated sludge configuration forcing the biomass to cycle between (1) anaerobic conditions in the presence of volatile fatty acids (VFA) from the influent and (2) aerobic conditions with minimal residual (VFAs) is the basis for the Enhanced Biological Phosphorus Removal (EBPR) process (Jenkins and Wanner, 2014).

While an activated sludge process configuration like the EBPR is superior to the physicochemical processes for P-removal such as P-precipitation with dissolved iron and ion exchange, due to comparatively low sludge production, the presence of the aerobic step makes it an energy-intensive and complex process (Bunce et al., 2018). Approximately 38-52% of the total energy required by a wastewater treatment plant is accounted for electrical energy (Rodziewicz et al., 2022), and aeration consumes 30% to 60% of total electrical energy supplied (Izadi et al., 2022). On the contrary, anaerobic processes can lower the energy requirement by eliminating the

aerated aerobic step from wastewater treatment processes.

To create a sustainable, resource-cycling process, the potential of recovering nutrients in their original form or as useful products should be considered in addition to energy reduction. Biosolids generated after anaerobic processing of municipal wastewater organics and sludges are expensive to dispose of, as they must be incinerated or landfilled when not used as fertilizers. Further, the safety of applying these biosolids directly on land is questionable (Marchuk et al., 2023). Wastewater contains valuable minerals and nutrients that can be 'mined' before it is disposed of as sludge. Aerobic treatment of wastewater has the potential to mineralize the organic components of wastewater, for example, up to 60% of nitrogen is converted to inorganic nitrogen (Magdoff and Chromec, 1977). Recovering the mineralized nutrients post-aerobic treatment is difficult as the nitrogen and phosphorus are released into the supernatant from the sludge and require additional processes for their recovery, including physicochemical or biological processes (Wang et al., 2014).

Anaerobic bacteria coupled with methanogenic archaea can treat the wastewater at a low cost while producing less residual sludge for disposal, and providing useful methane gas. These methanogenic processes utilize a low amount of energy and have a high organic matter removal efficiency (Zieliński et al., 2023). However, their very low biomass yield makes them extremely resourceful for the removal and recovery of N and P nutrients (Huang and Tang, 2007). Furthermore, their low growth rate requires long solids retention times (SRT) to achieve regulatory discharge limits (Forrez et al., 2011). This is an especially bad challenge in cold seasons like the Canadian winter, where the cold temperature further multiple the necessary

length of SRTs (Bhate, 2022). Therefore, it is necessary to find novel biological processes to optimize resource recovery in all climates.

1.2 Purple Non-Sulfur Bacteria

Purple non-sulfur bacteria (PNSBs) are a subset of photosynthetic bacteria that absorb light in the infrared region of the light spectrum. The low energy that PNSBs harvest defined their preferred electron donor and carbon source to be photoorganoheterotrophic in anaerobic conditions. Thus, they use organic acids and aromatic compounds as sources of relatively high energy electrons and of already fixed carbon (Adessi and De Philippis, 2013; Capson-Tojo et al., 2020; Fradinho et al., 2021; Imhoff, 1995). Nonetheless, they can also grow photolithoautotrophically in the presence of hydrogen or thiosulfate. The metabolic versatility and commercial potential of PNSBs in anaerobic conditions make them attractive candidates for cost-effective, low-energy, and sustainable wastewater treatment. Their utilization of light energy allows them to maintain relatively fast specific growth rates and to maintain high biomass yields even at low temperatures. From the perspective of organic value-added products, they are a good source of protein and carotenoids, which make the resulting biomass interesting as animal feed (Capson-Tojo et al., 2020). In the broader group, microalgae and PPBs have shown promise as low-energy nutrient accumulators, yielding high biomass. Their photosynthetic, anaerobic, and high yields make them attractive options for resource recovery (Zarezadeh et al., 2019). Although phosphorus accumulation has been observed in heterotrophic PAOs and other phototrophs like microalgae (Akbari et al., 2021), classical heterotrophic PAOs require aerobic conditions and are

difficult to maintain (Fall et al., 2022). However, PNSBs can utilize several inorganic electron donors when they employ photoautotrophic metabolism, unlike microalgae (Capson-Tojo et al., 2020; Hunter et al., 2008). Finally, with respect to phosphorus in wastewater (the nutrient of focus for this study), PNSBs can take it up and store it as polyphosphate (polyP) in addition to biomass synthesis. This forms the basis of employing PNSBs for wastewater valorization where the stored phosphorus in the form of polyP can be recovered and up-cycled. The importance of P-sequestration in the form of polyP has been extensively studied in EBPR systems (Fradinho et al., 2021; Rittmann and McCarty, 2012).

Notwithstanding experiments to understand the behaviour of pure cultures of PNSBs for phosphorus removal has been carried out in the past (Imhoff, 1995; Lai et al., 2017; Ohtake et al., 1985; Stante et al., 1997), it is only recently that PNSB behavior in large-scale open community systems is being explored. PNSBs can show a marked difference in their metabolism for nutrient accumulation when in pure culture versus in a consortium (Constanina et al., 2020). Thus, there is a need to understand the conditions that influence polyP accumulation in PNSB when present with other microbiota in actual wastewater treatment reactors.

1.3 Phosphate Removal and PHAs Accumulation Integrated System

As mentioned in the previous section, anaerobic treatment of wastewater sludge is superior to aerobic treatment due to low electrical energy input to the treatment plant, and possible

application in cold climates. In addition to these benefits and the high level of proteins and carotenoids in the biomass, the accumulation of storage compounds could in themselves additional value-added products. Beyond polyP accumulation, a number of PNSB species are known to accumulate polyhydroxyalkanoates (PHAs), which are bioplastic precursors. This is of special interest as both phosphate and PHAs are commercially useful products, and have the potential to be harvested sustainably from wastewater.

Depending on the biochemical transformation process needed to obtain the desired end product, several kinds of wastewater treatment configurations have been developed (Grady et al., 2011). One such configuration is the EBPR system, which utilizes heterotrophs in a cyclical anaerobic aerobic environment to remove phosphorus from the influent wastewater with the intermediate accumulation of PHAs. This process clearly establishes the metabolic relationship between polyP and PHAs accumulation in certain species. In aerobic-activated sludge systems, the enrichment of the microbial populations capable of PHAs accumulation is also favored by the feast and famine cycle that the biomass experiences in plug-flow reactors (Constanina et al., 2020). In these systems, polyP and PHAs accumulation provide energy storage for the cell allowing it to either take up substrate in the absence of an energy source (polyP in EBPR) or survive famine stages (PHAs in activated sludge). For PNSBs, at least for some species, the production of ATP over the carbon incorporation capacity of the cell leads to a significant increase in polyP accumulation (Fradinho et al., 2021). Inspired by the configurations in other wastewater treatment systems, it may be possible to engineer a selective environment that pushes for even greater accumulation of these storage compounds by PNSBs.

The photosynthetic enrichment method uses anaerobic operation and various illumination configurations to select polyP and PHAs accumulating organisms (Capson-Tojo et al., 2020; Kourmentza et al., 2017). Photosynthetic bacterial consortia live longer than other microorganisms in a permanently illuminated anaerobic feast phase (Kourmentza et al., 2017). Additionally, several of the existing studies focus on PHAs production using pure PPB cultures (Capson-Tojo et al., 2020; Montiel-Corona and Buitrón, 2021) or heterotrophic aerobic mixed cultures (Almeida et al., 2021; Higuchi-Takeuchi et al., 2016; Kourmentza and Kornaros, 2016). Although other factors are currently being explored that are necessary to understand the metabolism of PNSBs to enable their enrichment in open communities such as wastewater (Fradinho et al., 2021), this study aims to contribute to a better understanding of the wastewater treatment conditions that favor the enrichment of PNSBs and enable high uptake of carbon and phosphorus. In earlier experiments conducted in the Frigon Lab, polyphosphate was the nutrient of interest. Experiments were conducted to determine if it could be accumulated by PPBs in unoptimized anaerobic conditions. This led to an exploration of two questions on the polyP accumulating properties of PPBs in different environments: 1. How can different illumination parameters leading to light limitations affect PPB enrichment and poly-P uptake?; and 2. How does a short solid retention time affect the enrichment of PPBs and subsequently Poly-P accumulation? (Jaber, 2020) While these studies were undertaken, as an extension to the second question mentioned above, other operational parameters were explored as a part of this thesis.

The nutrient uptake by PNSBs can be optimized by adjusting the reactor conditions for the enrichment of bacteria. As mentioned above, a continuous feast with permanent illumination in an

anaerobic environment was found to promote polyP (Jentzsch et al., 2023) and PHAs (Constanina et al., 2020) accumulation. Additionally, in a photobioreactor, the light intensity (Cerruti et al., 2022; Katsuda et al., 2004), light path (González-Camejo et al., 2020), solid retention time (SRT), and hydraulic retention time (HRT) (Grady et al., 2011), organic loading rate (OLR) (Blansaer et al., 2022), ratios of carbon, nitrogen and phosphorus (Capson-Tojo et al., 2020; Hülsen et al., 2014) are important criteria in designing treatment systems that can concurrently become resource sinks.

Among the above-mentioned conditions, the SRT and HRT are critical factors in determining the microbial community within the reactor. The organic sources present in the waste lead to competition between microorganisms. A change in the retention time of the solids or liquids in wastewater alters its organic composition which can encourage the proliferation of bacteria with different specific growth rates (μ_{net}) according to Equation (1.1) (Reis et al., 2011):

$$\mu_{\text{net}} = \frac{1}{SRT} \tag{1.1}$$

Thus, SRT can drastically alter the microbial community composition in the reactor (Grady et al., 2011; Rittmann and McCarty, 2012). Optimizing the SRT and HRT to improve the population density of open bacterial communities in a wastewater treatment plant has been a well-researched topic (Chen et al., 2021; Solmaz and Isik, 2019; Xu et al., 2015; Zhang et al., 2021). As an extension to this, it has been observed that decoupling the SRT and HRT has some advantages. A higher SRT with lower HRT encourages the proliferation of slow-growing phototrophs, and high biomass accumulation by virtue of an increasing OLR (Zhang et al., 2021).

The separation of the SRT and HRT is called decoupling and has been used for enriching microalgae. However, the research to establish the effect of different SRT/HRT configurations on PNSB enrichment and nutrient removal is in its nascent stage. On extrapolating these parameters to the PNSBs studied here, some probing questions are raised: Does decoupling of SRT provide an advantage by boosting PNSB enrichment in reactors? What kind of microbial communities can be selected for when PPB-growth-inducing conditions are applied along with SRT/HRT decoupling? These questions remain to be explored in photobioreactors for PNSBs.

Similarly, among the several nutrients affecting the microbial community composition, the concentration of phosphorus in the influent can influence the population in the reactor. Further, inorganic orthophosphate (o-Pi) concentration in municipal wastewater can be a limiting component in PNSB growth. Very few studies have been conducted to explore the effect of o-Pi-deficiency on purple bacteria (Benning et al., 1993; Shaikh et al., 2023). Liang et al. (2010) studied PAOs in o-Pi-limited conditions with up to 23 mg PO_4^{3-}-P/L in the influent, and Dong et al. (2021) studied efficiency of o-Pi-removal for isolated *Rhodobacter spheroids* at 50 mg PO_4^{3-}-P/L. Further, previous experiments have shown that complete removal of o-Pi from the influent is not achieved in the low-o-Pi conditions of 23-25 mg PO_4^{3-}-P/L (unpublished data). As far as the knowledge and resource availability of the author goes, no study was found to understand if low o-Pi concentration can affect polyP accumulation in PNSBs. Thus, a new knowledge gap has been identified that this thesis aims to address: Can reducing the o-Pi concentration in the influent to less than 23 PO_4^{3-}-P/L have an effect on P-accumulation within the PNSBs? How does the microbial community change under extreme o-Pi limitation?

1.4 Objectives

PNSBs have the potential to be applied for both phosphorus and PHAs recovery. While species-level knowledge of PNSB metabolism exists, their behavior in an open community in wastewater is yet to be fully understood. Certain gaps in the literature were identified with respect to PNSB behavior. First, it is the effect of the retention time on PNSB enrichment and nutrient accumulation. Second, is exploring the tendencies of PNSB when o-Pi limitation is introduced. Additionally, the microbial community changes that may happen within the wastewater treatment community due to the above changes are also of interest. The possibility of enrichment of PNSBs can be identified by undertaking a 16S rRNA gene amplicon sequencing analysis to determine microbial population diversity.

To explore the possibilities of PNSB behavior and population dynamics by changing reactor conditions, the following objectives were defined:

1. To determine the effect of the specific growth rate of PNSB on phosphorus uptake and accumulation when SRT and HRT are decoupled;

2. To determine if P-limitation in the influent impacts P-uptake by purple bacteria.

1.5 Organization of Thesis

The thesis literature review and research content has been organized into four additional chapters described below:

Chapter 2 describes the existing literature on phosphorus, PHAs and studies carried out for

polyP accumulation in purple bacteria as well as microalgal mixed communities. It further discusses the knowledge gaps in the literature that require addressing.

Chapter 3 details the reactor setup and operation for the experiment which were used to test the impact of decoupling the SRT and HRT and varying phosphorus values. The same setup was divided into three phases where the reactor was cleaned to remove accumulated biofilm and yeast extract to attain the required P-limitation. This chapter also includes analytical methods employed for result assessment.

Chapter 4 describes and discusses the results of enriching the PNSBs. It describes the impact of decoupling SRT-HRT and the o-Pi concentrations (including the presence of P-rich yeast extract) in feed on the P removal by the bacterial community uptake. This chapter covers the results of operational parameters to establish a steady-state run of the reactor, subsequent changes within the microbial communities, and their possible causes.

Chapter 5 presents the final conclusions from this thesis by answering the hypotheses and objectives, and suggests possible future work that must be done to refine the existing work.

References

Adessi, A., De Philippis, R., 2013. Encyclopedia of Biological Chemistry (Second Edition). Academic Press, Waltham. book section Purple Bacteria: Electron Acceptors and Donors. pp. 693–699.

Akbari, A., Wang, Z., He, P., Wang, D., Lee, J., Han, I., Li, G., Gu, A.Z., 2021. Unrevealed roles of polyphosphate-accumulating microorganisms. Microb. Biotechnol. 14, 82–87.

Almeida, J.R., Serrano, E., Fernandez, M., Fradinho, J.C., Oehmen, A., Reis, M.A.M., 2021. Polyhydroxyalkanoates production from fermented domestic wastewater using phototrophic mixed cultures. Water Res. 197, 117101.

Benning, C., Beatty, J.T., Prince, R.C., Somerville, C.R., 1993. The sulfolipid sulfoquinovosyldiacylglycerol is not required for photosynthetic electron transport in *Rhodobacter sphaeroides* but enhances growth under phosphate limitation. Proc. Natl. Acad. Sci. 90, 1561–1565.

Bhate, V.M., 2022. Impact of wastewater temperature influent flow as the indicators of climate change on wastewater treatment systems. Thesis.

Blansaer, N., Alloul, A., Verstraete, W., Vlaeminck, S.E., Smets, B.F., 2022. Aggregation of purple bacteria in an upflow photobioreactor to facilitate solid/liquid separation: Impact of organic loading rate, hydraulic retention time and water composition. Bioresour. Technol. 348, 126806.

Bunce, J.T., Ndam, E., Ofiteru, I.D., Moore, A., Graham, D.W., 2018. A review of phosphorus removal technologies and their applicability to small-scale domestic wastewater treatment systems. Front. Environ. Sci. 6.

Burn, S., Muster, T., Kaksonen, A., 2014. Resource Recovery from Wastewater : A Research Agenda : WERF Research Report Series. IWA Publishing, London, UK.

Capson-Tojo, G., Batstone, D.J., Grassino, M., Vlaeminck, S.E., Puyol, D., Verstraete, W., Kleerebezem, R., Oehmen, A., Ghimire, A., Pikaar, I., Lema, J.M., Hülsen, T., 2020. Purple phototrophic bacteria for resource recovery: Challenges and opportunities. Biotechnol. Adv. 43.

Cerruti, M., Kim, J.H., Pabst, M., Van Loosdrecht, M.C.M., Weissbrodt, D.G., 2022. Light intensity defines growth and photopigment content of a mixed culture of purple phototrophic bacteria. Front. Microbiol. 13, 1014695.

Chen, G., Wu, W., Xu, J., Wang, Z., 2021. An anaerobic dynamic membrane bioreactor for enhancing sludge digestion: Impact of solids retention time on digestion efficacy. Bioresour. Technol. 329, 124864.

Constanina, K., Plácido, J., Venetsaneas, N., Burniol-Figols, A., Varrone, C., Gavala, H.N., Reis, M.A.M., 2020. Recent advances and challenges towards sustainable polyhydroxyalkanoate (pha) production, in: Koller, M. (Ed.), The Handbook of Polyhydroxyalkanoates. CRC Press, Boca, Raton, pp. 8–50.

Dong, D., Sun, H., Qi, Z., Liu, X., 2021. Improving microbial bioremediation efficiency of intensive aquacultural wastewater based on bacterial pollutant metabolism kinetics analysis. Chemosphere 265, 129151.

Fall, C., Barrón-Hernández, L.M., Gonzaga-Galeana, V.E., Olguín, M.T., 2022. Ordinary heterotrophic organisms with aerobic storage capacity provide stable aerobic granular sludge for c and n removal. J. Environ. Manage. 308, 114662.

Forrez, I., Boon, N., Verstraete, W., Carballa, M., 2011. 6.38 - Biodegradation of Micropollutants and Prospects for Water and Wastewater Biotreatment. Academic Press, Burlington. pp. 485–494. URL: https://www.sciencedirect.com/science/article/pii/B9780080885049005353, doi:https://doi.org/10.1016/B978-0-08-088504-9.00535-3.

Fradinho, J., Allegue, L.D., Ventura, M., Melero, J.A., Reis, M.A.M., Puyol, D., 2021. Up-scale challenges on biopolymer production from waste streams by purple phototrophic bacteria mixed cultures: A critical review. Bioresour. Technol. 327, 124820.

González-Camejo, J., Aparicio, S., Jiménez-Benítez, A., Pachés, M., Ruano, M.V., Borrás, L., Barat, R., Seco, A., 2020. Improving membrane photobioreactor performance by reducing light path: operating conditions and key performance indicators. Water Res. 172, 115518.

Grady, C., Daigger, G., Love, N., Filipe, C., 2011. Biological Wastewater Treatment. CRC Press.

Higuchi-Takeuchi, M., Morisaki, K., Toyooka, K., Numata, K., 2016. Synthesis of high-molecular-weight polyhydroxyalkanoates by marine photosynthetic purple bacteria. PLoS One 11, e0160981.

Huang, W.C., Tang, I.C., 2007. Chapter 8 - Bacterial and Yeast Cultures – Process Characteristics, Products, and Applications. Elsevier, Amsterdam. pp. 185–223. URL: https://www.sciencedirect.com/science/article/pii/B9780444521149500098, doi:https://doi.org/10.1016/B978-044452114-9/50009-8.

Hunter, C.N., Daldal, F., Thurnauer, M.C., Beatty, J.T., 2008. The Purple Phototrophic Bacteria. Springer Dordrecht.

Hülsen, T., Batstone, D.J., Keller, J., 2014. Phototrophic bacteria for nutrient recovery from domestic wastewater. Water Res. 50, 18–26.

Imhoff, J.F., 1995. Anoxygenic Photosynthetic Bacteria. Springer Netherlands, Dordrecht. book

section Taxonomy and Physiology of Phototrophic Purple Bacteria and Green Sulfur Bacteria. pp. 1–15.

Izadi, P., Izadi, P., Eldyasti, A., 2022. Evaluation of PAO adaptability to oxygen concentration change: Development of stable ebpr under stepwise low-aeration adaptation. Chemosphere 286, 131778.

Jaber, M., 2020. Purple bacteria for wastewater treatment and resource recovery. Https://escholarship.mcgill.ca/concern/theses/sq87bz79q.

Jenkins, D., Wanner, J., 2014. Activated Sludge - 100 Years and Counting : 100 Years and Counting. IWA Publishing, London, UK.

Jentzsch, L., Grossart, H.P., Plewe, S., Schulze-Makuch, D., Goldhammer, T., 2023. Response of cyanobacterial mats to ambient phosphate fluctuations: phosphorus cycling, polyphosphate accumulation and stoichiometric flexibility. ISME Communications 3, 6. URL: https://doi.org/10.1038/s43705-023-00215-x, doi:10.1038/s43705-023-00215-x.

Katsuda, T., Yegani, R., Fujii, N., Igarashi, K., Yoshimura, S., Katoh, S., 2004. Effects of light intensity distribution on growth of rhodobacter capsulatus. Biotechnol. Prog. 20, 998–1000.

Kourmentza, C., Kornaros, M., 2016. Biotransformation of volatile fatty acids to polyhydroxyalkanoates by employing mixed microbial consortia: The effect of ph and carbon source. Bioresour. Technol. 222, 388–398.

Kourmentza, C., Plácido, J., Venetsaneas, N., Burniol-Figols, A., Varrone, C., Gavala, H.N., Reis,

M.A.M., 2017. Recent advances and challenges towards sustainable polyhydroxyalkanoate (pha) production. Bioengineering 4, 55.

Lai, Y.C., Liang, C.M., Hsu, S.C., Hsieh, P.H., Hung, C.H., 2017. Polyphosphate metabolism by purple non-sulfur bacteria and its possible application on photo-microbial fuel cell. J. Biosci. Bioeng. 123, 722–730.

Liang, C.M., Hung, C.H., Hsu, S.C., Yeh, I.C., 2010. Purple nonsulfur bacteria diversity in activated sludge and its potential phosphorus-accumulating ability under different cultivation conditions. Appl. Microbiol. Biotechnol. 86, 709–719.

Madigan, M.T., Bender, K.S., Buckley, D.H., Sattley, W.M., Stahl, D.A., 2018. Brock biology of microorganisms. Fifteenth edition. ed., Pearson, NY, NY.

Magdoff, F.R., Chromec, F.W., 1977. Nitrogen mineralization from sewage sludge. J. Environ. Sci. Health A 12, 191–201.

Marchuk, S., Tait, S., Sinha, P., Harris, P., Antille, D.L., McCabe, B.K., 2023. Biosolids-derived fertilisers: A review of challenges and opportunities. Science of The Total Environment 875, 162555. URL: https://www.sciencedirect.com/science/article/pii/S0048969723011713, doi:https://doi.org/10.1016/j.scitotenv.2023.162555.

Montiel-Corona, V., Buitrón, G., 2021. Polyhydroxyalkanoates from organic waste streams using purple non-sulfur bacteria. Bioresour. Technol. 323.

Ohtake, H., Takahashi, K., Tsuzuki, Y., Toda, K., 1985. Uptake and release of phosphate by a pure culture of acinetobacter calcoaceticus. Water Research 19, 1587–1594.

Reis, M., Albuquerque, M., Villano, M., Majone, M., 2011. Comprehensive Biotechnology (Second Edition). Academic Press, Burlington. book section 6.51 - Mixed Culture Processes for Polyhydroxyalkanoate Production from Agro-Industrial Surplus/Wastes as Feedstocks. pp. 669–683.

Rittmann, B., McCarty, P., 2012. Environmental Biotechnology: Principles and Applications. Tata McGraw Hill Education Private Limited.

Rodziewicz, J., Mielcarek, A., Bryszewski, K., Janczukowicz, W., Kłobukowska, K., 2022. Energy consumption for nutrient removal from high-nitrate and high-phosphorus wastewater in aerobic and anaerobic bioelectrochemical reactors. Energies 15, 7251.

Schaum, C., 2018. Phosphorus - Polluter and Resource of the Future - Removal and Recovery from Wastewater. IWA Publishing.

Shaikh, S., Rashid, N., Onwusogh, U., McKay, G., Mackey, H.R., 2023. Effect of nutrients deficiency on biofilm formation and single cell protein production with a purple non-sulphur bacteria enriched culture. Biofilm 5, 100098.

Solmaz, A., Isik, M., 2019. Effect of sludge retention time on biomass production and nutrient removal at an algal membrane photobioreactor. Bioenerg. Res. 12, 197–204.

Stante, L., Cellamare, C., Malaspina, F., Bortone, G., Tilche, A., 1997. Biological phosphorus removal by pure culture of lampropedia spp. Water research 31, 1317–1324.

Wang, Y., Zheng, S.J., Pei, L.Y., Ke, L., Peng, D.C., Xia, S.Q., 2014. Nutrient release, recovery and removal from waste sludge of a biological nutrient removal system. Environ. Technol. 35, 2734–42.

Xu, M., Li, P., Tang, T., Hu, Z., 2015. Roles of srt and hrt of an algal membrane bioreactor system with a tanks-in-series configuration for secondary wastewater effluent polishing. Ecol. Eng. 85, 257–264.

Zarezadeh, S., Moheimani, N.R., Jenkins, S.N., Hülsen, T., Riahi, H., Mickan, B.S., 2019. Microalgae and phototrophic purple bacteria for nutrient recovery from agri-industrial effluents: Influences on plant growth, rhizosphere bacteria, and putative carbon- and nitrogen-cycling genes. Front. Plant Sci. 10.

Zhang, M., Leung, K.T., Lin, H., Liao, B., 2021. Effects of solids retention time on the biological performance of a novel microalgal-bacterial membrane photobioreactor for industrial wastewater treatment. J. Environ. Chem. Eng. 9, 105500.

Zieliński, M., Kazimierowicz, J., Debowski, M., 2023. Advantages and limitations of anaerobic wastewater treatment—technological basics, development directions, and technological innovations. Energies 16, 83.

Chapter 2

Background

2.1 Municipal Wastewater Treatment

The basic municipal wastewater treatment process was developed in the late 19^{th} century and includes primary and secondary treatments that remove, respectively, more than 60% and 85% of suspended solids, and 35% and 85% of BOD. An additional step of tertiary treatment is employed to remove excess dissolved nutrients namely phosphorus and nitrogen that may not be satisfactorily removed through the previous steps (Nathanson and Archis, 24 Jul. 2023).

The sludge generated during the secondary treatment has to be stabilized before disposal. One of the ways in which sludge is treated is through anaerobic digestion. The objective is to treat 70% of organic and 30% inorganic matter that is inseparable from the sludge water. During anaerobic digestion, the degradation of sludge happens in several steps including acid fermentation, stabilization, and gasification where nitrogenous and proteinaceous compounds are

converted with gas production (Cheremisinoff, 2002). This common route to recover energy from anaerobic digesters has been possible through the metabolism of microorganisms (Burn et al., 2014). The final products after digestion of sewage sludge contain phosphorus among other organic matter, minerals, and micronutrients, which have a potential application in agriculture, land remediation, and energy production (Rorat et al., 2019).

A boom in agriculture has facilitated the increasing human population of planet Earth. This has led to an excessive consumption of natural resources for the cultivation of plants and animals in farming. One of these resources is the fertilizer consisting of the three elements: nitrogen (N), phosphorus (P), and potassium (K), which have been applied generously on the farmlands to boost agronomy. Runoff from these cultivation lands is nutrient-rich and usually flows into natural water bodies without treatment. This P and N-rich water leads to eutrophication in lakes and lagoons, destabilizing the existing balance in nature. Thus, the need of the hour is to not only remove the nutrients from water to be disposed of but also utilize them for generating value-added commercial products.

2.2 Resource Recovery from Wastewater

Two commercially useful products namely phosphorus and polyhydroxyalkanoates (PHAs) have been researched as potential resources derived from municipal wastewater. They are the primary focus of research in the current study.

2.2.1 Phosphorus

Fertilizer consumption in agriculture in the world stands at 146.4 kg per hectare of arable land as of 2020 (World Bank). Phosphorus for fertilization is industrially obtained from processed phosphate rocks (Green, 2015). Although sewage sludge is a rich source of phosphorus, its direct application after removal from a treatment plant is restricted due to the presence of potential contaminants such as toxic organics, heavy metals, and pathogens (Lamastra et al., 2018). To address this, several P-removal technologies have been developed such as P-extraction from sewage sludge char (Atienza–Martínez et al., 2014; Havukainen et al., 2016), phosphorus as a precipitate in the form of struvite ($NH_4Mg(PO_4).6H_2O$) (Cañas et al., 2023), hydroxyapatite ($Ca_5(PO_4)_3(OH)$) or other calcium phosphates, and through electrodialysis (Cieślik and Konieczka, 2017). Barnard devised Enhanced Biological Phosphorus Removal (EBPR) process (specifically the BardenPho configuration), where it was observed that phosphate-accumulating organisms (PAOs) take up volatile fatty acids (VFAs) in the anaerobic zone (without nitrite, nitrate or oxygen) using their reserve polyP, and accumulated the carbon and energy in the form of PHAs and glycogen (Jenkins and Wanner, 2014). Then, in the anoxic zone (where nitrate or nitrite are the main electron acceptors) or the aerated zones (where oxygen is the electron acceptor), phosphate is taken back up and new biomass is formed driven by the consumption of the PHAs and glycogen pools as electron donors and the strong electron acceptors now available. This became the basis for the EBPR process widely used for P-treatment (Jenkins and Wanner, 2014).

The popular P-sequestration processes are energy intensive, and the production costs are high due to infrastructural and operation costs arising from aeration and resin usage among others (Egle

et al., 2016). EBPR-Sequence Batch Reactor (EBPR-SBR) process is efficient and produces less sludge waste (Khursheed et al., 2023) compared to other methods. Despite its advantages, the energy consumption and global warming potential of EBPR is high at 0.348–0.396 kWh/m^3 and 150 kg CO_2/kg PO_4^{3-} removed (Zhao et al., 2023). Anaerobic bacteria used in the anaerobic step of the above-mentioned process are viable as they reduce operation costs arising due to oxygen usage. Despite that, they have a lower maximum growth rate compared to aerobic bacteria. They are highly sensitive to low winter temperatures in Canada where reactors operate at less than 10-12°C for 4-6 months (Dale et al.). Therefore, there is a need to understand biological processes that will enhance the nutrient uptake into their biomass at lower energy consumption rates.

2.2.2 Polyhydroxyalkanoates (PHAs)

Polyhydroxyalkanoates are biodegradable, biocompatible, thermally, and mechanically malleable bio-polyesters identified as an excellent environment-friendly alternative for commercially available plastics. They are polymers of bioplastics popularly used in the medical and pharmaceutical fields. Depending on the monomers and side chains, the material properties of PHAs vary. The molecular constitution of PHAs is one of the deciding factors for choosing the conditions in which microbes are cultivated. It is interesting to note that the chemical production of PHAs is not as popular as its biological production because the latter results in higher yields (Chen et al., 2011).

Engineering of microbial metabolism through genetic modifications, or manipulation of ecosystems can induce PHA production within bacterial biomass. Genetically modified bacteria take part in a four-step process to synthesize and release PHAs: a) Quorum sensing – as soon as a

high cellular density is detected, O_2 uptake is suppressed; b) PHAs production is initiated; c) Space creation – additional products from metabolic pathways are restricted to create space for more PHAs; d) Self-disruption – the cell is programmed for autolysis (Constanina et al., 2020). Engineered bacteria can give higher PHAs yields, require less energy, have a wide temperature and pH tolerance, and be tailored for polymer function. However, inoculating and ensuring higher survival rates in variable real-time wastewater can be a challenge leading to high operational costs (Constanina et al., 2020). The high cost of production from pure cultures has prevented its profitable business within the large commercial plastic production industry (Fradinho et al., 2021).

Open microbial communities have been employed for the simultaneous treatment of wastewater and the production of PHAs (Ike et al., 2019; Pardelha, 2013). Along with the selection of bacteria in the treatment plant, the substrates that are present in wastewater to feed the bacteria determine the pathway taken to produce one of the three storage molecules - polyP, PHAs, or glycogen, or all depending on the culturing conditions (Constanina et al., 2020). In addition to the storage function of PHAs in bacteria, it has been observed that PHA metabolism is triggered in the presence of various stressors: low temperature, heat shock, osmotic shock, oxidative pressure, UV protection, and heavy metals (Obruca et al., 2020). Morgan-Sagastume et al. (2020) studied the PHAs accumulation in bacteria using feast-famine cycles to achieve up to 98% of COD removal and produce 0.7 gPHA/gVSS. A life cycle assessment of PHAs produced by the open communities by Roibàs-Rozas et al. (2020) utilized wastewater from a fish-canning industry showed an environmental impact of 3.51 kg CO_2 eq/kg biopolymer. Although the

coupling of operational steps has been undertaken to simplify the process of wastewater valorization using microbial consortia (Zeng et al., 2018), the step for open community enrichment using aerobic dynamic feeding (ADF), which uses substantial energy has not been omitted from the process steps. Therefore, phototrophic open communities may provide a cost-saving alternative as they photosynthesize in anaerobic conditions (Fradinho et al., 2013). Among the photosynthetic microbiota, purple bacteria may have the potential to operate with low energy input due to their versatile heterotrophic metabolism used in conjunction with biochemical energy derived from infrared (i.e., low energy) light. In addition to P-removal, they have the capacity to synthesize PHAs (Capson-Tojo et al., 2020; Fradinho et al., 2021).

2.3 Purple Bacteria for Resource Recovery

Purple bacteria are phototrophic bacteria that photosynthesize in often in the absence of oxygen (except in marine environments) using inorganic (e.g., sulfur and iron) or organic (e.g., volatile fatty acids) electron donors, and autotrophic or heterotrophic carbon metabolism. These facultative bacteria are metabolically versatile. The bacteriochlorophyll a and b present in purple bacteria absorbs light of wavelengths between 760-1130 nm, resulting in their characteristic purple colour (Fig. 2.1). Carotenoids in these bacteria absorb light at 400-500 nm, giving rise to the red colour present in lakes with algal bloom (Madigan et al., 2018). PPBs are predominantly anoxygenic, phototrophic, facultative anaerobes, and polyphosphate accumulating organisms (Capson-Tojo et al., 2020).

PPBs are grouped into two categories based on physiological properties: purple sulfur bacteria

(PSB) and purple non-sulfur bacteria (PNSB). PSBs use sulfide as an electron donor and store it intracellularly as elemental sulfur (Imhoff, 1995). Whilst the non-sulfur variant (PNSB) typically prefers organic electron donors; However, contrary to their name, they have also been found to be able to oxidize moderate concentrations of sulfide (<0.5 mM) to elemental sulfur granules, tetrathionate, or sulfate and excrete the granules (Imhoff, 1995). In fact, *R. capsulatus, R. spheroids*, and *Rhodospirillum* produce elemental sulfur as their final oxidized product, and *R. sulfidophilus* and several *Rhodobacter* and *Rhodopseudomonas* species oxidize sulfur to sulfate. Other more common electron donors for PNSBs are molecular H_2 oxidized by a membrane-bound hydrogen-ubiquinone oxidoreductase (McEwan, 1994). Their ability to metabolize high organic load and pollutants has been possible due to their unique glyoxylic acid cycle (GAC) metabolic pathway that affects VFA uptake and biomass synthesis. Further, they employ the Calvin–Benson cycle (CBB), tricarboxylic acid cycle (TCA), and Embden-Meyerhof-Parnas pathway (EMP) to generate several essential metabolic precursors for cell growth (McEwan, 1994; Petushkova et al., 2021).

2.4 Polyphosphate and PHAs in PNSBs

Inorganic polyphosphate (polyP) is important in multiple cellular functions, primarily as an ATP precursor and as phosphorus storage. PolyPs can form complexes with cellular constituents and with polyphosphate kinase (PPK), can assist in mobility, virulence, and stress control. The enzyme polyP kinase 1 (PPK1) is responsible for polyphosphate synthesis in the presence of excess phosphate, whereas exopolyphosphatase (PPX1) and endopolyphosphatase (PPN1)

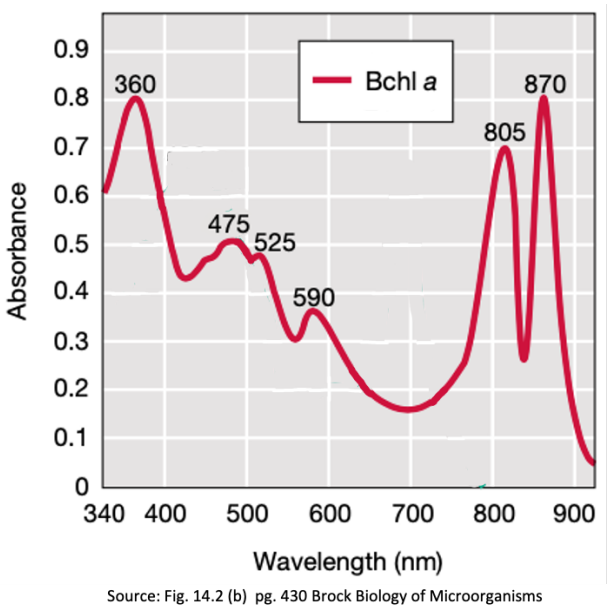

Figure 2.1: *Characteristic absorbance peaks shown by purple bacteria at 805 nm and 870 nm measured using spectrophotometry.*

degrade polyPs in their absence (Achbergerovà and Nahàlka, 2011; Hirota et al., 2010; Kornberg et al., 1999; Kulakovskaya et al., 2016; Rao et al., 2009). *R. palustris*, a model purple bacteria, have the ability to produce phosphoenolpyruvate (PEP) by combining the pyrophosphoryl group from ATP to pyruvate using PEP synthetase (PPS) or pyruvate-phosphate dikinase (PPDK) enzymes. The pyrophosphoryl group obtained from PEP or ATP combines with phosphate to form intracellular polyphosphate when excess phosphorus is present in their environment.

In the presence of excess substrates, for example, sugar or fatty acids, PNSBs follow different metabolic pathways. Depending on the type of substrate supplied, they form a variety of PHAs monomers, one of the storage molecules synthesized for famine conditions (Constanina et al., 2020; Khatami et al., 2021). When *R. palustris* G11 is subjected to an O_2 limited environment, it shows

an increase in NADH. Citrate synthase and isocitrate dehydrogenase are then inhibited by the high NADH level enabling acetyl-CoA redirection from the TCA cycle to the acetoacetyl-CoA formation cycle to form PHB using excess carbon (Lai et al., 2017).

2.5 Selection Factors for PNSB in Reactors

PNSBs generate ATP via photophosphorylation in ambient conditions and take up carbon in nutrient-limited conditions. This capability allows them to grow and accumulate PHAs in carbon-feast mode utilizing their internal cell-reducing power unlike the feast and famine ratio employed on mixed heterotrophic communities in Aerobic Dynamic Feeding (Almeida et al., 2021; Capson-Tojo et al., 2020). In Aerobic Dynamic Feeding, alternating cycles of short carbon-feast and long carbon-famine phases are employed to select PHA-accumulating bacteria which depends on their ability to grow on the accumulated PHAs (Almeida et al., 2021; Jayakrishnan et al., 2021). Almeida et al. (2021) enrich PPBs in the continuous C-feast regime using pre-treated domestic wastewater and molasses as substrate. In the first few weeks of operation, their reactor showed an average of 12% PHA content with a phosphorus uptake and release profile under P-limiting conditions. Interestingly, the suspension later saw an increase in sugar concentration (20% of total organics) that led to a fermentation process. This fermentation condition caused a decline in biomass.

Of several factors dictating the behaviour of purple bacteria in reactors, the retention time (RT) has an important effect on the type of VFA generated and thus, the microbial community in a nutrient recovery system. The contact period between biocatalysts and substrate is determined

by HRT. The amount of time anaerobic bacteria are exposed to the substrate is measured by the SRT (Jayakrishnan et al., 2021). The effects of decoupling the SRT and HRT for improved performance in microalgal-bacteria photobioreactors have been widely studied with algae-based reactors and not PNSBs. Gonzàlez-Camejo et al. (2019) observed that a lower SRT of 4.5 to 9 days and HRT of 3.5 days were optimum for phosphorus consumption and carbon fixation in outdoor photobioreactors. Typically, anaerobic filter (AF), packed bed (PB), expanded bed reactor ((EBR)), and membrane-bound reactors have enabled attached growth for decoupling of SRT in microalgal or open community-based reactors (Sattler, 2014). Chen et al. (2021) demonstrated that anaerobic digester performance increases with increasing SRTs (30 to 50 days) and a decrease in *Acidobacteria* and *Bacteriodetes*. Settling of biomass at rates of 24 gVSS $h^{-1}m^{-3}$ (Cerruti et al., 2020) or measured as settleability of algae at 77-90% (Arias et al., 2019) has been applied for SRT decoupling. Hafez et al. (2009) utilized the decoupled system to generate H_2 from glucose in a reactor enriched with *Clostridium* sp. Algal-bacterial photobioreactors have been extensively used in experiments to study the effect of uncoupling SRT and HRT on the enrichment and nutrient removal performances which showed promising results with P-removal rates of 0.4 mg PO_4^{3-}-P/L day^{-1} (Solmaz and Işik, 2019), with 55% to 91% TP removal efficiency (Arias et al., 2019; Xu et al., 2015; Zhang et al., 2021). Furthermore, a number of studies have been carried out to understand the polyP removal and PHA-accumulation capacities of isolated PNSB strains in reactor systems (Blansaer et al., 2022; Lai et al., 2017; Monroy and Buitrón, 2020). However, no study has been undertaken to assess the impact of decoupling the SRT and HRT on PNSBs in a photobioreactor. The influence of those parameters on phosphorus and PHAs accumulation in mixed PNSB cultures

is unclear. Therefore, the goal of this study is to improve our knowledge in these gap areas.

Finally, the effects of P-limitation on PNSB mixed culture enrichment and corresponding polyP and PHAs accumulation remain to be explored. Carstensen et al. (2018) recently presented a biological model describing the disruption in photosystem I (PSI) due to reduced inorganic orthophosphate. This caused lumen acidification in chloroplasts of barley, leading to reduced ATP synthase activity. However, bacteria can adapt to P-limitation by degrading phosphoglycerolipids and replacing them with glycoglycerolipids. Purple bacteria can also synthesize glycoglycerolipids and sulfoquinovosyldiacylglycerol as their lipid membranes which facilitates their survival (Tamot and Benning, 2009). A pure culture of *R. spheroids* NR3 began accumulating polyP only at concentrations over 10 mM external o-P_i in media (Hiraishi et al., 1991). The hypothesis would be that in a P-limited phototrophic-microbial reactor, PNSB selection and carbon uptake will be encouraged due to their survival capacity. Although picocyanobacteria (a member of the phototrophic microbial community) can out-compete heterotrophic bacteria by the above mechanism (Tamot and Benning, 2009), lipid remodelling during P-deficiency is more common than assumed as shown in marine heterotrophic bacteria (Sebastián et al., 2016). In mixed culture photobioreactors, low-P conditions of <25 mg P/L have not been studied yet (Section 1.3), which necessitates further exploration.

References

Achbergerovà, L., Nahàlka, J., 2011. Polyphosphate - an ancient energy source and active metabolic regulator. Microbial Cell Factories 10, 63. doi:10.1186/1475-2859-10-63.

Almeida, J.R., Serrano, E., Fernandez, M., Fradinho, J.C., Oehmen, A., Reis, M.A.M., 2021. Polyhydroxyalkanoates production from fermented domestic wastewater using phototrophic mixed cultures. Water Research 197, 117101. doi:https://doi.org/10.1016/j.watres.2021.117101.

Arias, D.M., Rueda, E., García-Galán, M.J., Uggetti, E., García, J., 2019. Selection of cyanobacteria over green algae in a photo-sequencing batch bioreactor fed with wastewater. Science of The Total Environment 653, 485–495. doi:https://doi.org/10.1016/j.scitotenv.2018.10.342.

Atienza–Martínez, M., Gea, G., Arauzo, J., Kersten, S.R.A., Kootstra, A.M.J., 2014. Phosphorus recovery from sewage sludge char ash. Biomass and Bioenergy 65, 42–50. doi:https://doi.org/10.1016/j.biombioe.2014.03.058.

Blansaer, N., Alloul, A., Verstraete, W., Vlaeminck, S.E., Smets, B.F., 2022. Aggregation of purple bacteria in an upflow photobioreactor to facilitate solid/liquid separation: Impact of organic loading rate, hydraulic retention time and water composition. Bioresource Technology 348, 126806. doi:https://doi.org/10.1016/j.biortech.2022.126806.

Burn, S., Muster, T., Kaksonen, A., 2014. Resource Recovery from Wastewater : A Research Agenda : WERF Research Report Series. IWA Publishing, London, UNITED KINGDOM.

Cañas, J., Àlvarez-Torrellas, S., Hermana, B., García, J., 2023. Phosphorus recovery from sewage sludge as struvite. Water 15, 2382.

Capson-Tojo, G., Batstone, D.J., Grassino, M., Vlaeminck, S.E., Puyol, D., Verstraete, W., Kleerebezem, R., Oehmen, A., Ghimire, A., Pikaar, I., Lema, J.M., Hülsen, T., 2020. Purple phototrophic bacteria for resource recovery: Challenges and opportunities. Biotechnology Advances 43. doi:10.1016/j.biotechadv.2020.107567.

Carstensen, A., Herdean, A., Schmidt, S.B., Sharma, A., Spetea, C., Pribil, M., Husted, S., 2018. The impacts of phosphorus deficiency on the photosynthetic electron transport chain. Plant Physiol 177, 271–284. doi:10.1104/pp.17.01624.

Cerruti, M., Stevens, B., Ebrahimi, S., Alloul, A., Vlaeminck, S.E., Weissbrodt, D.G., 2020. Enrichment and aggregation of purple non-sulfur bacteria in a mixed-culture sequencing-batch photobioreactor for biological nutrient removal from wastewater. Frontiers in Bioengineering and Biotechnology 8. doi:10.3389/fbioe.2020.557234.

Chen, G., Wu, W., Xu, J., Wang, Z., 2021. An anaerobic dynamic membrane bioreactor for enhancing sludge digestion: Impact of solids retention time on digestion efficacy. Bioresource Technology 329, 124864. doi:https://doi.org/10.1016/j.biortech.2021.124864.

Chen, G.Q., Wu, Q., Jung, Y.K., Lee, S.Y., 2011. 3.21 - PHA/PHB. Academic Press, Burlington. pp. 217–227. doi:https://doi.org/10.1016/B978-0-08-088504-9.00179-3.

Cheremisinoff, N.P., 2002. Chapter 12 - Treating the Sludge. Butterworth-Heinemann, Woburn. pp. 496–600. doi:https://doi.org/10.1016/B978-075067498-0/50015-2.

Cieślik, B., Konieczka, P., 2017. A review of phosphorus recovery methods at various steps of wastewater treatment and sewage sludge management. the concept of “no solid waste generation”

and analytical methods. Journal of Cleaner Production 142, 1728–1740. doi:https://doi.org/10.1016/j.jclepro.2016.11.116.

Constanina, K., Plácido, J., Venetsaneas, N., Burniol-Figols, A., Varrone, C., Gavala, H.N., Reis, M.A.M., 2020. Recent advances and challenges towards sustainable polyhydroxyalkanoate (pha) production, in: Koller, M. (Ed.), The Handbook of Polyhydroxyalkanoates. CRC Press, Boca, Raton, pp. 8–50.

Dale, C., Laliberte, M., Oliphant, D., Ekenberg, M., . Wastewater treatment using mbbr in cold climates, in: Conference Proceedings of Mine Water Solutions in Extreme Environments, pp. 12–15.

Egle, L., Rechberger, H., Krampe, J., Zessner, M., 2016. Phosphorus recovery from municipal wastewater: An integrated comparative technological, environmental and economic assessment of p recovery technologies. Science of The Total Environment 571, 522–542. doi:https://doi.org/10.1016/j.scitotenv.2016.07.019.

Fradinho, J., Allegue, L.D., Ventura, M., Melero, J.A., Reis, M.A.M., Puyol, D., 2021. Up-scale challenges on biopolymer production from waste streams by purple phototrophic bacteria mixed cultures: A critical review. Bioresource Technology 327, 124820. doi:https://doi.org/10.1016/j.biortech.2021.124820.

Fradinho, J.C., Domingos, J.M.B., Carvalho, G., Oehmen, A., Reis, M.A.M., 2013. Polyhydroxyalkanoates production by a mixed photosynthetic consortium of bacteria and algae.

Bioresource Technology 132, 146–153. doi:https://doi.org/10.1016/j.biortech.2013.01.050.

Gonzàlez-Camejo, J., Jim/'enez-Benítez, A., Ruano, M.V., Robles, A., Barat, R., Ferrer, J., 2019. Optimising an outdoor membrane photobioreactor for tertiary sewage treatment. Journal of Environmental Management 245, 76–85. doi:https://doi.org/10.1016/j.jenvman.2019.05.010.

Green, B.W., 2015. 2 - Fertilizers in aquaculture. Woodhead Publishing, Oxford. pp. 27–52. doi:https://doi.org/10.1016/B978-0-08-100506-4.00002-7.

Hafez, H., Baghchehsaraee, B., Nakhla, G., Karamanev, D., Margaritis, A., El Naggar, H., 2009. Comparative assessment of decoupling of biomass and hydraulic retention times in hydrogen production bioreactors. International Journal of Hydrogen Energy 34, 7603–7611. doi:https://doi.org/10.1016/j.ijhydene.2009.07.060.

Havukainen, J., Nguyen, M.T., Hermann, L., Horttanainen, M., Mikkilä, M., Deviatkin, I., Linnanen, L., 2016. Potential of phosphorus recovery from sewage sludge and manure ash by thermochemical treatment. Waste Management 49, 221–229.

Hiraishi, A., Yanase, A., Kitamura, H., 1991. Polyphosphate accumulation by *Rhodobacter sphaeroides* grown under different environmental conditions with special emphasis on the effect of external phosphate concentrations. Bulletin of Japanese Society of Microbial Ecology 6, 25–32. doi:10.1264/microbes1986.6.25.

Hirota, R., Kuroda, A., Kato, J., Ohtake, H., 2010. Bacterial phosphate metabolism and its application to phosphorus recovery and industrial bioprocesses. Journal of Bioscience and Bioengineering 109, 423–432. doi:https://doi.org/10.1016/j.jbiosc.2009.10.018.

Ike, M., Okada, Y., Narui, T., Sakai, K., Kuroda, M., Soda, S., Inoue, D., 2019. Potential of waste activated sludge to accumulate polyhydroxyalkanoates and glycogen using industrial wastewater/liquid wastes as substrates. Water science and technology : a journal of the International Association on Water Pollution Research 80, 2373–2380. doi:10.2166/wst.2020.059.

Imhoff, J.F., 1995. Taxonomy and Physiology of Phototrophic Purple Bacteria and Green Sulfur Bacteria. Springer Netherlands, Dordrecht. pp. 1–15. doi:10.1007/0-306-47954-0_1.

Jayakrishnan, U., Deka, D., Das, G., 2021. Waste as feedstock for polyhydroxyalkanoate production from activated sludge: Implications of aerobic dynamic feeding and acidogenic fermentation. Journal of Environmental Chemical Engineering 9, 105550. doi:https://doi.org/10.1016/j.jece.2021.105550.

Jenkins, D., Wanner, J., 2014. Activated Sludge - 100 Years and Counting : 100 Years and Counting. IWA Publishing, London, UNITED KINGDOM.

Khatami, K., Perez-Zabaleta, M., Owusu-Agyeman, I., Cetecioglu, Z., 2021. Waste to bioplastics: How close are we to sustainable polyhydroxyalkanoates production? Waste Management 119, 374–388. doi:https://doi.org/10.1016/j.wasman.2020.10.008.

Khursheed, A., Munshi, F.M.A., Almohana, A.I., Alali, A.F., Kamal, M.A., Alam, S., Alrehaili, O., Islam, D.T., Kumar, M., Varjani, S., Kazmi, A.A., Tyagi, V.K., 2023. Resolution of conflict of reduced sludge production with ebpr by coupling osa to a2/o process in a pilot scale sbr. Chemosphere 318, 137945. doi:https://doi.org/10.1016/j.chemosphere.2023.137945.

Kornberg, A., Rao, N.N., Ault-Riché, D., 1999. Inorganic polyphosphate: a molecule of many functions. Annu Rev Biochem 68, 89–125. doi:10.1146/annurev.biochem.68.1.89.

Kulakovskaya, T., Ryasanova, L., Dmitriev, V., Zvonarev, A., 2016. The Role of Inorganic Polyphosphates in Stress Response and Regulation of Enzyme Activities in Yeast. Springer International Publishing, Cham. pp. 3–14. doi:10.1007/978-3-319-41073-9_1.

Lai, Y.C., Liang, C.M., Hsu, S.C., Hsieh, P.H., Hung, C.H., 2017. Polyphosphate metabolism by purple non-sulfur bacteria and its possible application on photo-microbial fuel cell. Journal of Bioscience and Bioengineering 123, 722–730.

Lamastra, L., Suciu, N.A., Trevisan, M., 2018. Sewage sludge for sustainable agriculture: contaminants' contents and potential use as fertilizer. Chemical and Biological Technologies in Agriculture 5, 10. doi:10.1186/s40538-018-0122-3.

Madigan, M.T., Bender, K.S., Buckley, D.H., Sattley, W.M., Stahl, D.A., 2018. Brock biology of microorganisms. Fifteenth edition. ed., Pearson, NY, NY.

McEwan, A.G., 1994. Photosynthetic electron transport and anaerobic metabolism in purple non-sulfur phototrophic bacteria. Antonie Van Leeuwenhoek 66, 151–64. doi:10.1007/bf00871637.

Monroy, I., Buitrón, G., 2020. Production of polyhydroxybutyrate by pure and mixed cultures of purple non-sulfur bacteria: A review. Journal of Biotechnology 317, 39–47. doi:https://doi.org/10.1016/j.jbiotec.2020.04.012.

Morgan-Sagastume, F., Bengtsson, S., De Grazia, G., Alexandersson, T., Quadri, L., Johansson, P., Magnusson, P., Werker, A., 2020. Mixed-culture polyhydroxyalkanoate (pha) production integrated into a food-industry effluent biological treatment: A pilot-scale evaluation. Journal of Environmental Chemical Engineering 8. doi:10.1016/j.jece.2020.104469.

Nathanson, J.A., Archis, A., 24 Jul. 2023. Wastewater treatment. doi:https://www.britannica.com/technology/wastewater-treatment. accessed: 09 Aug. 2023.

Obruca, S., Sedlacek, P., Slaninova, E., Fritz, I., Daffert, C., Meixner, K., Sedrlova, Z., Koller, M., 2020. Novel unexpected functions of pha granules. Applied Microbiology and Biotechnology 104, 4795–4810. doi:10.1007/s00253-020-10568-1.

Pardelha, F.A.G., 2013. Constraint-based modelling of mixed microbial populations: Application to polyhydroxyalkanoates production. Thesis.

Petushkova, E., Mayorova, E., Tsygankov, A., 2021. Tca cycle replenishing pathways in photosynthetic purple non-sulfur bacteria growing with acetate. Life (Basel) 11. doi:10.3390/life11070711.

Rao, N.N., Goòmez-Garciìa, M.R., Kornberg, A., 2009. Inorganic polyphosphate: essential for growth and survival. Annual review of biochemistry 78, 605–47. doi:10.1146/annurev.biochem.77.083007.093039.

Roibàs-Rozas, A., Mosquera-Corral, A., Hospido, A., 2020. Environmental assessment of complex wastewater valorisation by polyhydroxyalkanoates production. The Science of the total environment 744, 140893. doi:10.1016/j.scitotenv.2020.140893.

Rorat, A., Courtois, P., Vandenbulcke, F., Lemiere, S., 2019. 8 - Sanitary and environmental aspects of sewage sludge management. Butterworth-Heinemann. pp. 155–180. doi:https://doi.org/10.1016/B978-0-12-815907-1.00008-8.

Sattler, L.M., 2014. Anaerobic municipal wastewater treatment: A beneficial option for developing countries. Current Environmental Engineering 1, 126–135. doi:dx.doi.org/10.2174/22127178016661407071610 49.

Sebastián, M., Smith, A.F., González, J.M., Fredricks, H.F., Van Mooy, B., Koblížek, M., Brandsma, J., Koster, G., Mestre, M., Mostajir, B., Pitta, P., Postle, A.D., Sánchez, P., Gasol, J.M., Scanlan, D.J., Chen, Y., 2016. Lipid remodelling is a widespread strategy in marine heterotrophic bacteria upon phosphorus deficiency. The ISME Journal 10, 968–978. URL: https://doi.org/10.1038/ismej.2015.172, doi:10.1038/ismej.2015.172.

Solmaz, A., Işik, M., 2019. Effect of sludge retention time on biomass production and nutrient removal at an algal membrane photobioreactor. BioEnergy Research 12, 197–204. doi:10.1007/s12155-019-9961-4.

Tamot, B., Benning, C., 2009. The Purple Phototrophic Bacteria. Springer Netherlands, Dordrecht. book section Membrane Lipid Biosynthesis in Purple Bacteria. pp. 119–134. doi:10.1007/978-1-4020-8815-5_7.

World Bank, . Accessed: Aug 2023.

Xu, M., Li, P., Tang, T., Hu, Z., 2015. Roles of srt and hrt of an algal membrane bioreactor system with a tanks-in-series configuration for secondary wastewater effluent polishing. Ecological Engineering 85, 257–264. doi:https://doi.org/10.1016/j.ecoleng.2015.09.064.

Zeng, S., Song, F., Lu, P., He, Q., Zhang, D., 2018. Improving pha production in a sbr of coupling pha-storing microorganism enrichment and pha accumulation by feed-on-demand control. AMB Express 8, 1–12. doi:10.1186/s13568-018-0628-x.

Zhang, M., Leung, K.T., Lin, H., Liao, B., 2021. Effects of solids retention time on the biological performance of a novel microalgal-bacterial membrane photobioreactor for industrial wastewater treatment. Journal of Environmental Chemical Engineering 9, 105500. doi:https://doi.org/10.1016/j.jece.2021.105500.

Zhao, Q., Ying, H., Liu, Y., Wang, H., Xu, J., Wang, W., Ren, J., Meng, S., Wang, N., Mu, R., Wang, S., Li, J., 2023. Towards low energy-carbon footprint: Current versus potential p recovery paths in domestic wastewater treatment plants. Journal of Environmental Management 344, 118653. doi:https://doi.org/10.1016/j.jenvman.2023.118653.

Chapter 3

Materials & Methods

3.1 Growth Medium

The medium is prepared according to Biebl and Pfennig (1981) with modifications in the phosphate (0.02 g/L, 0.06 g/L and 0.1 g/L of KH_2PO_4 fed to each reactor) and substrate (Table 3.1). All the solutions were stored in glass bottles in the dark. Stock solutions of yeast extract broth and potassium phosphate solutions were autoclaved separately before storage. The pH was adjusted between 7 and 8 by adding 1N HCl to the glass bottles containing the media.

Table 3.1: *Compositions of media fed to the reactors (Modified from (Biebl and Pfennig, 1981))*

Medium composition per litre of distilled water	
$MgSO_4.7H_2O$	0.2 g
NaCl	0.4 g
NH_4Cl	0.4 g
$CaCl_2.2H_2O$	0.05 g
Acetate or Propionate	0.5 g
Yeast extract	0.2 g
Fe-citrate solution (0.1 g/ 100 mL)	5 mL
Trace element solution	1 mL

Trace element solution composition per litre of distilled water	
HCl (25%)	1 mL
$ZnCl_2$	70 mg
$MnCl_2.4H_2O$	100 mg
H_3BO_3	60 mg
$CoCl_2.2H_2O$	200 mg
$CuCl_2.2H_2O$	20 mg
$NiCl_2.6H_2O$	20 mg
$NaMoO_4.2H_2O$	40 mg

3.2 Experimental Design

A total of 24 reactors were set up in 50-mL falcon™ tubes filled to the rim, manipulated in an anaerobic hood, and incubated on a shaker in normal air conditions (modified from Jaber (2020)). All the reactors were inoculated with 100 μ L of secondary sludge from La Prairie wastewater treatment plant located in St. Hyacinthe, Quebec. Out of the 24 reactors, 12 were fed with acetate, and others with propionate added as the sole substrate to a mineral medium containing yeast extract (Section 3.1). The 24 reactors were divided into two batches of 12 reactors each. Six reactors in each of the VFA-fed reactors were operated with decoupled SRT (7 days) and HRT (2

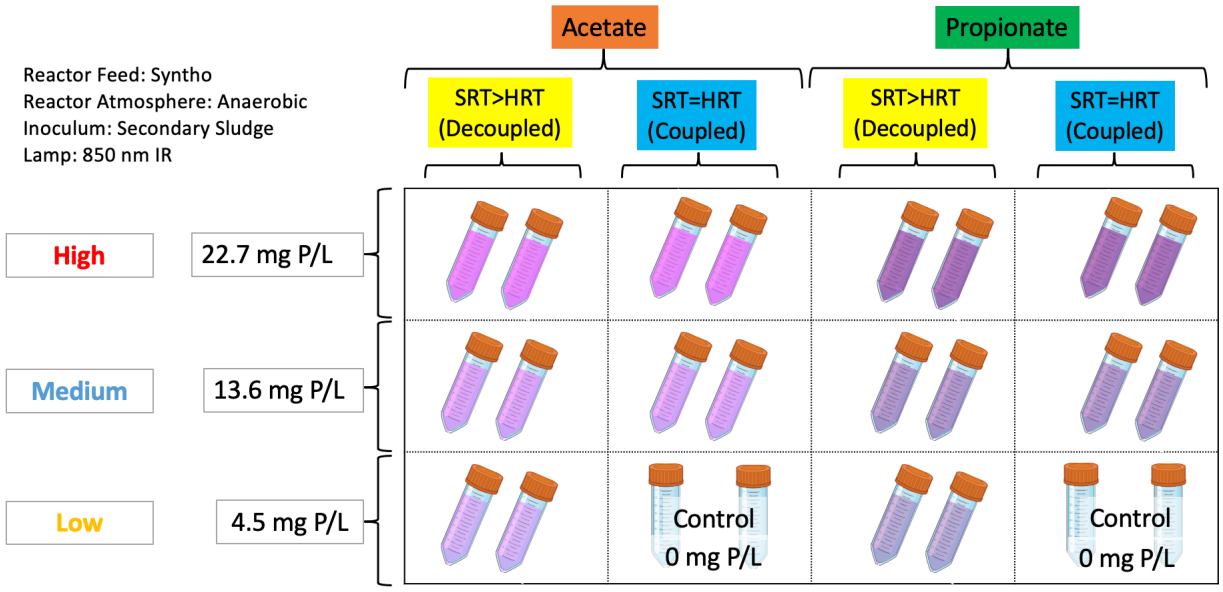

Figure 3.1: *Schematics of the experimental design. Each row of reactors corresponds to an amount of phosphate added to the mineral medium independently of the yeast extract. Each pair of columns indicates the intended sole substrate besides yeast extract (acetate or propionate), and the SRT-HRT configuration (decoupled or coupled as described above). Duplicates of reactors were employed in the experiment.*

days), whilst four reactors were operated with coupled SRT = HRT (2 days). In each of these sets, duplicates of reactors were fed with different concentrations of PO_4^{3-}, that is, 22.7 mg P/L; 13.6 mg P/L; and 4.5 mg P/L. Each SRT-HRT configuration had a control in which no phosphorus was added (Fig. 3.1). The reactors were operated for a total of 232 days between April 2022 to December 2022.

3.3 Reactor Setup and Operation

The reactor operation lasted 232 days and was adjusted in 3 different phases to address questions raised by the observations made on the reactors as the experiment developed. In Phase 1 (50 days of operation), the reactors were operated semi-continuously with feeding and wastage without special cleaning of the cell walls. This led to the accumulation of biofilm on the reactors' surfaces, which was judged undesirable. In Phase 2 (117 days of operation), the biofilms were scraped off every two weeks using a lab brush saved exclusively for this experiment under running hot water. In Phase 3 (48 days of operation), the wall cleaning was continued as during Phase 2, and yeast extract was removed from the growth medium because it was suspected that it was contributing phosphorus and degradable carbon substrates to the medium, which was thought to preclude adequate assessment of the questions the study attempted to address. Thus, yeast extract broth was eliminated from the feed composition. The wastage volume and frequency of wastage was changed for phase 2 and 3, details of which are in Table 3.2.

For the reactors with decoupled HRT & SRT, the 50-mL screw cap tubes (i.e., reactors) were centrifuged at 5000 rpm in a centrifuge (Thermo Scientific ™ Sorvall ™ Legend™ Micro 21R Microcentrifuge) for 40 min. to settle the biomass.

Out of 50 mL volume of cell suspension in each reactor, 15-25% of suspension and 35-50% of supernatant were discarded as per HRT of 2 days without disturbing the biofilm, if any. For the 4 coupled reactors in each batch, 50% of cell suspension was discarded every day. Each of the reactors was then refilled to 50 mL with fresh feed solution (Table 3.2).

The pH of the reactors was measured on the bench (pH probe: LE422 electrode, Mettler Toledo,

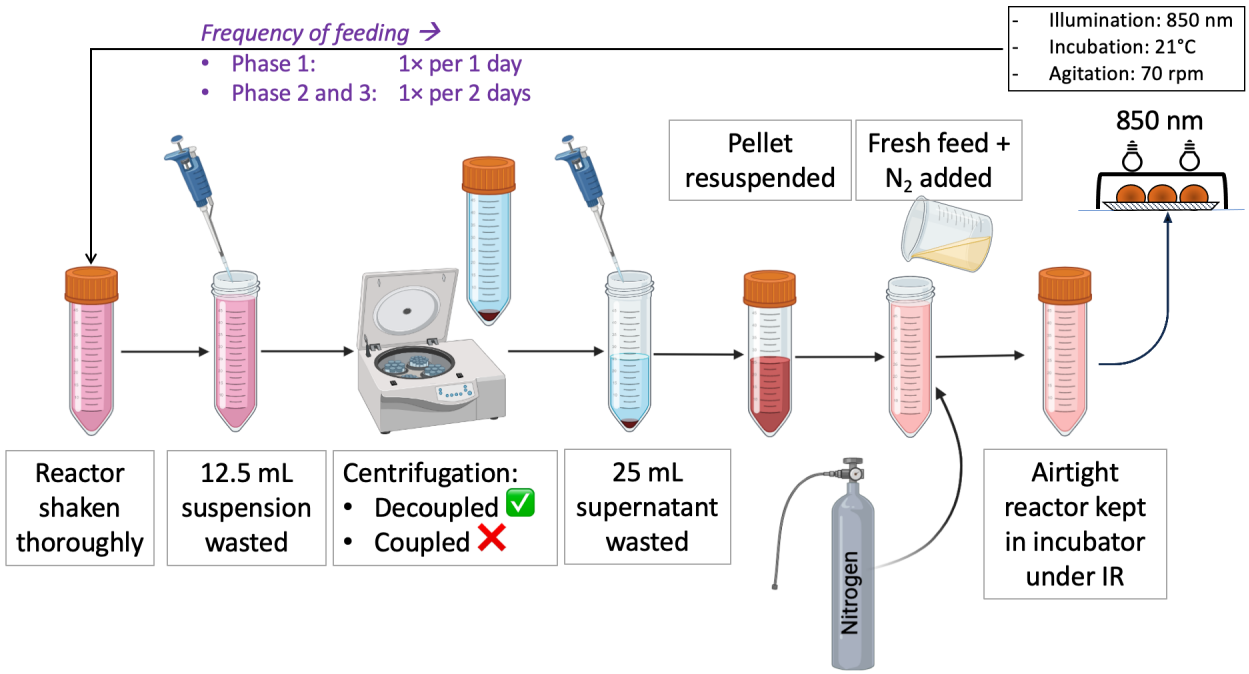

Figure 3.2: *The operational steps are described. For decoupling the SRT and HRT, the cell suspension was centrifuged and the supernatant was removed. The centrifugation step was skipped for coupled reactors.*

Material No.: 30089747; pH meter: Orion Star™ A211).

The headspace of the 24 reactors was filled with inert N_2 using a nozzle from N_2 gas cylinder at low pressure (0.1 psi) for 2 minutes per reactor to create an oxygen-free environment. The reactors were then screwed closed and checked for leaks by wrapping the tubes with brown hand paper (Superior Sany Solutions). Before placing them in the incubator, the reactors were randomly arranged on a tray to eliminate biased irradiation from the lamp (Fig. 3.2).

Table 3.2: *Wastage and feeding volume and frequency*

	SRT>HRT (Decoupled)		SRT=HRT (Coupled)	
	Cell Suspension Wastage Volume (mL)	Supernatant Wastage Volume (mL)	Cell Suspension Wastage Volume (mL)	Frequency of Wastage (Days)
Phase 1	7	18	25	1
Phase 2	12.5	25	37.5	2
Phase 3	12.5	25	37.5	2

3.4 Analytical Methods

3.4.1 Operation Parameters

Every time the reactors were maintained (i.e., every day in Phase 1 and every 2 days in Phases 2 and 3), the OD, orthophosphate and pH were measured. Every week at the end of an SRT (7 days), the TSS, VSS, sCOD, and VFA were measured.

Every feeding day

Two types of measurements were carried out for the OD. In the first type of measurement, the absorbance was measured at 660, 805, and 870 nm using the spectrophotometer. In the second type, the absorbance was measured in a spectrum from 400 nm to 900 nm to highlight the wavelengths at which the absorbance was the highest.

The pH measurement was carried out using a pH probe (LE422 electrode, Mettler Toledo, Material No.: 30089747) every time after the reactors were fed.

The samples were prepared before orthophosphate measurement was carried out. About 2

mL of the sample was centrifuged at 20,000 g for 20 minutes in phase 1 and up to 40 minutes in phases 2 and 3 and the supernatant was used for orthophosphate measurement, protocol given in APHA (2012). The supernatant (200 μL) was taken in triplicates in a 96-well plate and 50 μL of vanadate–molybdate reagent was added to it. After the color developed at 10 minutes, the absorbance of the samples was measured at 470 nm, and turbidity at 800 nm using a SpectraMax UV-Vis spectrophotometer.

Every SRT = 7 days

Once a week, the total suspended solids (TSS) and volatile suspended solids (VSS) were measured following standard methods 2540D and 2540E (APHA, 2012) respectively.

The sCOD was measured every week or at the end of each SRT following the steps in APHA (2012).

VFAs were measured at the same time as the TSS, VSS and sCOD using a gas chromatograph (7820A Agilent, Agilent Technologies, USA) and CP7485 Agilent column (25 $\times$ 0.32 nm $\times$ 0.3 um) using helium as the carrier gas, with a flow rate of 6.5 L/min.

3.4.2 16S rRNA Gene Amplicon Sequencing Analysis

Every 7 days the biomass was archived for subsequent community analyses. On these days, 2 mL of mixed liquor was centrifuged, the water discarded and the pellet placed at -80°C until analysis.

DNA was extracted from the pellets Qiagen DNeasy Powersoil Kit (Qiagen, Germany) according to the manufacturer's instructions. The samples were purified using PCR purification

kits (Qiagen, Canada, Cat no. 28106; and Bio Basic, Canada, Part no. 9K-006-0004). DNA within the samples was amplified using 806R and 515F primer sets in a PCR (Caporaso et al., 2012) and its concentration was measured using NanoDrop™(OneC Microvolume UV-Vis Spectrophotometer, Thermo Scientific™). The PCR conditions applied are mentioned in Appendix A.3. All the samples were barcoded, checked for quality using P5, P7 primers, and purified again. 10 ng of DNA from each sample was pooled in two samples, and quantified using Quant-iT PicoGreen dsDNA Reagent. The samples were then sent to Génome Québec for sequencing using Illumina Miseq technology. The results were processed using Qiime2 software (Bolyen et al., 2018) and analyzed (Appendix D).

3.4.3 DAPI and LP2 Staining

The samples were centrifuged and the biomass pellet was taken with a pipette. The pellet was then washed with 1× PBS. After centrifugation at 10,000× g for 5 min, the supernatant was discarded and the samples were stained following the steps below. Samples were stained with 4'6-Diamidino-2-Phenylindole (DAPI) (Terashima et al., 2020) to visualize polyP and Lipid Green 2 (LP2) (Kettner and Griehl, 2020) for PHAs. The samples were plated, dried using ethanol 70%, and washed with 1× PBS twice. The samples were stained with DAPI and incubated in the dark for 20 minutes. The slides were washed with PBS thrice and stored at 4°C before observation under Zeiss LSM 710 confocal microscope with 100× oil immersion objective. The 405 nm blue diode laser 30 mW, and Ar Ion laser 458/488/514 nm 25 mW with fluorescence cubes Zeiss FS 49 (DAPI) and Zeiss FS 38 (eGFP) for LP2 were employed for imaging. The image processing was performed on ZEN (Zeiss

Efficient Navigation) software.

References

APHA, 2012. Standard Methods for the Examination of Water and Wastewater. American Public Health Association.

Biebl, H., Pfennig, N., 1981. Isolation of Members of the Family Rhodospirillaceae. Springer Berlin Heidelberg, Berlin, Heidelberg. pp. 267–273. doi:10.1007/978-3-662-13187-9_14.

Bolyen, E., Rideout, J.R., Dillon, M.R., Bokulich, N.A., Abnet, C., Al-Ghalith, G.A., Alexander, H., Alm, E.J., Arumugam, M., Asnicar, F., 2018. QIIME 2: Reproducible, interactive, scalable, and extensible microbiome data science. Report 2167-9843. PeerJ Preprints.

Caporaso, J.G., Lauber, C.L., Walters, W.A., Berg-Lyons, D., Huntley, J., Fierer, N., Owens, S.M., Betley, J., Fraser, L., Bauer, M., Gormley, N., Gilbert, J.A., Smith, G., Knight, R., 2012. Ultra-high-throughput microbial community analysis on the illumina hiseq and miseq platforms. The ISME Journal 6, 1621–1624. doi:10.1038/ismej.2012.8.

Jaber, M., 2020. Purple bacteria for wastewater treatment and resource recovery. Https://escholarship.mcgill.ca/concern/theses/sq87bz79q.

Kettner, A., Griehl, C., 2020. The use of lipidgreen2 for visualization and quantification of intracellular poly(3-hydroxybutyrate) in cupriavidus necator. Biochemistry and Biophysics Reports 24, 100819. doi:https://doi.org/10.1016/j.bbrep.2020.100819.

Terashima, M., Kamagata, Y., Kato, S., 2020. Rapid enrichment and isolation of polyphosphate-accumulating organisms through 4'6-diamidino-2-phenylindole (dapi) staining with fluorescence-activated cell sorting (facs). Front Microbiol 11, 793. doi:10.3389/fmicb.2020.00793.

Chapter 4

Results

4.1 Reactor Operation

The reactors were inoculated with activated sludge and operated for a duration of 232 days, and the characteristic red colouration of PNSB was observed within the first 7 days of operation for each of the phases (Fig. 4.1). During the entire operation, reactors were fed semi-continuously with a synthetic influent medium containing either acetate or propionate, and different concentrations of added phosphate (mg PO_4^{3-}-P/L: 22.7, 13.6, 4.5, and 0 - no-growth control) with the objective of observing the effect of P limitation. Biomass wasting was adjusted such that half of the reactors had SRT=HRT (i.e., *Coupled* retention times) and the other half had SRT>HRT (i.e., *Decoupled* retention times), to determine the impact of the average growth rate on the biomass (Fig. 4.1).

The experimental run was divided into 3 phases depending on the observations and the adjustments made to the protocol to meet the objectives. In Phase 1 (Day 1 - 65), biofilm

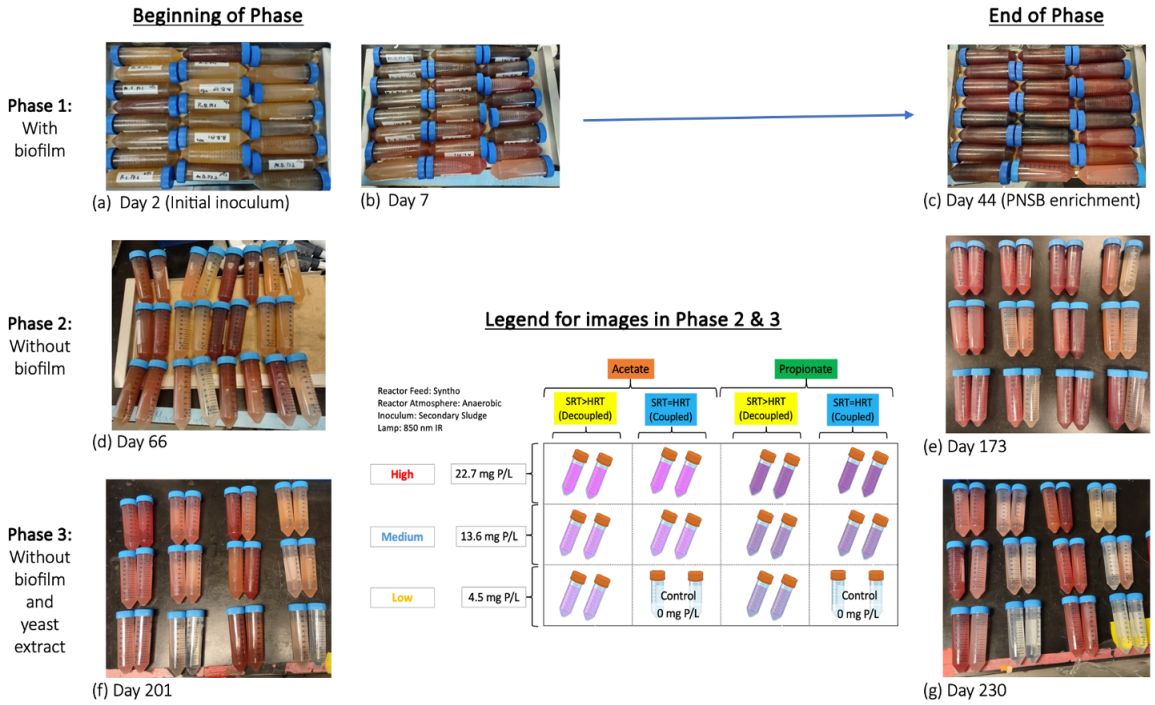

Figure 4.1: *PNSB suspensions in Falcon™ tube reactors. Pictures showing progressive change in colour (yellow-orange to red) and intensity (pale red to dark brown due to biofilm formation in some reactors). (a-c)Phase 1: (a) Day 2; (b) Day 7; (c) Day 44. (d-e) Phase 2: (d) Day 66 (e) Day 173. (f-g) Phase 3: (f) Day 201 (g) Day 230*

accumulation was observed, which was not desirable because it precluded adequate control of the SRT. In Phase 2 (Day 66 - 182) and 3 (Day 183 - 232), walls were cleaned to remove biofilm. However, yeast extract was presumed to contribute additional degradable COD and P in Phase 2; thus, the communities likely did not experience P limitation. In Phase 3, yeast extract was then removed from the influent medium to observe true P-limited conditions. All reactor conditions were duplicated in independent reactors. The detailed observations are presented below.

4.1.1 Visual Inspection

Throughout the operation period, PNSB growth was monitored by visual inspection (Fig. 4.1) and by OD measurements. Within the first few days of inoculation, a pink-red colouration developed within all the reactors (Fig. 4.1(a),(b)). The presence of purple bacteria in the reactor was confirmed by the observation of characteristic absorbance peaks of BChl *a* pigment at 805 and 870 nm (Fig. 4.2). However, by the end of Phase 1, thick biofilm formations with deep red and almost black colouration were observed in most reactors (Fig. 4.1 (c)).

The accumulation of biofilms in all reactors precluded the accurate comparison between coupled and decoupled SRT & HRT conditions because of very long solids retention in the biofilms. Consequently, in Phase 2 and 3, reactor walls were cleaned. As a result, the red color remained relatively more intense in the reactors with decoupled SRT & HRT than in the reactors with SRT equal to the HRT (Fig. 4.1(d),(f)). This was according to expectations.

During Phase 1 and 2, two pairs of replicate reactors received minimal medium without added mineral phosphate. It was expected that no biomass would grow in these reactors. However, a similar red colouration could be observed in these reactors as was in the other reactors with coupled SRT & HRT and receiving the medium with phosphate addition (Fig. 4.1 (e)). Therefore, it was hypothesized that yeast extract was the remaining source of P in the medium, and it was removed in the hope of establishing at least one P-limited condition. As a result, no biomass grew in the reactors not receiving phosphates as it was expected (Fig. 4.1 (g)).

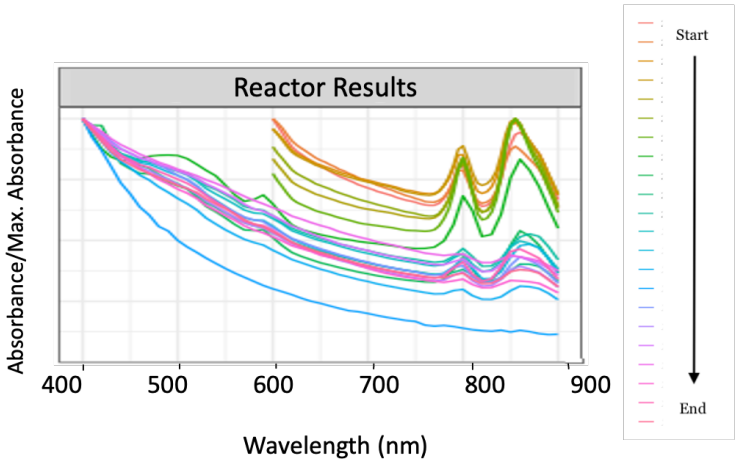

Figure 4.2: *Normalized curves for absorbance of IR wavelengths. The average values of absorbance for the duplicate reactors fed with propionate and 13.6 mg PO_4^{3-}/L and coupled configuration are presented here. The spectral plots for other reactors are in Appendix A.4. The peaks correspond to the peaks at 805 nm and 870 nm characteristic of PNSBs (Fig. 2.1).*

4.1.2 Performance Parameters

Optical Density (OD)

Optical Density measurements were taken at 660, 805, and 870 nm to estimate bacterial density and establish bacteriochlorophyll a (BChl a) containing PNSBs in the reactors.

Beginning from Day 0, the OD at 660 nm measurements rapidly increased and reached a steady state after approximately 15 days and remained steady for the rest of Phase 1 (Fig. 4.3 (b), 4.4(b)). The ratios of ODs 870 nm/660 nm & 805 nm/660 nm (Appendix A.3) steadily increased during Phase 1 for approximately half of the Phase 1 period, likely indicating an increase in the biomass level of BChl a (Fig.4.3(c,d), Fig.4.4(c,d)).

In Phase 2, the OD at 660 nm measurements decreased slightly with respect to their values at

the end of Phase 1, and stabilized by Day 95 with higher values in the decoupled than in the coupled reactors as observed in Phase 1 (Fig. 4.3(a), 4.4(a)). Drops in the 870 nm/660 nm and 805 nm/660 nm ratios compared to Phase 1 values were observed under all reactor conditions, suggesting that the PPB enrichment had been impacted by the removal of biofilm accumulation. Nonetheless, their values remained higher in both acetate-fed and propionate-fed decoupled than in coupled reactors (Fig. 4.3(c,d), 4.4(c,d)), suggesting a higher enrichment of BChl *a* at longer SRT. Finally, during the period of steady measurements of OD at 600 nm, the values were not markedly different between high (22.7 mg PO_4^{3-}-P/L), medium (13.6 mg PO_4^{3-}-P/L), and low (4.5 mg PO_4^{3-}/L) P-fed reactors, and the no P addition (0 mg PO_4^{3-}-P/L) reactors (Fig. 4.3(a,b),4.4(a,b)). This was unexpected and a source of P was suspected to be present in the medium, which was hypothesized to be the yeast extract.

In Phase 3, the OD at 660 nm dropped to half of Phase 1 indicating lower biomass concentrations due to the removal of yeast extract and biofilm from the reactors. However, the behaviour of the OD across the reactors with different phosphate in feed and SRT-HRT configuration remained similar to the previous phases, for instance, the decoupling of SRT continued to influence the biomass enrichment. OD ratios at 870 nm/660 nm and 805 nm/660 nm were relatively constant at approximately 1 for all the decoupled reactors and at slightly lower values for the coupled reactors. The spectral graph (Fig. 4.2, Appendix A.4) continues to show peaks at 805 and 870 nm denoting the presence of BChl *a* in the reactor suspensions. Finally, the OD 600 nm in the no phosphate control (0 mg PO_4^{3-}-P/L) reactors rapidly decreased, and the OD ratio 870 nm/600 nm also decreased, indicating that the biomass as a whole could not sustain itself and that PNSB was

decreasing in relative abundances.

Total and Volatile Suspended Solids

The Total Suspended Solids (TSS) and Volatile Suspended Solids (VSS) were measured to estimate the biomass accumulated within the reactor. This was done to complement the data obtained from OD measurements.

The TSS and VSS values followed a similar temporal profile as the OD measurements and showed high concentrations of solids in Phase 1, which declined through Phases 2 and 3. In Phase 1, the average VSS values were between 594±80 and 2002±191 mg/L. When walls were cleaned of the biofilms containing bacteria starting with Phase 2, the VSS dropped to average values between 399±40 and 1817±195 mg/L. Then, they continued to reduce in Phase 3 with VSS averages of 231±24 and 964±81 mg/L. The VFA (acetate or propionate) fed to the reactor and coupling or decoupling HRT and SRT did not have any visible effect on the accumulated VSS/TSS ratios. Finally, with the exception of the no phosphate control (0 mg PO_4^{3-}-P/L) reactors during Phase 3, changing the phosphate added to the feed medium did not affect the VSS concentration across the reactors (Fig. 4.3,4.4). Changing the VFA fed to the reactor - acetate or propionate did not change the TSS concentrations

Residual Soluble COD

The enriched PNSB-based communities were successful in removing COD from the wastewater. The mean residual soluble COD (sCOD) in Phase 1 was significantly higher in the effluent of coupled reactors than decoupled reactors fed with 22.7 mg PO_4^{3-}-P/L at 189 mg COD/L ($p=0.026$

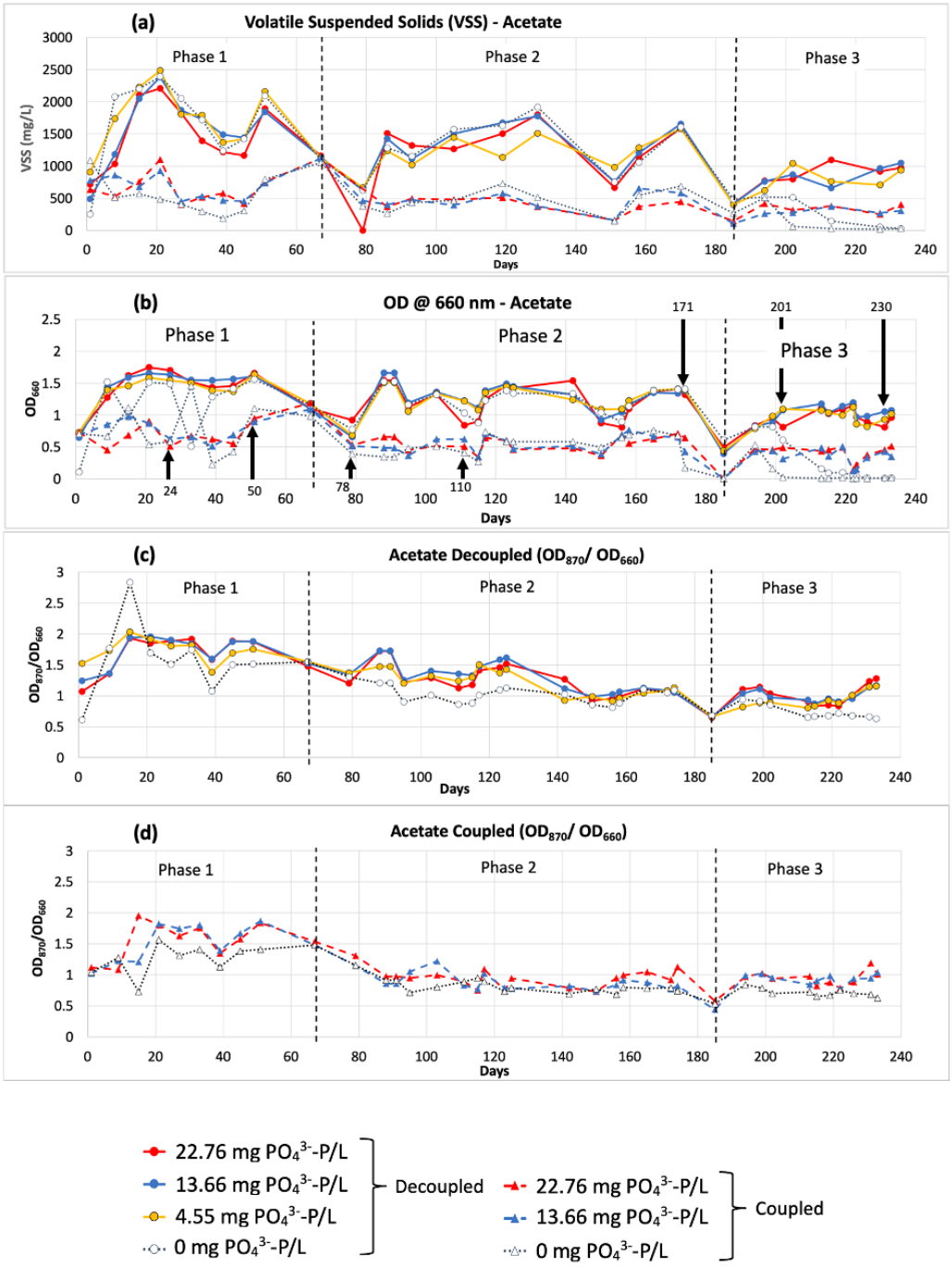

Figure 4.3: *Performance parameters of Acetate-fed reactors with different phosphate concentrations and SRT decoupled or coupled to HRT. (a) VSS profiles; (b) OD at 660 nm measurements; (c) Ratio of OD at 870 nm to OD at 660 nm for decoupled reactors; (d) Ratio OD at 870 nm to OD at 660 nm for coupled reactors. The ratios point to values*

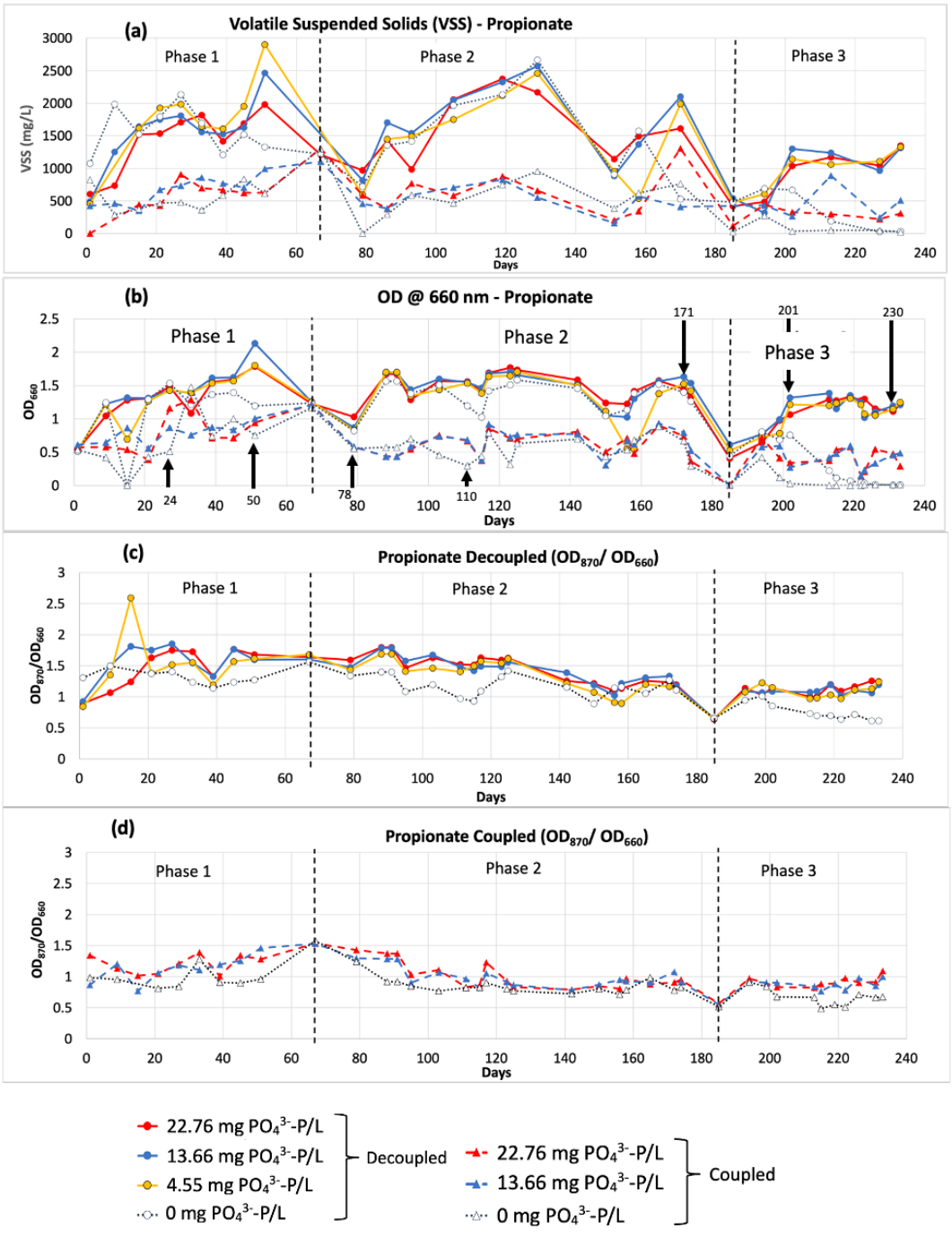

Figure 4.4: *Performance parameters of Propionate-fed reactors with different phosphate concentrations and SRT decoupled or coupled to HRT.. (a) VSS profiles; (b) OD at 660 nm measurements; (c) Ratio of OD at 870 nm to OD at 660 nm for decoupled reactors; (d) Ratio of OD at 870 nm to OD at 660 nm for coupled reactors.*

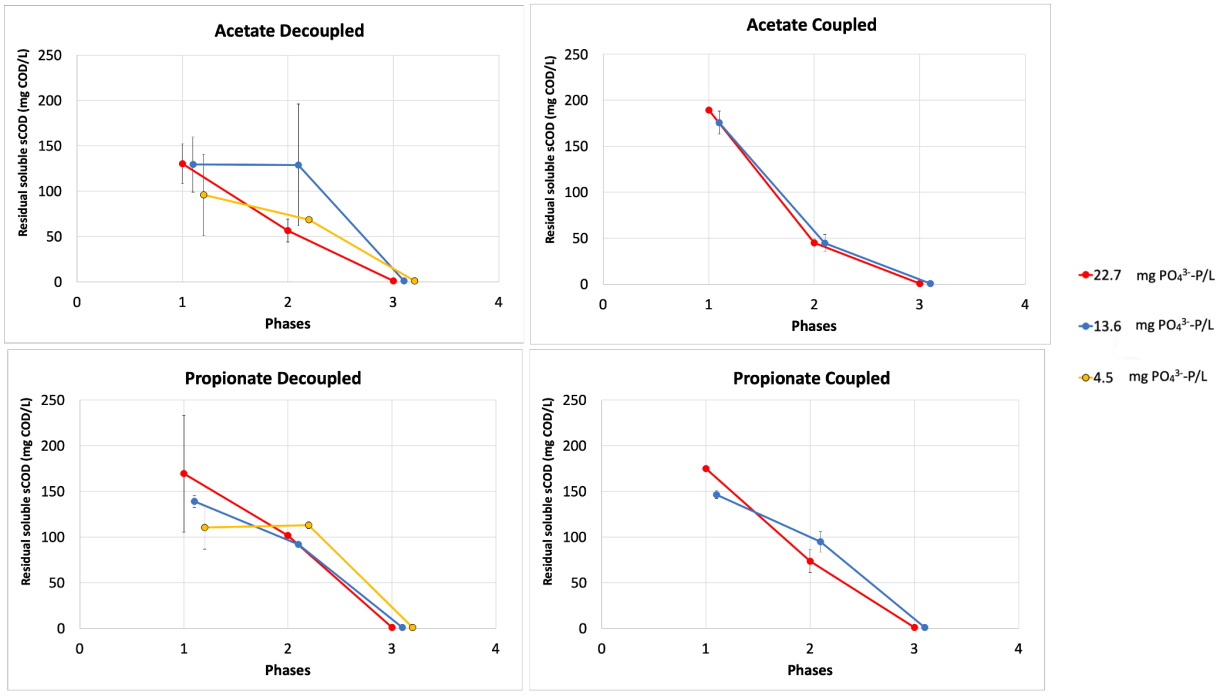

Figure 4.5: *Average residual sCOD concentrations for duplicate reactors fed different VFAs and added phosphate concentrations. For a given phase, values for reactors that received feeds containing different P concentrations were plotted with slight offset to visualize error bars. acetate-fed decoupled (a) and coupled (b) reactors; propionate-fed decoupled (c) and coupled (d) reactors. Error bars are the half-range of the two duplicate reactors.*

at α=0.05) for acetate-fed reactors. No such significant difference was found for propionate-fed reactors (p=0.45). Removal of the biofilm and subsequently yeast extract led to lower sCOD concentrations of 129 and 113 mg COD/L for acetate- and propionate-fed reactors, respectively, in Phase 2, and to sCOD being below detection in Phase 3 (Figure 4.5). The value of residual sCOD: below the detection level during Phase 3 suggested that yeast extract was contributing non-degradable COD.

Residual Orthophosphate (PO_4^{3-}-P)

Throughout the three phases, the measured residual orthophosphate concentrations by colourimetric measurements appeared to be proportional to their added phosphate in the feed medium (Fig.4.6). However, two observations made during Phase 1 attracted attention. First, as the solids accumulated through the phase, the residual orthophosphate concentrations unexpectedly increased. Second, whilst the phosphate concentrations in the feed medium were not measured in Phase 1, the residuals appeared to be higher than the added phosphate in all reactors. Additionally, the control reactors without phosphate added to their feed medium had residual phosphate concentrations similar to the ones measured in the reactors receiving medium supplement with 4.55 mg PO_4^{3-}-P/L (i.e., low-P) reactors. At this point, it was hypothesized that the extra-long SRT due to the accumulation of biofilm may have had the effect of concentrated phosphates. Therefore, it was further hypothesized that stopping biofilm accumulation would solve the discrepancies, and it was resolved to start measuring the orthophosphate in the feed medium (which was implemented starting on Day 66).

At the beginning of Phase 2 between 90 and 118 days, the residual phosphate concentrations rapidly lowered to concentrations well below the ones added to the feed media (Fig. 4.6(e)). This behaviour was seen across all the reactors irrespective of the VFA fed. This was perhaps due to the change of lamps that might have affected the light intensity and path incident on the reactors. Nonetheless, these observations were short-lived and the orthophosphate concentrations in the reactor effluent were once again above the measured concentrations of the feed media by the end of Phase 2. On the basis of these observations, it was then hypothesized that the yeast extract could

be contributing much more phosphate than anticipated, and yeast extract was removed from the medium formulation.

In the control reactors containing zero phosphate in feed, the effluent of the reactors did not detect any phosphate once the biomass had almost completely washed out of these reactors. However, despite the removal of yeast extract from the feed medium, the residual phosphate concentrations measured in the effluent of all the reactors with phosphate added to the feed media remained higher than the phosphate concentrations of the influent (Fig.4.6). Therefore, it appears that the biomass somehow interfered with the colourimetric measurement of orthophosphate in these experiments (Fig. 4.6(e)).

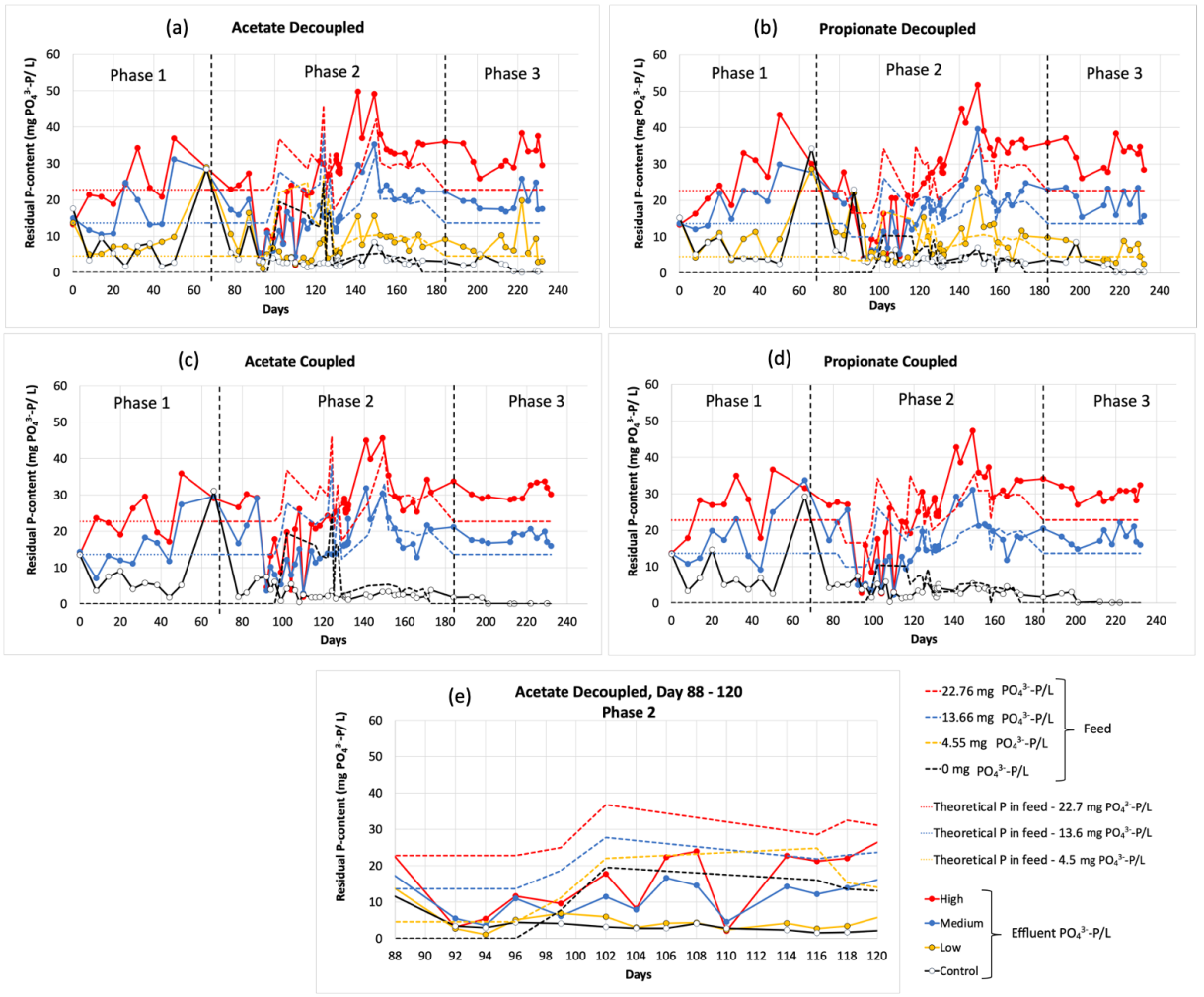

Figure 4.6: *Orthophosphate concentrations in the feed and the effluent of the reactors fed acetate (a,c,e) or propionate (b,d) with SRT decoupled (a,b,e) or coupled (c,d) to HRT. Panel (e) is an expansion (Day 88 to 120) of Panel (a) to visualize a period when the effluent residual phosphate concentrations were below the influent concentrations.*

High Residual Phosphate Value Corrections

The measured orthophosphate concentrations in the effluent of the reactors being higher than the influent concentrations were not plausible. The possible causes were investigated. The results of

the experimental investigation are all presented in Appendix B. Whilst the exact reason for the odd measurement of PO_4^{3-}-P in the reactors is yet to be determined, it was concluded that the bacterial biomass in the reactor was producing a compound interfering with the colourimetric assay, which caused the residual phosphate concentrations to be overestimated. It was hypothesized that the changing compositions of the microbial communities could provide possible explanations for this anomalous behaviour (Section 4.2).

4.2 Microbial Community Analysis

Biomass samples to determine the microbial community composition by 16S rRNA gene amplicon sequencing analysis were generally chosen at two points of each phase, one when the reactors reached a steady state, and the second, after the phase ended (Fig. 4.3(b),4.4(b)). During Phase 2, a third point was selected at Day 110 because it corresponded to a period when the effluent orthophosphate concentrations were not higher than the ones in the feed media as measured by the colourimetric assay. Thus, it was hypothesized that the biomass composition could be a factor in this observation.

4.2.1 Phase 1

Principal Coordinate Analysis (PCoA) was used to visualize the Bray-Curtis dissimilarities between communities developed at different reactor conditions from the beginning of the steady state (defined based on OD600 temporal stability) and the end of Phase 1 (Fig. 4.7). Acetate and

propionate addition to the growth medium gave rise to distinctly different communities, well separated along the PCoA1 axis (Fig. 4.7). While the acetate-fed microbial communities did not change much through the steady-state period as symbols representing communities at the beginning and the end of the Phase 1 steady-state period appear close to each other, propionate-fed communities drifted in the PCoA plot in a similar direction down the PCoA2 axis irrespective of the amount of phosphate added to the medium, indicating similar changes in the population profiles of the communities. These variations in ASV profiles were accompanied by the development of more diverse communities when the added VFA was propionate than when it was acetate as seen in Fig. 4.9 (c,d). All the acetate-fed reactors were enriched with more than 50% of *Rhodopseudomonas* whereas propionate-fed reactors saw a mix of genera from families *Rhodobacteraceae* and *Xanthobacteraceae*, as well as fermentative bacterial genera from the family *Dysgonomonadaceae*.

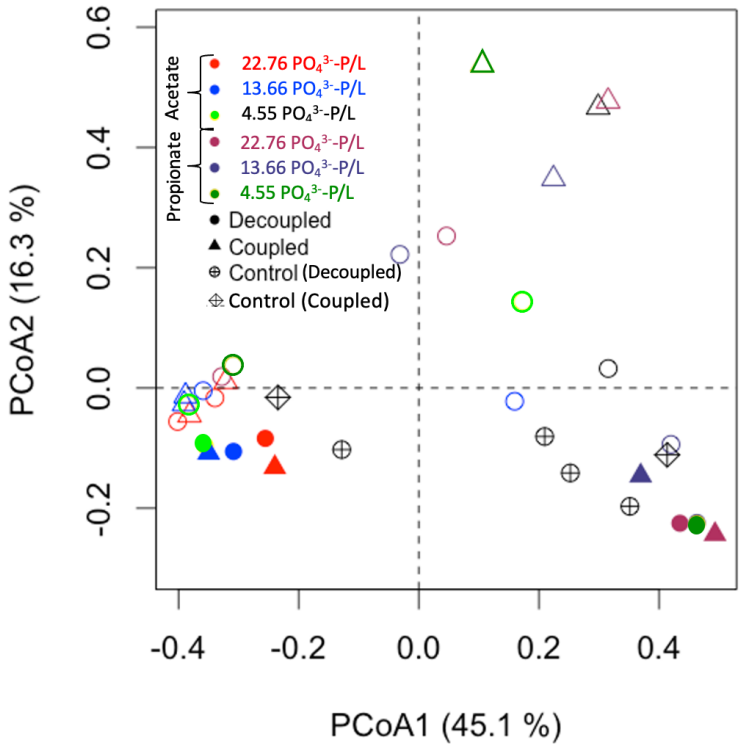

Figure 4.7: *Principal Coordinate Analysis visualizing the Bray-Curtis dissimilarities between communities present in the reactors during Phase 1. Colour legend corresponds to different VFA (acetate and propionate) and orthophosphate concentrations added to the feed media; control means no orthophosphate added. Coupled means SRT = HRT, Decoupled mean SRT > HRT. Solid symbols are samples from the beginning of the steady state (Day 24) and empty symbols are from the end of Phase 1 (Day 50).*

At the beginning of the steady-state period of Phase 1, the communities fed acetate comprised at least 78% of amplicon reads from the phylum *Proteobacteria*, whilst this proportion was only 60% (with 50% when no phosphate was added) with the remaining being reads mainly from *Firmicutes* or *Bacteroidetes* (Fig. 4.8(a)). The differences in the distribution of reads among phyla between the communities receiving acetate and propionate remained similar until the end of

Phase 1 (Fig. 4.8(b)). The majority of the proteobacterial reads were associated with the genera *Rhodopseudomonas* and *Rhodoplanes* belonging to the family *Xanthobacteriaceae*, and the genera *Rhodobacter* and unclassified ASVs both belonging to the family *Rhodobacteriaceae* (Fig. 4.13).

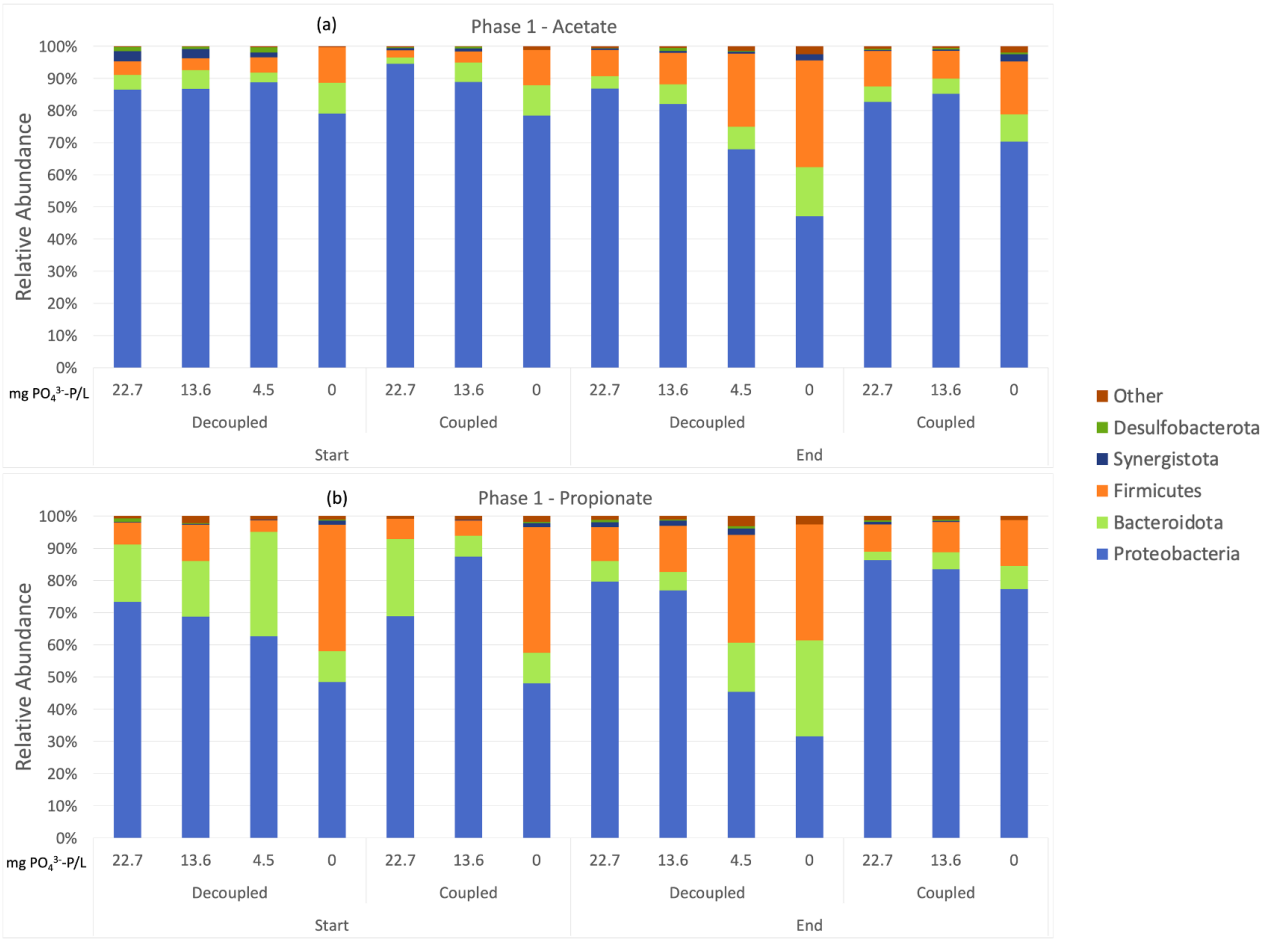

Figure 4.8: *Phyla of Phase 1. The microbial community at the start (Day 24) and the end of the phase (Day 50) for both decoupled and coupled reactors are plotted. Community in reactors fed by (a) acetate and (b) propionate show an abundance of Proteobacteria throughout the Phase for acetate more than propionate.*

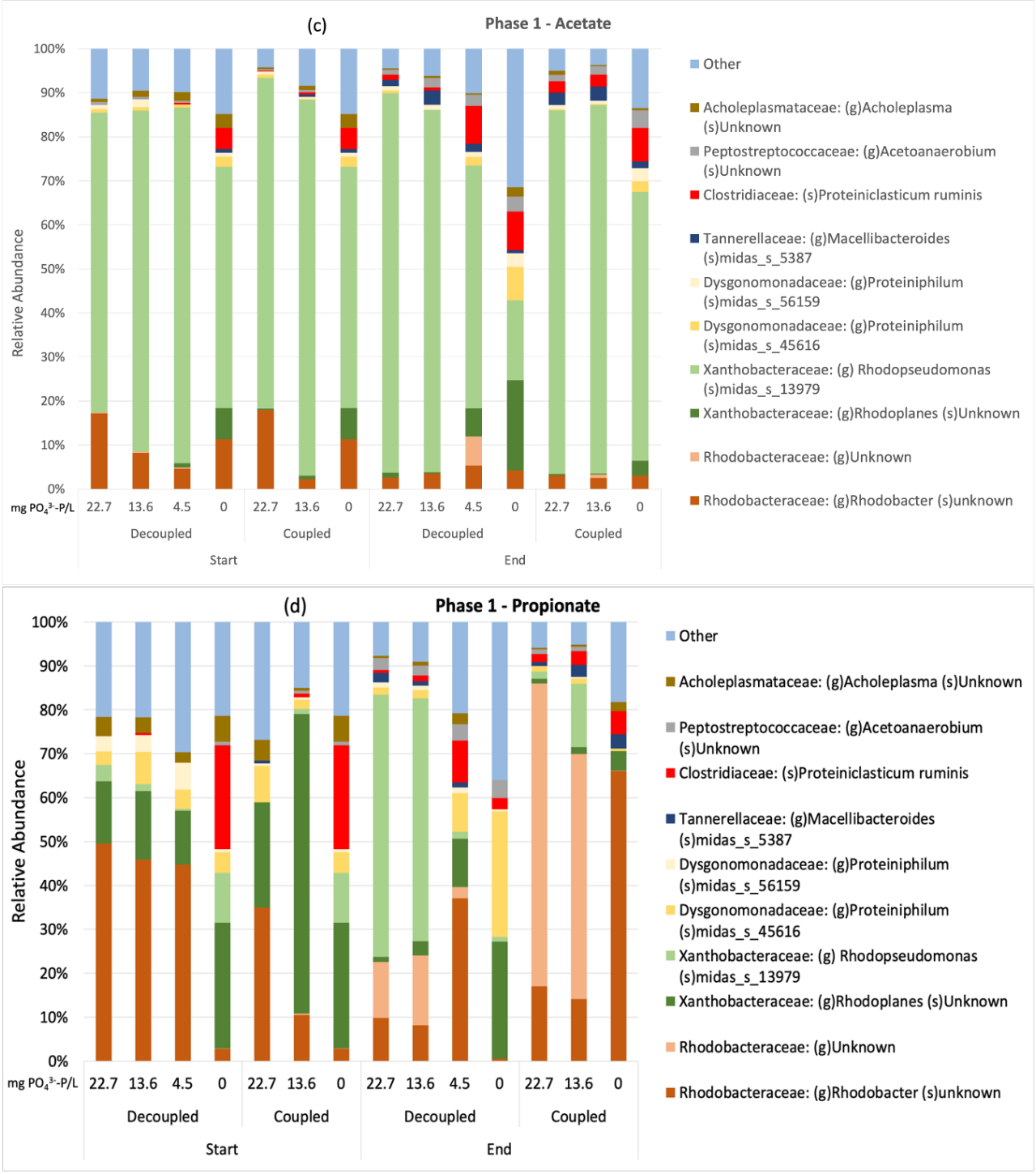

Figure 4.9: *The top 10 species from (c) acetate and (d) propionate of Phase 1. A change in the community can be seen in the decoupled and coupled propionate-fed reactors at the start (Day 24) and end (Day 50) of reactor operation. No major difference in the communities between the start and end of the reactor operation was seen in decoupled and coupled acetate-fed reactors.*

The significance of the impact of the manipulated experimental parameters was tested by redundancy analysis (RDA) (Fig. 4.10). The three parameters exerted a significant impact on the compositions of the communities. These differences appeared related to the composition of the PNSB populations. The main differences were due to the VFA fed to the photoreactors, with two genera within *Rhodobacteraceae* (one unclassified and the other one being *Rhodobacter* itself, to a lesser extent) being both in higher abundances when propionate was in the growth medium (Fig. 4.10 and 4.9). The coupling of SRT and HRT (decoupled vs. coupled) appeared to correlate with the proportions of *Rhodopseudomonas* (higher in reactors with decoupled SRT & HRT) and *Rhodobacter* (slightly higher in reactors with coupled HRT & SRT in corresponding phosphate concentrations) (Fig. 4.10 and 4.9). However, the reason for this impact is not clear because the accumulation of biofilms retained the biomass for a long time in both reactors. Finally, the abundances of the genus *Rhodoplanes* appeared to increase at low phosphate additions (Fig. 4.9(c)(d)).

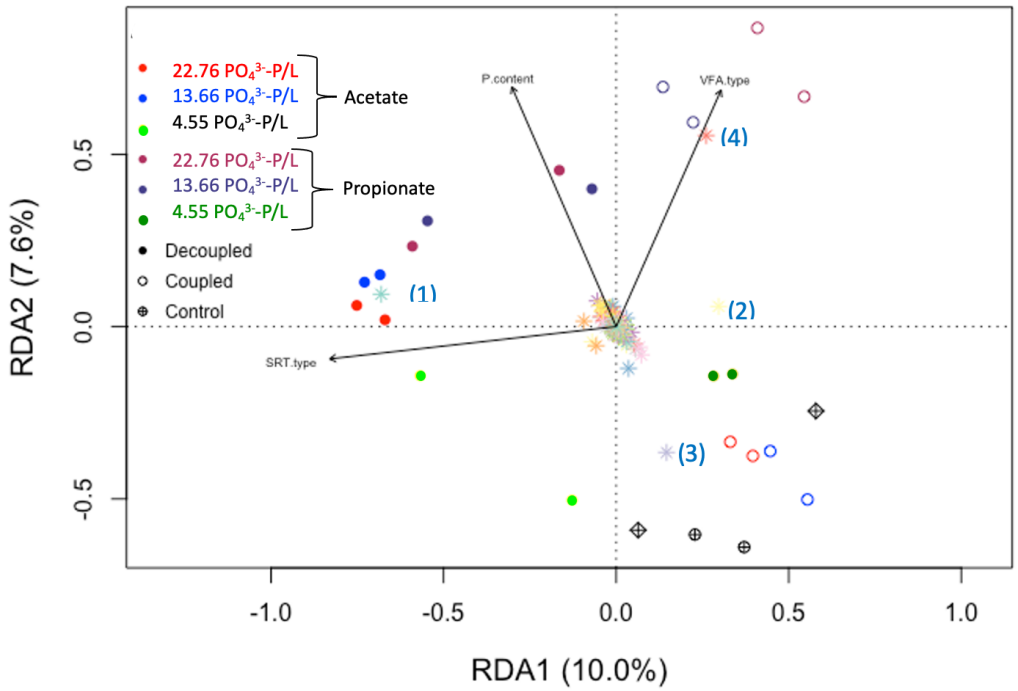

Figure 4.10: *Redundancy Analysis (RDA) of bacterial community compositions defined at the species level during Phase 1. Overall model p-value = 0.001. Explanatory variables were experimental design parameters: VFA-type (acetate or propionate) p-value = 0.004, SRT type (Decoupled or Coupled) p-value = 0.001, and added phosphate to influent (P content) p-value = 0.001. Axes p-value (RDA1=RDA2) = 0.001. The numbers next to star symbols are a specific genus projection: (1) Midas 13979 from Rhodopseudomonas, (2) Unknown species from Rhodobacter, (3) Unknown species from Rhodoplanes, (4) Unknown species of the family* Rhodobacteraceae. *Open and solids circles are from the beginning of the steady-state period (Day 24) and the end of Phase 1 (Day 50), respectively.*

4.2.2 Phase 2

Once regular cleaning of the tube walls was instituted to remove biofilms, the compositions of communities drifted away from their compositions at the end of Phase 1. By Day 78, the OD660

became more stable, which can be defined as the beginning of the Phase 2 steady-state period (Fig. 4.3(b), 4.4(b)); thus, a first series of Phase 2 biomass samples were chosen for 16S rRNA gene sequencing. Approximately a week after (i.e., by Day 92), the measured phosphate concentrations in the reactor effluents by colourimetric assay were found to be much lower than the measured concentrations in the influent (Fig. 4.6), as it should be expected. This lasted until approximately Day 110; this change in the behaviour of colourimetric phosphate measurements prompted the selection of the biomass samples of Day 110 to determine the community compositions. Finally, the phosphate concentrations remaining high in the effluents after Day 110, prompted the initiation of Phase 3 with yeast extract removed, and the biomass samples of Day 171 were chosen to be analyzed for the communities.

The PCoA visualizations of the Bray-Curtis dissimilarities between the communities in these 3 dates during Phase 2 revealed that at steady-state the communities in reactors fed acetate or propionate similarly changed in time as that in Phase 1 (Fig. 4.11). After achieving a steady state, operation between days 80-120 when the reactor showed low residual PO_4-P concentrations in the effluents of the reactors (Fig. 4.6), the microbial community compositions drifted along the PCoA2 axis from the south-west quadrant to the north-west one (Fig. 4.11). Nonetheless, in these clusters, a clear distinction remained between the communities between reactors with coupled and decoupled HRT & SRT. The community compositions changed considerably by the end of Phase 2, as they appeared on the right of PCoA1 opposite to the communities from earlier sampling points in Phase 2 (Fig. 4.11).

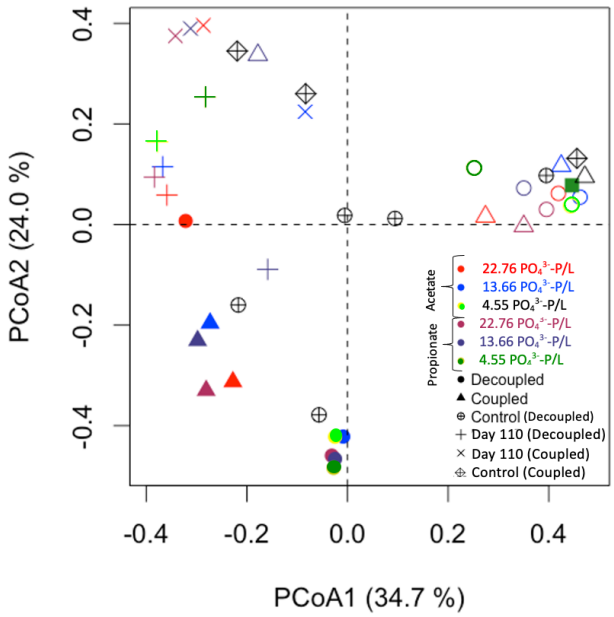

Figure 4.11: *Principal Coordinate Analysis visualizing the Bray-Curtis dissimilarities between communities present in the reactors during Phase 2. Colour legend corresponds to different VFA (acetate and propionate) and orthophosphate concentrations added to the feed media; control means no orthophosphate added. Coupled means SRT = HRT, Decoupled mean SRT > HRT. Solid symbols are samples from the beginning of the steady state (Day 80), crosses from (Day 110), and empty symbols from the end of Phase 2 (Day 171).*

The compositions of the communities sampled in the early days of Phase 2 were dominated by members of the phylum *Proteobacteria*, with populations of noticeable abundances from the phyla *Firmicutes* and the *Bacteroidota* (Fig. 4.12). However, by the end of Phase 2, the community composition revealed by the PCoA analysis (Fig. 4.11) was characterized by a sharp decrease of the abundances of *Proteobacteria* in almost all reactors and proportional increases of the two other phyla (Fig. 4.12).

The variations in community compositions between Day 78 (start of Phase 2 steady-state period)

and Day 110 visible on the PCoA plot (Fig. 4.11) were mainly due to changes in PNSB populations members of the *Proteobacteria* phylum. Generally, the main PNSB population in the reactor was a member of the *Xanthobacteraceae* family (either genera *Rhodoplanes*, *Rhodopseudomonas*, or two species unclassified at the genus level including Midas 40482). These populations were replaced by PNSB classified within the *Rhodobacteraceae* family (genus *Rhodobacter*, and another unclassified species) (4.13). This implies that PNSBs were successfully enriched up to Day 110.

The communities found in the reactors at the end of Phase 2 comprised lower relative abundances of PNSB (typically found to be the majority of the *Proteobacteria* phylum in the current study). Instead, the communities appeared to have become dominated by population that could be associated with fermentative organisms such as the genera *Proteiniphilum* (phylum *Bacteroidota*), *Proteiniclasticum* (phylum *Firmicutes*), and *Exeguobacterium* (phylum *Firmicutes*).

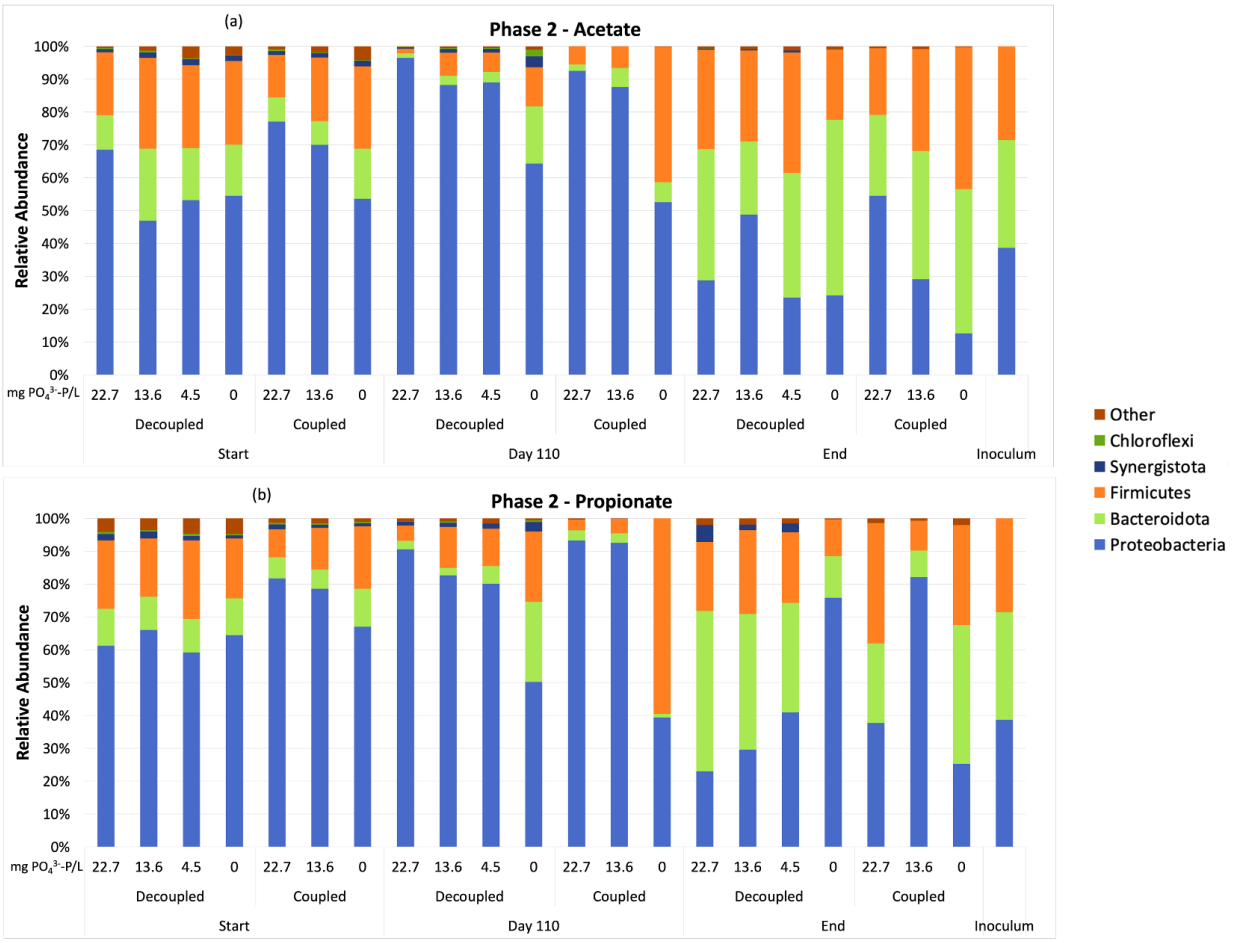

Figure 4.12: *Phyla in Phase 2. The* start (Day 78), Day 110 *and* end (Day 171) *are plotted. (a) Acetate and (b) propionate-fed reactor communities show a dynamic shift in the community composition. Proteobacteria abundance increases in the Day 80-120 window, which is replaced by Bacteroidota and Firmicutes by the* end *of reactor operation.*

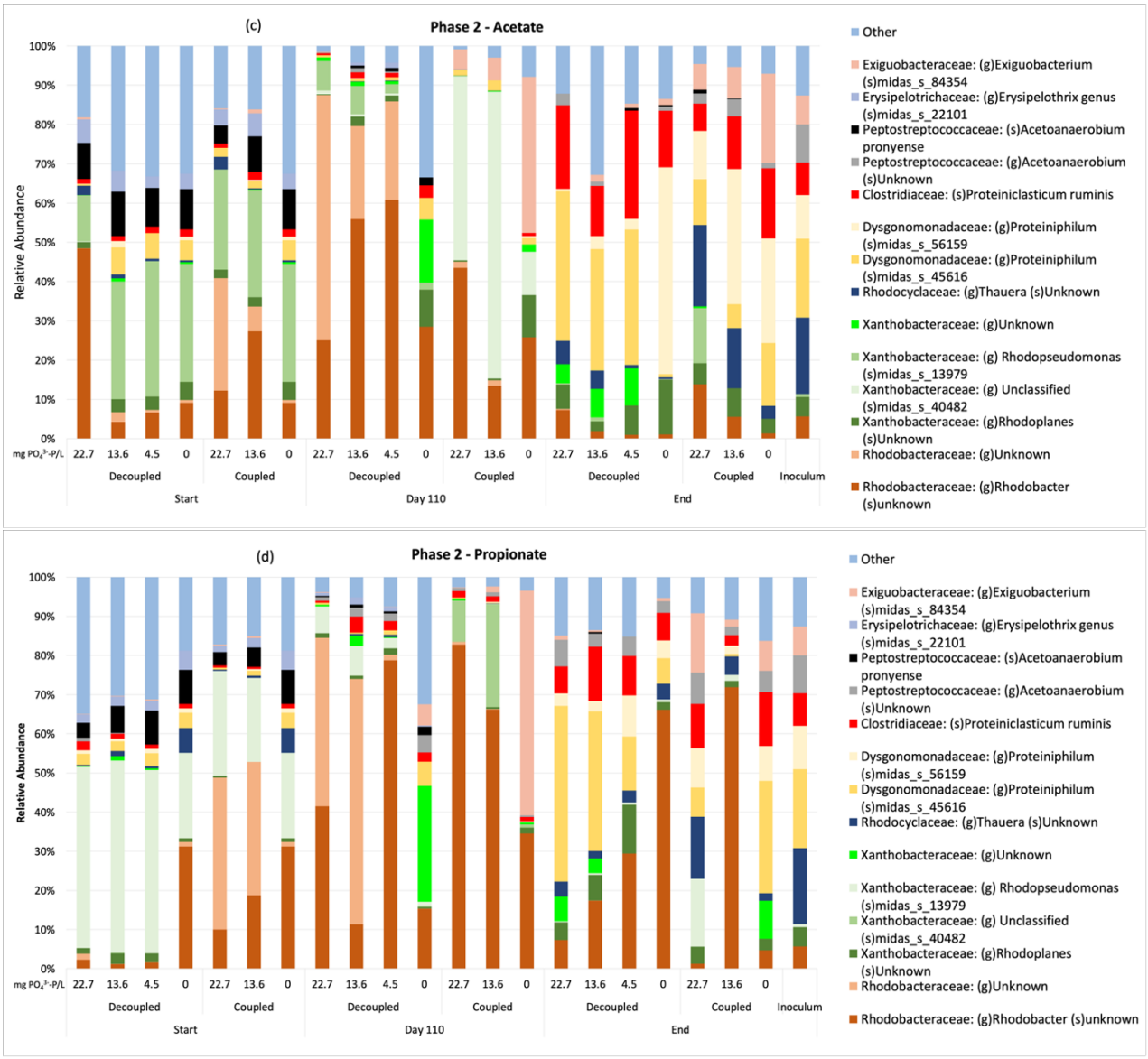

Figure 4.13: *The top 10 species from (c) acetate and (d) propionate of Phase 2. The change in the community can be seen across the start and end of reactor operation. A distinct difference in the community composition of decoupled and coupled systems was observed for Day 110.*

The significance of the experimental conditions on the variations in community compositions

through Phase 2 was also evaluated by redundancy analysis (RDA). The analysis was conducted for Days 110 and 171 together (including sampling time in the model) and separately (Fig. 4.14). As expected form the magnitude of changes observed above, the time of sampling (Day 110 or 171) was highly significant (Fig. 4.14(a)). Additionally, the SRT type was also significant in this analysis (Fig. 4.14(a)), as SRT and HRT coupling vs. decoupling appeared to have impacted both the PNSB and presumed fermentative populations similarly on the two sampling days. For PNSB populations, long SRT (i.e., low net average growth rate) due to decoupling from HRT led to higher abundances of the family *Rhodobacteriaceae* (both the genus *Rhodobacter* and an unclassified population), whilst some *Xanthobacteriaceae* (Midas 40482 and *Rhodopseudomonas*) populations were somewhat more abundant at low SRT coupled with HRT (4.13). For presumed fermentative populations, long SRT (decoupled) led to higher abundances of the population Midas 45616 of the genus *Proteiniphylum* (phylum *Bacteroidota*), whilst short SRT (coupled) led to higher relative abundances of the populations *Thauera* (phylum *Proteobacteria*), Midas 56159 of the genus *Proteiniphylum*, and *Exeguobacterium* (phylum *Firmicutes*).

On close inspection of the RDA results, the added concentrations of phosphate to the feed media were the second most significant model parameters for Days 110 and 171 (Fig. 4.14(b, c)). The main differences are between the control (i.e., no phosphate added to feed) reactors and the others. For Day 110, the relative abundances of PNSB populations (both *Rhodobacteriaceae* and *Xanthobacteraceae* related populations; Fig. 4.14(b), points (4) and (6), respectively) were markedly lower when no phosphate was added to the influent (4.13). Opposingly, the Midas 84354 from *Exiguobacter* genus (Fig. 4.14(b), point (10)) showed higher relative abundances when no

phosphate was added to the feed, especially in reactors with coupled SRT & HRT (4.13).

For Day 171, the observations with respect to phosphate addition to the influent remained largely similar from the *Exiguobacter* genus population (4.13). For the other presumptive fermentative populations, the *Thauera* genus was found to be much lower in relative abundances when phosphate was not added to the feed. At the same time, there is a slight effect on the two *Proteiniphylum* populations with Midas 45616 being more abundant when phosphate was added to the feed and Midas 56159 being more abundant when it was not (4.13).

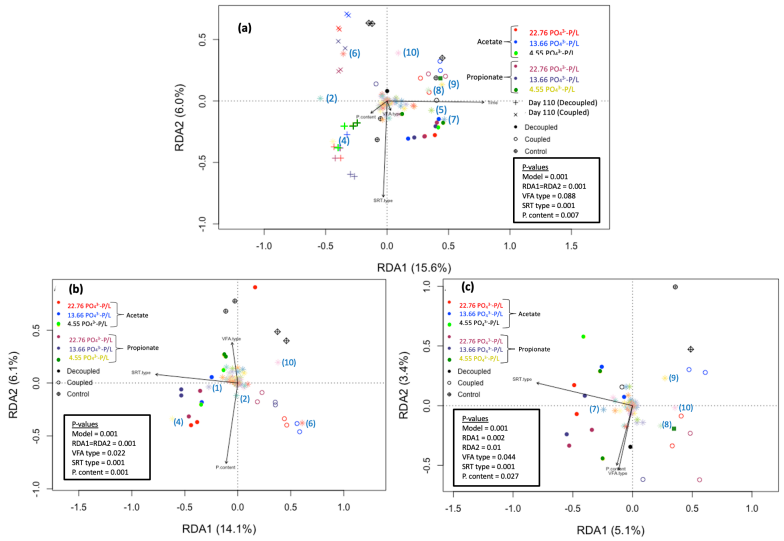

Figure 4.14: *Redundancy Analysis (RDA) of bacterial community compositions defined at the species level during Phase 2. The p-values of the model, explanatory variables, and axes are mentioned in the figures. (a) RDA for biomass from both Day 110 and the end of Phase 2 (Day 171). The time axis is an additional explanatory variable (p=0.001); (b) RDA for biomass from Day 110 (c) RDA for biomass from the end of Phase 2 (Day 171). The numbers next to star symbols are a specific genus projection: (1) Midas 13979 from Rhodopseudomonas (b), (2) unknown species of Rhodobacter (a,b), (4) unknown species of the family Rhodobacteraceae (a,b), (5) Proteiniclasticum ruminis (a), (6) Midas 40482 from the Xanthobacteraceae family (a,b), (7) Midas 45616 from Proteiniphilum genus (a,c), (8) unknown species from Thauera (a,c), (9) Midas 56159 from Proteiniphilum (a,c), (10) Midas 84354 from Exiguobacterium (a,c). Solid symbols are from the beginning of the steady-state period and the open symbols are from the end of Phase 1. The Day 110 reactors are denoted by plus and cross symbols.*

4.2.3 Phase 3

During Phase 3, biofilm was removed from the reactors and no yeast extract was supplied in the feed media. The PCoA of the community compositions at the beginning and end of the steady-state period revealed distinct communities for acetate-fed and propionate-fed reactors (separated along the PCoA1 axis; Fig. 4.15). In the PCoA plot, phosphate addition to the feed and the SRT type did not appear to influence the community structures markedly. Nonetheless, the community compositions in the majority of the reactors drifted towards the upper-left between Day 201 and Day 230 as visualized in the PCoA plot (Fig. 4.15).

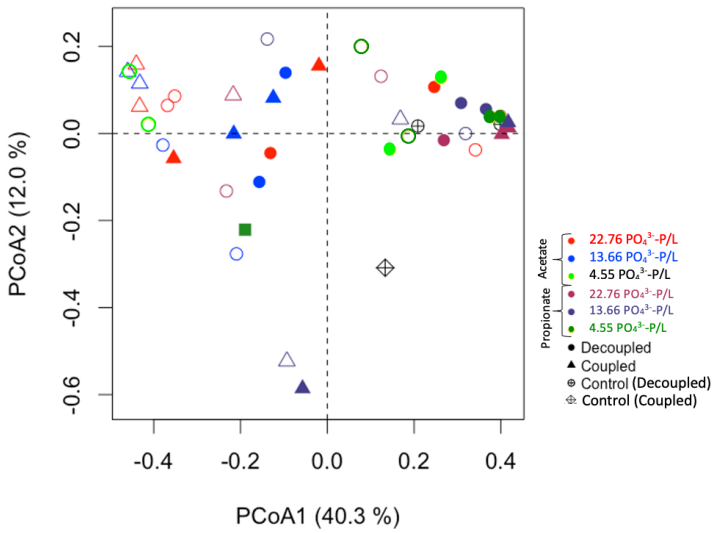

Figure 4.15: *Principal Coordinate Analysis visualizing the Bray-Curtis dissimilarities between communities present in the reactors during Phase 3. Colour legend corresponds to different VFA (acetate and propionate) and orthophosphate concentrations added to the feed media; control means no orthophosphate added. The control from the start of the Phase is shown. No biomass was present in the control at the end of Phase 3. Coupled means SRT = HRT, Decoupled means SRT > HRT. Solid symbols are samples from the beginning of the steady state (Day 201), and open symbols are from the end of Phase 3 (Day 230).*

Although a fresh inoculum (composed of a mixture of biomass from all reactors of Phase 1) and new reactor vessels were used for this phase, a similar trend as in Phase 2 was observed in the variations in the community structures. While *Proteobacteria* constituted more than 80% of the community at the beginning of the steady-state period (Day 201), the drift in community structures observed in the PCoA visualization is explained by a sharp decrease in the relative abundances *Proteobacteria* (as in previous phases dominated by *Rhodobactereaceae*-related and *Xanthobacteriaceae*-related PNSB populations; Fig. 4.17) to well below 80% in most reactors and reaching as low as 28% in reactors with decoupled SRT & HRT and receiving acetate in the feed (Fig. 4.16). Like in Phase 2, *Bacteroidota* and *Firmicutes* reached together between 30% and 70% of the communities at the end of the Phase 3 steady-state period (Day 230, Fig. 4.16). In Phase 3, the main population members of the two presumptive fermentative phyla were members of the genera *Proteiniclasticum* (phylum *Firmicutes*) and *Proteiniphilum* (two populations: Midas 45616 and 56159; phylum *Bacteroidota*), and *Thauera* (phylum *Proteobacteria*; Fig. 4.17).

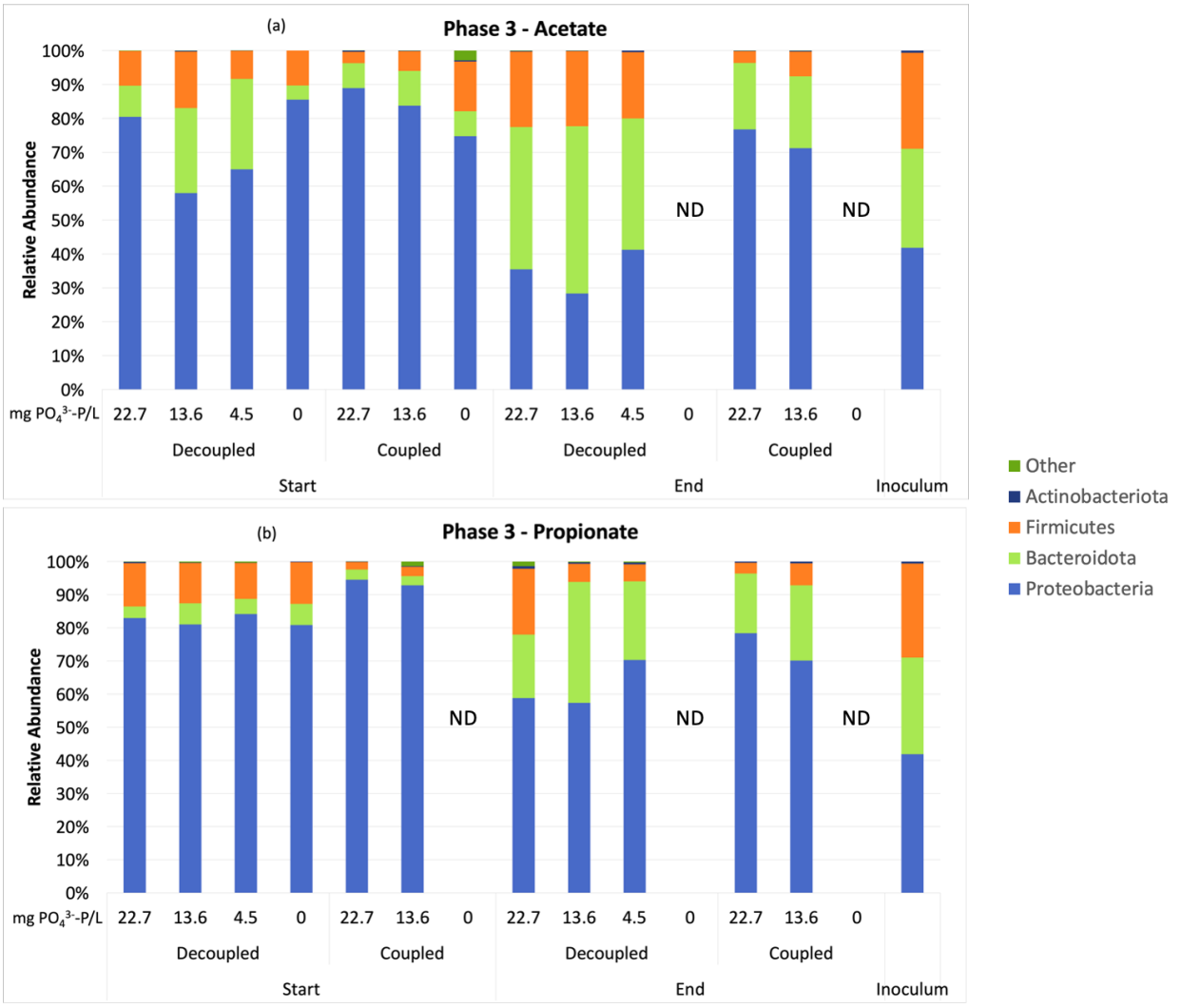

Figure 4.16: *Phyla of Phase 3. The microbial community at the start and the end of the reactor phase are plotted in the diagram, separated by the red dotted line. Acetate and propionate-fed reactors are separated by the black dashed lines. There is a shift in the abundance of Proteobacteria by the end of the phase with an abundance of Bacteroidota. ND = Not Detected due to biomass washout or depletion.*

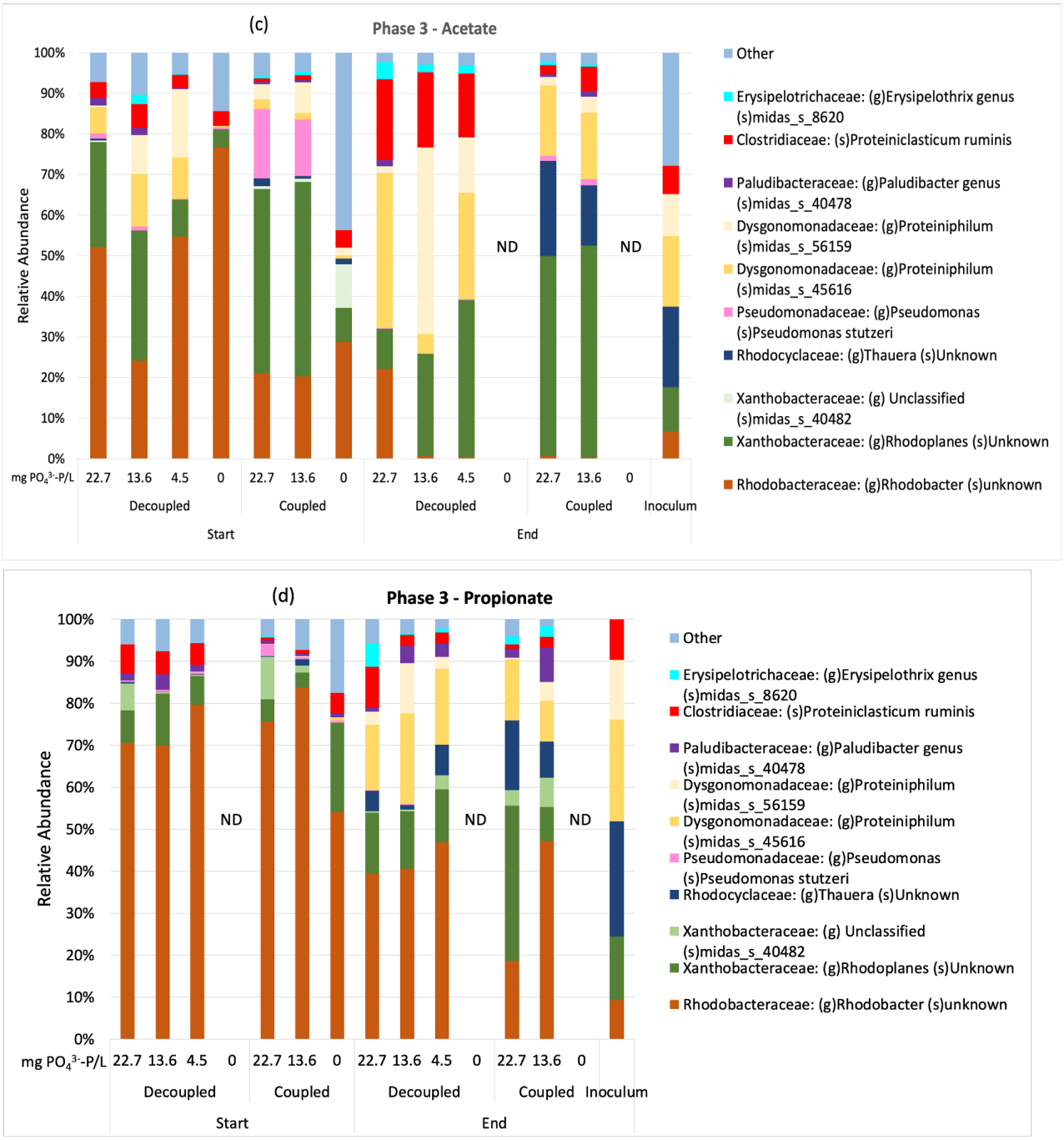

Figure 4.17: *The top 10 species from acetate (a) and propionate (b) of Phase 3. The change in the community can be seen at the start and end of the reactor operation. There is a shift in communities from PNSBs to fermentors. No difference is seen between decoupled and coupled reactors.*

When the experimental factors were tested for their significance in affecting the community compositions by RDA performed on data at the end (Day 230) of Phase 3, the VFA in the feed medium was the only significant factor, although the SRT type showed some tendency to significance (p-value = 0.065; Fig. 4.18). With respect to PNSB, propionate in the feed led to higher relative abundances of *Rhodobacter* (Fig. 4.18, point(2)), whilst acetate in the feed supported higher abundances of Rhodoplanes (Fig. 4.18, point(3); Fig. 4.17). For the presumptive fermentative bacteria, *Thauera* were at slightly higher abundances when propionate was the carbon and electron source (Fig. 4.18, point(8)), whilst *Proteiniphilum* (Fig. 4.18, point (9)) and *Proteiniclasticum* (Fig. 4.18, point(5)) were at higher abundances in acetate-fed reactors (Fig. 4.17).

4.3 Fluorescent Visualization

4.3.1 DAPI for Polyphosphate Visualization

One of the objectives of this thesis was to evaluate the impact of operation parameters on the P uptake and accumulation by PNSB. Despite the difficulties in quantifying the orthophosphate residual concentrations, they were similar in all conditions that received the same phosphate additions to the feed media except at some exceptional times (e.g., Day 78 to 110 in Phase 2). Nonetheless, the question remained about the possible storage of P, likely in the form of polyphosphate (polyP). DAPI has been used for the quantification of polyP without the interference of DNA (Aschar-Sobbi et al., 2008). On staining with DAPI, the blue fluorescence indicated the enrichment of bacteria, and the pink fluorescence (Fig 4.19) was visible

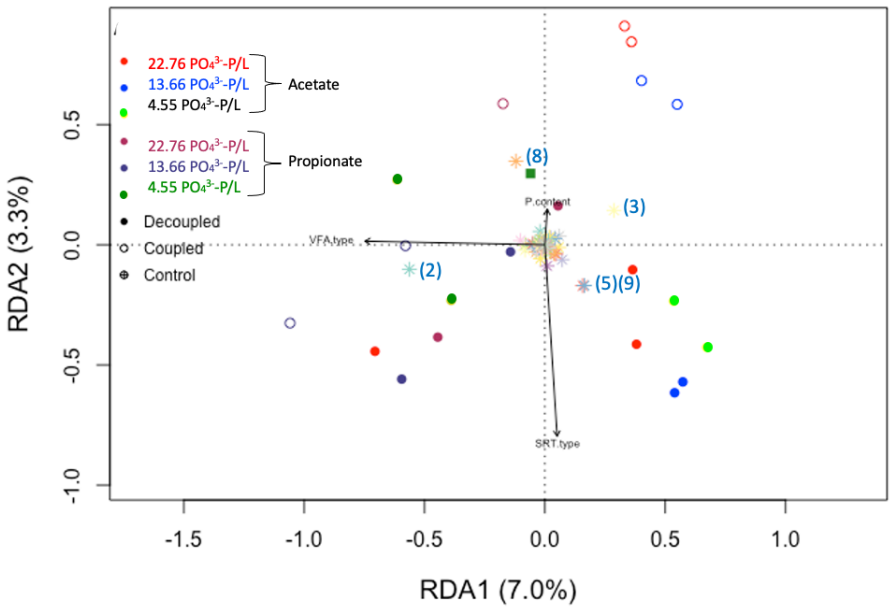

Figure 4.18: *Redundancy Analysis (RDA) of bacterial community compositions defined at the species level during Phase 3. Overall model p-value = 0.004. Explanatory variables were experimental design parameters: VFA-type (acetate[low] or propionate[high]) p-value = 0.006, SRT type (Decoupled or Coupled) p-value = 0.065, and added phosphate to influent (P content) p-value = 0.242. Axes p-value RDA1 = 0.033; RDA2 = 0.188. The numbers next to star symbols are a specific genus projection: (2) Rhodobacter, (3) Rhodoplanes, (5) Proteiniclasticum ruminis (8) Thauera, (9) Proteiniphilum. Open and solids circles are from the beginning of the steady-state period and the end of Phase 2, respectively.*

intracellularly which might indicate the presence of polyP. Decoupled reactors - high-P in influent (a), low-P in influent (b), and coupled reactors high-P in influent (c) did not differ in their fluorescence of polyP.

Three samples were chosen for discussion as representative of typical observations under widespread conditions. Acetate-fed decoupled reactors with high phosphate addition (Fig. 4.19 (a)) and low phosphate addition in the influent (Fig. 4.19 (b)) showed the presence of polyP. The biomass in the acetate-fed coupled reactors with 22.7 mg PO_4^{3-}/L in the influent were similar to the other two fluorescent images. As Terashima et al. (2020) note, the fluorescence from lipids faded rapidly as opposed to polyP, which indicated that some polyP accumulation was achieved within the cultured biomass.

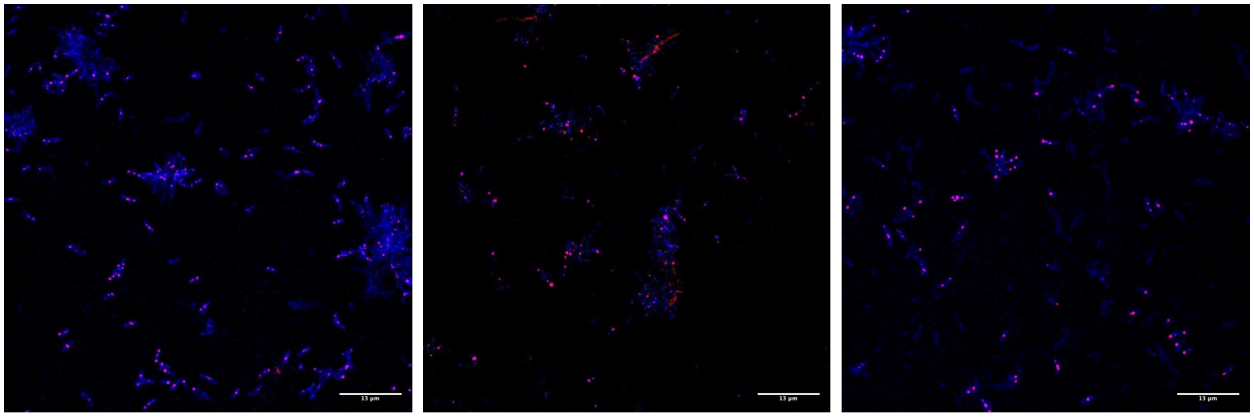

Figure 4.19: *DAPI stained cells. The nucleus of the cells emitted a blue fluorescence which is an indicator of the enrichment of bacteria. The pink fluorescence was visible intracellularly indicating the presence of polyP. Biomass from acetate-fed reactors was sampled. Decoupled reactors with (a) 22.7 mg PO_4^{3-}/L in influent, (b) 4.5 mg PO_4^{3-}/L in influent, and (c) coupled reactors with 22.7 mg PO_4^{3-}/L in influent showed fluorescence by polyP and nucleus.*

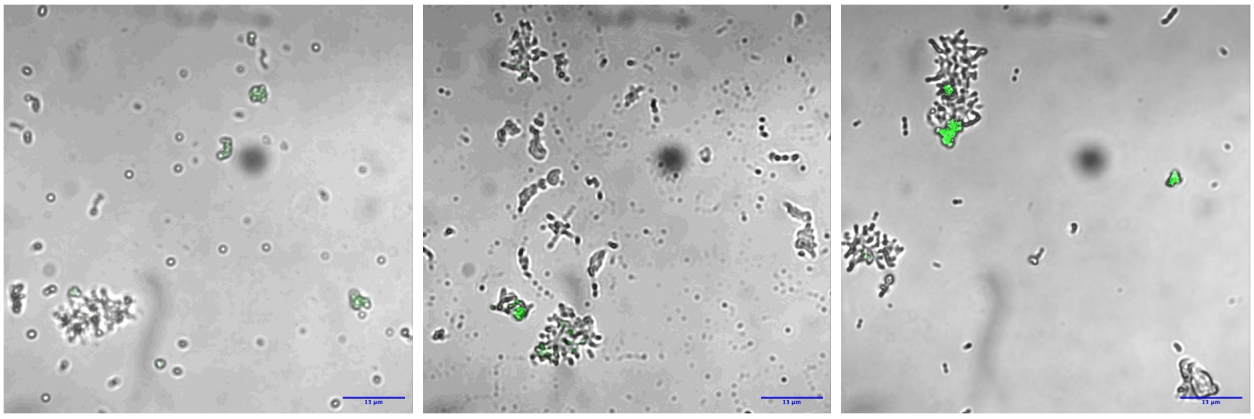

Figure 4.20: *LP2 stained cells. The black dots are the biomass visualised. The green fluorescence might be because of PHAs staining in the biomass. Acetate-fed decoupled reactors with (a) 22.7 mg PO_4^{3-}/L, and (b) 4.5 mg PO_4^{3-}/L in the influent are shown against a (c) propionate-fed, decoupled reactor with 13.6 mg PO_4^{3-}/L in the influent.*

4.3.2 LP2 for Polyhydroxyalkanoate Visualization

PNSBs can store carbon in the form of polyhydroxyalkanoates as described in the Literature Review. Apart from the defined objectives it was of interest to know if the enriched PNSBs in this experiment accumulated PHAs. Lipid-Green 2 (LP2) stains polyhydroxyalkanoates (PHAs) and emits fluorescence indicating the presence (Higuchi-Takeuchi et al., 2016; Kettner and Griehl, 2020). Selected acetate and propionate-fed reactors were chosen for LP2 staining as all the reactors did not produce a detectable fluorescence. For the biomass accumulated in the reactors, the LP2 stained some cells especially those present in clusters, which might indicate some PHAs accumulation. However, there was no clear fluorescence from individual cells to draw any conclusion (Fig. 4.20).

References

Aschar-Sobbi, R., Abramov, A.Y., Diao, C., Kargacin, M.E., Kargacin, G.J., French, R.J., Pavlov, E., 2008. High sensitivity, quantitative measurements of polyphosphate using a new dapi-based approach. Journal of Fluorescence 18, 859–866. doi:10.1007/s10895-008-0315-4.

Higuchi-Takeuchi, M., Morisaki, K., Toyooka, K., Numata, K., 2016. Synthesis of high-molecular-weight polyhydroxyalkanoates by marine photosynthetic purple bacteria. PLoS One 11, e0160981. doi:10.1371/journal.pone.0160981.

Kettner, A., Griehl, C., 2020. The use of lipidgreen2 for visualization and quantification of intracellular poly(3-hydroxybutyrate) in cupriavidus necator. Biochemistry and Biophysics Reports 24, 100819. doi:https://doi.org/10.1016/j.bbrep.2020.100819.

Terashima, M., Kamagata, Y., Kato, S., 2020. Rapid enrichment and isolation of polyphosphate-accumulating organisms through 4'6-diamidino-2-phenylindole (dapi) staining with fluorescence-activated cell sorting (facs). Front Microbiol 11, 793. doi:10.3389/fmicb.2020.00793.

Chapter 5

Discussion

5.1 Enrichment of PNSBs and the Emergence of Fermenters

Throughout the reactor operation of 232 days, the bacterial community changed dynamically. PNSB's ability to grow anaerobically and phototrophically under infrared radiation was utilized for its enrichment in anaerobic reactors. The reactor setup with IR lamps enriched for purple bacteria at the beginning of all the phases. The quantification of the biomass was done through OD and VSS measurements that showed biomass enrichments similar to that found by Cerruti et al. (2020) for biomass grown at similar SRTs and illuminated with similar light. The biomass enrichment measured through OD_{660} was higher in the reactors of this experiment than that obtained by Hülsen et al. (2014), who used real settled wastewater to enrich for purple bacteria. These two

experiments were considered for comparison as they successfully enrich PNSBs. The development of the deep red colour of the cultures and the absorbance of light at 805 and 870 nm are characteristics of PPB bacteria (Fig. 2.1) (Madigan et al., 2018). The OD_{870}/OD_{660} ratio indicated that a high proportion of the microbial community was rich in BChl *a* containing microorganisms. This high ratio of the OD_{870}/OD_{660} ratio was maintained in the reactors throughout all the phases, which could indicate a consistent presence of PNSBs within the reactors.

In Phase 1, it was likely that the presence of biofilm enabled the emergence and maintenance of PPB population in the reactors. An experiment by Shaikh et al. (2023) gave rise to protein-rich biomass consisting of PNSBs through biofilm formation in nutrient-sufficient conditions. They observed no PNSB enrichment in the form of a biofilm when the influent was P-deficient. Further, Capson-Tojo et al. (2023) conducted a systematic study of suspended vs. attached PNSBs grown in an outdoor flat plate reactor and found that a higher relative abundance of PPB, and a higher enrichment of biomass in general, was achieved in the biofilms than the suspended solution (Capson-Tojo et al., 2023). This could be observed through the VSS values that were the highest in Phase 1 compared to the other phases. Further, more than 60% of cumulative relative abundance of *Rhodopseudomonas*, *Rhodoplanes*, *Rhodobacter*, and other unclassified PNSB related *Rhodobacteraceae* and *Xanthomonaceae* populations were enriched in all the reactors in this experiment (Fig. 4.9). Thus confirming the positive enrichment of PNSBs.

By Phase 2, a drop in the total VSS was observed which could be due to the removal of biofilm that could have been contributing to more substrate through its decay due to higher retention time (Rittmann and McCarty, 2012). The reduction in the OD_{870}/OD_{660} ratio could be explained by

the top 10 species in Phase 2 (Fig. 4.13), which saw the relative abundance of PNSBs fall from 50-80% to 30%. In Phase 3, the lowest amount of VSS was detected, which could be due to the removal of yeast extract that was contributing to cell growth (Morsy et al., 2019).

It was interesting to note that although the VSS reduced from Phase 1 to Phase 3, in terms of operation, the residual sCOD reached a value of almost zero in all the reactors by the time Phase 3 was reached. It is possible that in Phase 1 the decay of the biofilm microbes and a subsequent release of the soluble microbial products from their consumption by other microorganisms could have led to the increase in the residual sCOD in the system (Rittmann and McCarty, 2012). Further, in Phase 2, the yeast extract could have acted as an additional source of sCOD due to its carbon content (Sparviero et al., 2023). By the time Phase 3 was reached, these additional sources of sCOD that were contributing to its measurement were removed and hence the residual sCOD reached zero.

The high percentage of relative abundance of fermenters was a recurring phenomenon at the end of all three phases of reactor operation. The community went from a high abundance of PNSB-related populations (70 to 90%) to almost 60% *Proteiniphilum* in Phase 3. Two possible causes may be i) attenuation of light in the bulk of decoupled reactor (Capson-Tojo et al., 2022); and (ii) natural reactor instability (He et al., 2017; Maus et al., 2020) as indicated by the growth of *Proteiniphilum*. *Proteiniphilum* is an obligately anaerobic, chemoorganotrophic, proteolytic organism known for producing acetic acid and propionic acid from yeast extract (Trujillo et al., 2015). Since no external source of protein was fed to the reactor, the high enrichment of protein-rich PNSBs (Alloul et al., 2019; Hülsen et al., 2022; Wang et al., 2021) in all the reactors across the phases could have led to their decay and subsequent scavenging by *Proteiniphilum*. The decrease in PNSB biomass

by the end of each phase may be due to adjustments made by the microbial community in the new conditions created by stepwise removal of biofilm and yeast extract in Phase 2 and Phase 3 respectively (Sepúlveda-Muñoz et al., 2022). An alkaline environment developed in the reactor within 24 hours (Fig. A.6) could have encouraged the growth of *Proteiniphilum* (Wang et al., 2021). The presence of *Proteiniphilum* has been associated with process failure in food waste digesters due to high oil, salt, or protein conditions (He et al., 2017). An increase in OLR conditions gives rise to fermenters (Khafipour et al., 2020; Maus et al., 2020). Almeida et al. (2021) saw that an upsurge of sugars (glucose and fructose) in the influent caused acidification and subsequent decrease in biomass due to decay giving rise to fermenters in stage 2 of their reactor operation. Therefore, an OLR imbalance could be a possibility for Phase 1 and 2 as the biofilm and yeast extract were sources of carbon, but not for Phase 3.

5.2 P-uptake and PNSB enrichment between Day 88-110 of Phase 2

Throughout all the phases, decoupling SRT-HRT directly enriched different populations of PPB. It was seen through the RDA plots (Fig. 4.10, 4.14, 4.18) that a significant difference in the community compositions was achieved by decoupling SRT-HRT. Studies have been conducted to utilize the effect of decoupling SRT and HRT on changing the microscopic-microalgal morphology (Zhang et al., 2021), selection of cyanobacteria (Arias et al., 2019), nutrient removal, and algal enrichment (Solmaz and Isik, 2019; Xu et al., 2015). Cerruti et al. (2020) mentioned that the

decoupling of reactors had a positive impact on PPB enrichments. In addition to achieving PNSB enrichment, it was shown that different populations could be enriched.

In Phase 2, the distinction between the communities of decoupled and coupled reactors is significant. Further, the PNSB community was able to take up phosphate and leave a residue well below the phosphate fed. This may be attributed to a change in the lamps carried out to address technical problems in the beginning of Phase 2. The sudden change in the intensity and positioning of lamp could have acted as a stressor to induce such a behaviour within the PNSBs. An increase in light intensity up to an optimum level has a favourable effect on P-removal by purple bacteria (Liang et al., 2010; Liu et al., 2019). A simultaneous change in the light path due to the repositioning of the lamp could have an effect on P-uptake behaviour (González-Camejo et al., 2020). Similar to the P-uptake and transformation between inorganic and organic phosphorus seen in *Scenedesmus*, extracellular and intracellular polymeric substances from PNSBs may have an effect on its P-uptake behaviour (Wu et al., 2021). However, although the light path and intensity were not disturbed afterwards, the residual PO_4^{3-}-P reverted to its earlier behaviour as seen in Phase 1, reaching values over that present in the feed.

5.3 Effect of P-concentration and VFA in the feed on the microbial community

Feeding 3 different phosphate concentrations up to 22.7 mg PO_4^{3-}/L did not have any effect on the microbial community. It was seen in the RDA plots that the P-content was perhaps not a

significant explanatory variable for Phase 2 and 3, except for Day 88-110. While the low P-content were supposed to induce some P-limitation in the reactors affecting the microbial community, no significant effect was observed. Shaikh et al. (2023) carried out an experiment with P-limitation showing its effect on biofilm formation, and confirming the enrichment alone.

In all the reactors, the PNSBs showed higher abundance when propionate was in the feed instead of acetate. In Phase 1, it was observed that *Rhodopseudomonas* showed high abundance in acetate-fed reactors, which has been found earlier (Cerruti et al., 2020; Okubo and Hiraishi, 2007). However, statistically, the VFA was the least significant parameter when the RDAs were scrutinized for the end of Phase 2 and all of Phase 3, although a comparatively higher abundance of PNSBs was found in propionate reactors compared to acetate reactors (Fig. 4.13, 4.17).

The experiments carried out for this thesis had their limitations. Firstly, the formation of biofilm and the addition of yeast extract influenced the concentration of PO_4^{3-}-P in the feed, but it was addressed in Phase 3. Secondly, the higher values of residual PO_4^{3-}-P were unexpected and were addressed through several corrective tests (Appendix B). However, promising results were obtained in terms of PNSB enrichment at the beginning of each of the phases and selective microbial communities with decoupled SRT-HRT.

References

Alloul, A., Wuyts, S., Lebeer, S., Vlaeminck, S.E., 2019. Volatile fatty acids impacting phototrophic growth kinetics of purple bacteria: Paving the way for protein production on fermented wastewater. Water Research 152, 138–147. doi:https://doi.org/10.1016/j.watres.2018.

12.025.

Almeida, J.R., Serrano, E., Fernandez, M., Fradinho, J.C., Oehmen, A., Reis, M.A.M., 2021. Polyhydroxyalkanoates production from fermented domestic wastewater using phototrophic mixed cultures. Water Research 197, 117101. doi:https://doi.org/10.1016/j.watres.2021.117101.

Arias, D.M., Rueda, E., García-Galán, M.J., Uggetti, E., García, J., 2019. Selection of cyanobacteria over green algae in a photo-sequencing batch bioreactor fed with wastewater. Science of The Total Environment 653, 485–495. doi:https://doi.org/10.1016/j.scitotenv.2018.10.342.

Capson-Tojo, G., Batstone, D.J., Grassino, M., Hülsen, T., 2022. Light attenuation in enriched purple phototrophic bacteria cultures: Implications for modelling and reactor design. Water Research 219, 118572. doi:https://doi.org/10.1016/j.watres.2022.118572.

Capson-Tojo, G., Zuo Meng Gan, A., Ledezma, P., Batstone, D.J., Hülsen, T., 2023. Resource recovery using enriched purple phototrophic bacteria in an outdoor flat plate photobioreactor: Suspended vs. attached growth. Bioresource Technology 373, 128709. doi:https://doi.org/10.1016/j.biortech.2023.128709.

Cerruti, M., Stevens, B., Ebrahimi, S., Alloul, A., Vlaeminck, S.E., Weissbrodt, D.G., 2020. Enrichment and aggregation of purple non-sulfur bacteria in a mixed-culture sequencing-batch photobioreactor for biological nutrient removal from wastewater. Frontiers in Bioengineering and Biotechnology 8. doi:10.3389/fbioe.2020.557234.

González-Camejo, J., Aparicio, S., Jiménez-Benítez, A., Pachés, M., Ruano, M.V., Borrás, L., Barat, R., Seco, A., 2020. Improving membrane photobioreactor performance by reducing light path: operating conditions and key performance indicators. Water Research 172, 115518. doi:https://doi.org/10.1016/j.watres.2020.115518.

He, Q., Li, L., Peng, X., 2017. Early warning indicators and microbial mechanisms for process failure due to organic overloading in food waste digesters. Journal of Environmental Engineering 143, 04017077. doi:doi:10.1061/(ASCE)EE.1943-7870.0001280.

Hülsen, T., Barnes, A.C., Batstone, D.J., Capson-Tojo, G., 2022. Creating value from purple phototrophic bacteria via single-cell protein production. Current Opinion in Biotechnology 76, 102726. doi:https://doi.org/10.1016/j.copbio.2022.102726.

Hülsen, T., Batstone, D.J., Keller, J., 2014. Phototrophic bacteria for nutrient recovery from domestic wastewater. Water Research 50, 18–26. doi:https://doi.org/10.1016/j.watres.2013.10.051.

Khafipour, A., Jordaan, E.M., Flores-Orozco, D., Khafipour, E., Levin, D.B., Sparling, R., Cicek, N., 2020. Response of microbial community to induced failure of anaerobic digesters through overloading with propionic acid followed by process recovery. Frontiers in Bioengineering and Biotechnology 8. doi:10.3389/fbioe.2020.604838.

Liang, C.M., Hung, C.H., Hsu, S.C., Yeh, I.C., 2010. Purple nonsulfur bacteria diversity in activated sludge and its potential phosphorus-accumulating ability under different cultivation conditions. Applied Microbiology and Biotechnology 86, 709–719. doi:10.1007/s00253-009-2348-2.

Liu, S., Daigger, G.T., Kang, J., Zhang, G., 2019. Effects of light intensity and photoperiod on pigments production and corresponding key gene expression of rhodopseudomonas palustris in a photobioreactor system. Bioresource Technology 294, 122172. doi:https://doi.org/10.1016/j.biortech.2019.122172.

Madigan, M.T., Bender, K.S., Buckley, D.H., Sattley, W.M., Stahl, D.A., 2018. Brock biology of microorganisms. Fifteenth edition. ed., Pearson, NY, NY.

Maus, I., Tubbesing, T., Wibberg, D., Heyer, R., Hassa, J., Tomazetto, G., Huang, L., Bunk, B., Spröer, C., Benndorf, D., Zverlov, V., Pühler, A., Klocke, M., Sczyrba, A., Schlüter, A., 2020. The role of petrimonas mucosa ing2-e5at in mesophilic biogas reactor systems as deduced from multiomics analyses. Microorganisms 8, 2024.

Morsy, F.M., Elbahloul, Y., Elbadry, M., 2019. Photoheterotrophic growth of purple non-sulfur bacteria on tris acetate phosphate yeast extract (tapy) medium and its hydrogen productivity in light under nitrogen deprivation. International Journal of Hydrogen Energy 44, 9282–9290. doi:https://doi.org/10.1016/j.ijhydene.2019.02.086.

Okubo, Y., Hiraishi, A., 2007. Population dynamics and acetate utilization kinetics of two different species of phototrophic purple nonsulfur bacteria in a continuous co-culture system. Microbes and Environments 22, 82–87. doi:10.1264/jsme2.22.82.

Rittmann, B., McCarty, P., 2012. Environmental Biotechnology: Principles and Applications. Tata McGraw Hill Education Private Limited.

Sepúlveda-Muñoz, C.A., Hontiyuelo, G., Blanco, S., Torres-Franco, A.F., Muñoz, R., 2022. Photosynthetic treatment of piggery wastewater in sequential purple phototrophic bacteria and microalgae-bacteria photobioreactors. Journal of Water Process Engineering 47, 102825. doi:https://doi.org/10.1016/j.jwpe.2022.102825.

Shaikh, S., Rashid, N., Onwusogh, U., McKay, G., Mackey, H.R., 2023. Effect of nutrients deficiency on biofilm formation and single cell protein production with a purple non-sulphur bacteria enriched culture. Biofilm 5, 100098.

Solmaz, A., Isik, M., 2019. Effect of sludge retention time on biomass production and nutrient removal at an algal membrane photobioreactor. BioEnergy Research 12, 197–204. doi:10.1007/s12155-019-9961-4.

Sparviero, S., Dicke, M.D., Rosch, T.M., Castillo, T., Salgado-Lugo, H., Galindo, E., Peña, C., Büchs, J., 2023. Yeast extracts from different manufacturers and supplementation of amino acids and micro elements reveal a remarkable impact on alginate production by a. vinelandii atcc9046. Microbial Cell Factories 22, 99. URL: https://doi.org/10.1186/s12934-023-02112-3, doi:10.1186/s12934-023-02112-3.

Trujillo, M., Dedysh, S., DeVos, P., Hedlund, B., Kämpfer, P., Rainey, F., Whitman, W., 2015. Proteiniphilum. pp. 1–2. doi:https://doi.org/10.1002/9781118960608.gbm00247.

Wang, X., Zhang, Y., Li, Y., Luo, Y.L., Pan, Y.R., Liu, J., Butler, D., 2021. Alkaline environments benefit microbial k-strategists to efficiently utilize protein substrate and promote valorization of

protein waste into short-chain fatty acids. Chemical Engineering Journal 404, 127147. doi:https://doi.org/10.1016/j.cej.2020.127147.

Wu, Q., Guo, L., Li, X., Wang, Y., 2021. Effect of phosphorus concentration and light/dark condition on phosphorus uptake and distribution with microalgae. Bioresource Technology 340, 125745. doi:https://doi.org/10.1016/j.biortech.2021.125745.

Xu, M., Li, P., Tang, T., Hu, Z., 2015. Roles of srt and hrt of an algal membrane bioreactor system with a tanks-in-series configuration for secondary wastewater effluent polishing. Ecological Engineering 85, 257–264. doi:https://doi.org/10.1016/j.ecoleng.2015.09.064.

Zhang, M., Leung, K.T., Lin, H., Liao, B., 2021. Effects of solids retention time on the biological performance of a novel microalgal-bacterial membrane photobioreactor for industrial wastewater treatment. Journal of Environmental Chemical Engineering 9, 105500. doi:https://doi.org/10.1016/j.jece.2021.105500.

Chapter 6

Conclusions & Future Work

6.1 Conclusion

The current study explored the potential of PNSBs as versatile organisms that can hold the key to developing energy-efficient and sustainable nutrient-recovery wastewater treatment facilities. They can be selected in open communities by applying selection pressure by changing the light, nutrient concentration, pH, temperature, and SRT-HRT among other parameters. This study determined additional factors that impact their enrichment as well as phosphate and PHA accumulating capabilities in an SBR. The reactors were excellent anaerobic digesters in phases 2 and 3, removing most of the COD from the influent. It was shown that a successful enrichment of PNSB in both coupled and decoupled reactors is possible in the presence of biofilm. Since microbial community development within an open community is a dynamic process and changes with time even if conditions are maintained constantly, it led us to ask further questions on

maintaining community stability and performance in realistic conditions. This study shows that decoupling the SRT significantly affects the microbial community composition and reactor performance. However, phosphorus quantities lower than 25 mg PO_4^{3-}-P/L did not have a visible effect on the microbial community or P-accumulation within the reactors. The conclusions to the defined objects are listed below:

SRT-HRT Decoupling

1. PNSBs form distinctly different communities on uncoupling SRT and HRT where certain bacteria prefer decoupled SRT while others grow in coupled systems.

2. The decoupling of SRT and HRT does not form distinct open communities in the presence of biofilm in the reactors.

P-content in influent

3. Altering the P-content in the influent below 25 mg PO_4^{3-}-P/L did not have any visible effect on the open communities diversity within the reactors.

16S analysis of open community

4. The development of fermenters in the suspension despite the maintenance of reactor conditions reflects some challenges in growing PNSBs. A constant OLR to the reactors led to the activation of metabolic pathways within PNSB that converted the excess carbon to pyruvate encouraging heterotrophic fermenters to replace the PNSBs.

5. Phosphorus measurement can be hindered by substances produced by the mixed culture. Since the exact mechanism of operation of open communities during a nutrient recovery operation is still unknown, the exopolymeric substances produced by them pose an exciting field of discovery.

Although out of the scope of this study, the development of biofilm had a significant impact on the community development within the reactor which can be further explored (Capson-Tojo et al., 2023). Yeast extract in the reactors was not apparent in their influence on the P-uptake behavior but it perhaps had an influence on the growth of fermenters (Maus et al., 2020).

To conclude, mixed purple bacteria cultures in photobioreactors can be successfully employed to extract nutrients from wastewater leaving a low carbon footprint. However, akin to any realistic operation of a reactor, it is imperative to assess all the parameters that require constant monitoring to ensure the growth of the right microbial communities and high recovery efficiency.

6.2 Future Work

This study aimed to broaden the knowledge in a relatively niche and unexplored field of open communities in PBRs. While important observations related to the microbial communities were made, tests need to be conducted to improve phosphorus measurement techniques and open community stability in reactors.

6.2.1 Interference in P-measurement

Appendix B details the results from tests conducted to determine the cause of P-measurement offset. The presence of an interferent in the supernatant is confirmed but the element or compound causing this is unknown. Currently, ion chromatography is being carried out in the MiCel lab to determine the interferent. This knowledge can help in developing accurate methods for P-assessment for future studies in wastewater treatment. Further, if the interferent is an exo-polymer, it can provide insights into the dynamics of the microbial community within the reactors.

The orthophosphate measurements were performed using metavanadate for quick assessment. The development of yellow coloration during testing is a factor of time (Rice et al., 2012) along with a concentration (Dabkowski and White, 2015). Thus, it is essential to optimize the duration in which the color development is allowed before the reading is taken on a spectrophotometer. The color development also depends on the redox potential of the sample which is in turn a function of the pH of the solution (Zeitoun and Biswas, 2020). A similar principle applies to orthophosphate measurement using ascorbic acid. All of these factors play a role in determining the final concentration of orthophosphate measured in the reactor suspension and must be optimized before beginning the experiments.

6.2.2 Operation Improvement

The P-value offset in the study raised several questions that open space for further research. Although phosphorus measurement optimization is out of the scope of this study, further investigation may be carried out in that direction. Additional periodic tests may be carried out

on some parameters while optimizing P-measurement namely pH, redox potential, and interfering ions.

Fermenter growth in the reactors is a natural possibility within a reactor with open communities as discussed in Chapter 4. While predation and phage attacks are inevitable possibilities till their mechanism is fully understood, maintenance of purple bacteria in the wastewater treatment systems requires constant monitoring. While undertaking future experiments it is advised to monitor VFAs regularly throughout the operation period to ensure no shock loading of organic matter takes place causing the proliferation of fermenters. If a high load of OLR is registered, adjustment to original levels can revert the microbial community to its original composition (Khafipour et al., 2020).

The distance between the lamp and the reactor as well as its intensity should be monitored regularly. The lamp's light being infrared has the possibility of altering the temperature to which the bacteria is exposed which may have an effect on the metabolic pathway leading to change in microbe communities and P-uptake behavior (George et al., 2020).

It may be interesting to take into account the role of quorum sensing by the PNSBs to accumulate phosphorus effectively. Operating the reactors at low volumes of cell suspension (Appendix B) may be more conducive to enriching PNSBs and removing phosphorus. It may also lead to lower production of exopolymeric substances that probably interfere with the P-measurements (Dow, 2021; Zhang et al., 2019).

Further experiments must be designed taking together all the parameters into account while assessing P-uptake by open communities.

6.2.3 Microbial Community Exploration

Other than the genus *Proteiniphilum* discussed in Chapter 4, several other genera were identified that could provide insights into open community behavior in real wastewater treatment reactors. A summary of the different genera and their properties are given in Appendix C. Some of the non-PNSBs such as *Thauera* can remove phosphorus, synthesize PHAs, and produce exopolysaccharides. Similarly, *Exiguobacterium* is also a PHA-accumulating genus. In fact, they can alter polystyrene properties by forming a biofilm on its surface. Although PHAs accumulation was not discussed in this study, polyP accumulation by PNSBs in open communities can form a building block to understand PHAs accumulation by the consortia. Further experiments may be carried out to understand the role of non-PNSB, polyP, and PHAs accumulating organisms in a mixed culture such as the ones identified in this study.

6.2.4 Optimizing Quantification using LP2

To be able to quantitatively assess PHAs in the bacteria periodically, an attempt was made to apply LP2 staining for PHAs measurement in PPBs. The protocol developed by Kettner and Griehl (2020) was modified for this purpose. A brief description of the modifications in the protocol for PHA quantification in PPBs is given in Appendix E. Further work and tests must be conducted to accurately deploy the staining technique for quick quantification of PHAs. Future work may also include extraction of PHAs from the cells and characterization.

Closing Remarks

Thus, knowledge from this experiment determined the importance of reactor decoupling and microbial community stability. Results from this study along with suggestions for improvement can pave the way to create energy-efficient, cost-effective wastewater valorization systems using open communities.

References

Capson-Tojo, G., Zuo Meng Gan, A., Ledezma, P., Batstone, D.J., Hülsen, T., 2023. Resource recovery using enriched purple phototrophic bacteria in an outdoor flat plate photobioreactor: Suspended vs. attached growth. Bioresource Technology 373, 128709. doi:https://doi.org/10.1016/j.biortech.2023.128709.

Dabkowski, B., White, M., 2015. Understanding the different phosphorus tests. URL: https://www.hach.com/asset-get.download-en.jsa?id=50989301315, doi:DOC040.53.10108.May16.

Dow, L., 2021. How do quorum-sensing signals mediate algae-bacteria interactions? Microorganisms 9. doi:10.3390/microorganisms9071391.

George, D.M., Vincent, A.S., Mackey, H.R., 2020. An overview of anoxygenic phototrophic bacteria and their applications in environmental biotechnology for sustainable resource recovery. Biotechnology Reports 28, e00563. doi:https://doi.org/10.1016/j.btre.2020.e00563.

Kettner, A., Griehl, C., 2020. The use of lipidgreen2 for visualization and quantification of

intracellular poly(3-hydroxybutyrate) in cupriavidus necator. Biochemistry and Biophysics Reports 24, 100819. doi:https://doi.org/10.1016/j.bbrep.2020.100819.

Khafipour, A., Jordaan, E.M., Flores-Orozco, D., Khafipour, E., Levin, D.B., Sparling, R., Cicek, N., 2020. Response of microbial community to induced failure of anaerobic digesters through overloading with propionic acid followed by process recovery. Frontiers in Bioengineering and Biotechnology 8. doi:10.3389/fbioe.2020.604838.

Maus, I., Tubbesing, T., Wibberg, D., Heyer, R., Hassa, J., Tomazetto, G., Huang, L., Bunk, B., Spröer, C., Benndorf, D., Zverlov, V., Pühler, A., Klocke, M., Sczyrba, A., Schlüter, A., 2020. The role of petrimonas mucosa ing2-e5at in mesophilic biogas reactor systems as deduced from multiomics analyses. Microorganisms 8, 2024.

Rice, E., Bridgewater, L., Association, A.P.H., Association, A.W.W., Federation, W.E., 2012. Standard Methods for the Examination of Water and Wastewater. American Public Health Association. book 4500-P C.

Zeitoun, R., Biswas, A., 2020. Potentiometric determination of phosphate using cobalt: A review. Journal of The Electrochemical Society 167, 127507.

Zhang, Z., Yu, Z., Wang, Z., Ma, K., Xu, X., Alvarezc, P.J.J., Zhu, L., 2019. Understanding of aerobic sludge granulation enhanced by sludge retention time in the aspect of quorum sensing. Bioresource Technology 272, 226–234. doi:https://doi.org/10.1016/j.biortech.2018.10.027.

Appendix A

Experimental Results

Table A.1: *Reactor operation parameters describing the SRTs, HRTs, Organic Loading, and phosphorus content of different phases of the experiment*

Process Parameters	Units	Phase I	Phase II & III
Solid Retention Time			
Decoupled	Day (d)	7	6.67
Coupled	d	2	2.53
Hydraulic Retention Time			
Decoupled	d	2	2.33
Coupled	d	2	2.53
Loadings			
Organic Loading per feed frequency			
Acetate	mg COD L^{-1}	532.85	532.85
Propionate	mg COD L^{-1}	755.93	755.93
Phosphorus			
High	mg PO_4-P L^{-1}	22.76	22.76
Medium	mg PO_4-P L^{-1}	13.66	13.66
Low	mg PO_4-P L^{-1}	4.55	4.55

Table A.2: *Results from reactor operation in all three phases. The table enlists all the values with corresponding standard deviations found during the reactor operation period*

Measured Parameters	Units	P-in feed (mg PO_4-P/L)	Phase 1: Biofilm				Phase 2: Yeast extract				Phase 3: No biofilm & yeast extract			
			Acetate		Propionate		Acetate		Propionate		Acetate		Propionate	
			Decoupled	Coupled	Decoupled	Coupled	Decoupled	Coupled	Decoupled	Coupled	Decoupled	Coupled	Decoupled	Coupled
TSS	mg solids/ L	22.76	1853.81± 179.58	724.76±9 8.04	1795.71± 77.54	701.90± 66.20	1565.42± 138.26	490.42± 42.73	1916.67± 181.19	644.58±9 3.63	1006.67 ±62.46	385.83± 27.43	1253.33± 67.09	310.00±20. 09
		13.66	2005.24± 150.83	658.57±7 7.56	1991.90± 205.76	785.71± 94.05	1640.83± 122.53	568.33± 56.04	2085.83± 202.71	693.75±8 1.44	940 ±85.65	390.83± 53.70	1281.67± 85.36	513.33±157 .29
		4.55	2014.76± 161.49	-	2037.62± 225.43	-	1545.00± 82.05	-	1895.00 ±240.64	-	935 ±73.06	-	1235.00± 54.54	-
VSS	mg solids/ L	22.76	1617.22± 171.66	626.67±1 07.79	1690.00± 81.75	657.22± 63.07	1349.58± 121.89	399.17± 39.90	1656.251 ±76.35	640.00±1 24.53	756.67± 63.12	268.67± 33.04	918.67±7 3.04	230.67±23. 59
		13.66	1793.33± 138.44	593.89±8 0.06	1788.33± 142.82	788.89± 48.43	1388.75± 121.34	451.67± 55.72	1817.08± 194.74	523.75±7 2.61	708.00± 83.23	244.00± 23.98	964.00±8 1.29	380.67±149 .77
		4.55	1893.44± 174.99	-	2002.22± 191.48	-	1275.00± 79.35	-	1595.00± 221.83	-	689.33± 77.99	-	928.00±5 8.13	-
sCOD	mg O_2/L	22.76	128.22 ±55.95	189.39 ±75.64	169.58 ±60.29	151.77 ±71.51	57.44 ±19.65	45.25 ±13.38	101.74 ±46.02	73.55 ±17.41	0.8771 ±0.02	0.8769 ±0.02	0.8900 ±0.02	0.8774 ±0.02
		13.66	129.47 ±50.98	185.66 ±77.80	115.14 ±46.68	155.49 ±64.94	63.06 ±28.51	43.70 ±10.39	92.58 ±31.01	92.75 ±19.70	0.8869 ±0.02	0.8868 ±0.02	0.8871 ±0.02	0.8873 ±0.02
		4.55	95.80 ±31.75	-	102.21 ±31.67	-	68.44 ±26.19	-	97.96 ±18.90	-	0.8770 ±0.02	-	0.8774 ±0.02	-
Maximum Removal	%		82.02	65.16	86.48	79.92	89.22	91.80	87.75	90.27	99.84	99.83	99.88	99.88

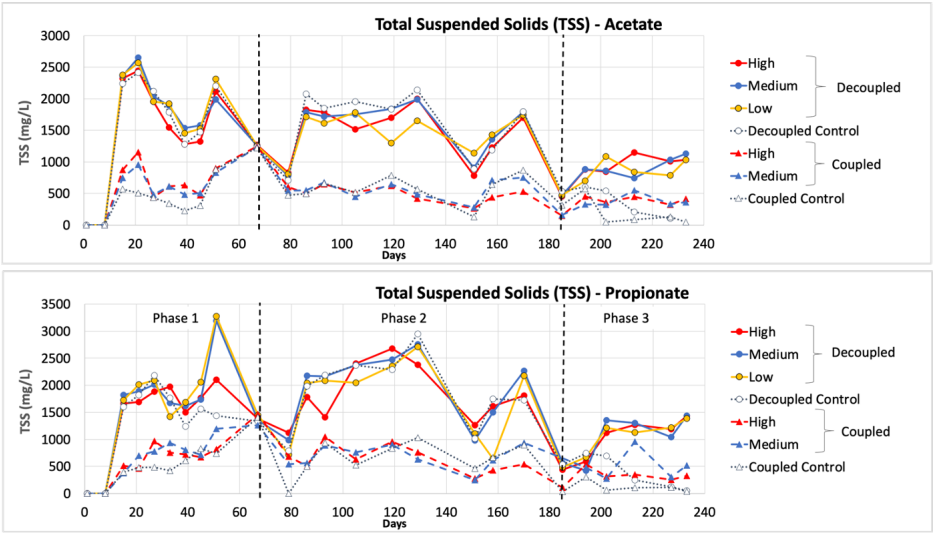

Figure A.1: *TSS of (a) acetate and (b) propionate fed reactors across all the three phases*

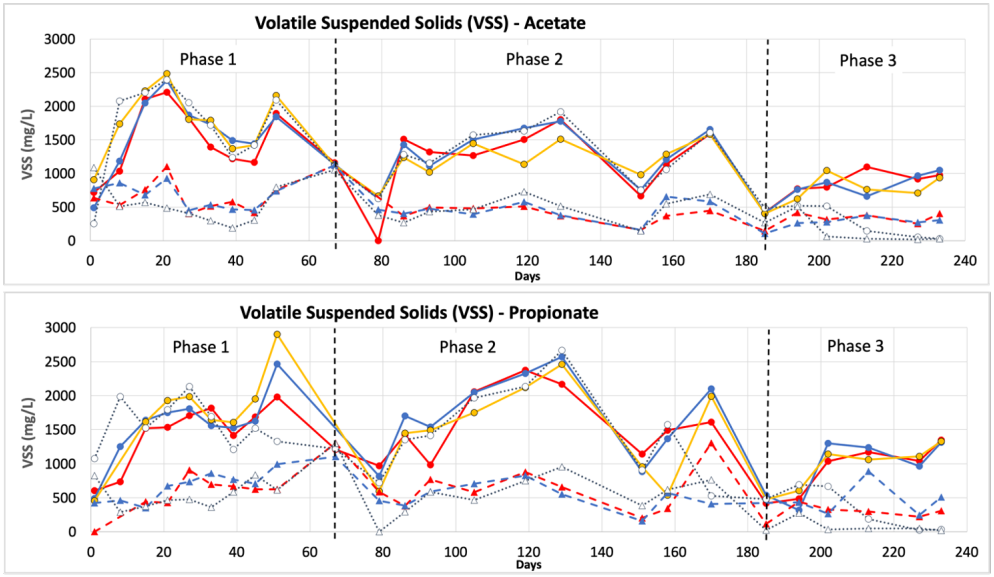

Figure A.2: *VSS of (a) acetate and (b) propionate fed reactors across all the three phases*

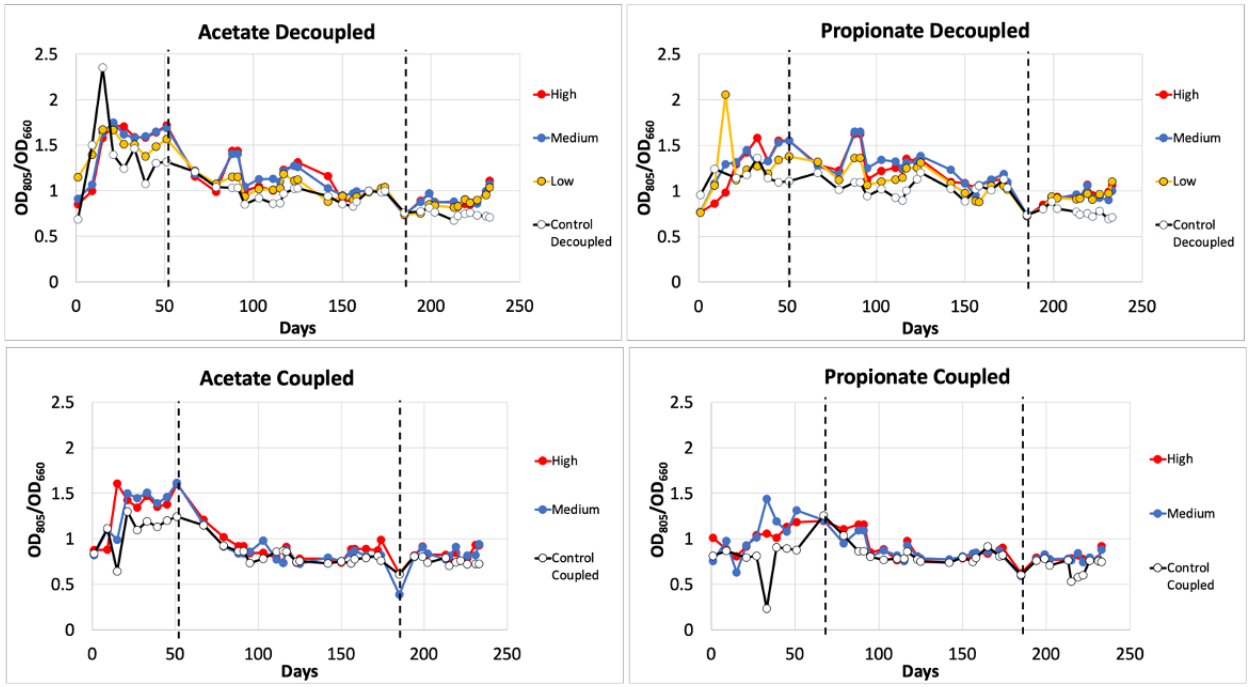

Figure A.3: *OD_{805}/OD_{660} for acetate and propionate-fed reactors showing one of the peaks for BChl a*

Table A.3: *PCR reaction conditions. The primers are 515F + 806R. The PCR was run 25× for amplification.*

Step	Temperature	Time
Initial denaturation	94°	3 min
Denaturation	94°	45 sec
Annealing	50°	60 sec
Elongation	68°	45 sec
Final elongation	68°	10 sec
Cooling	4°	∞

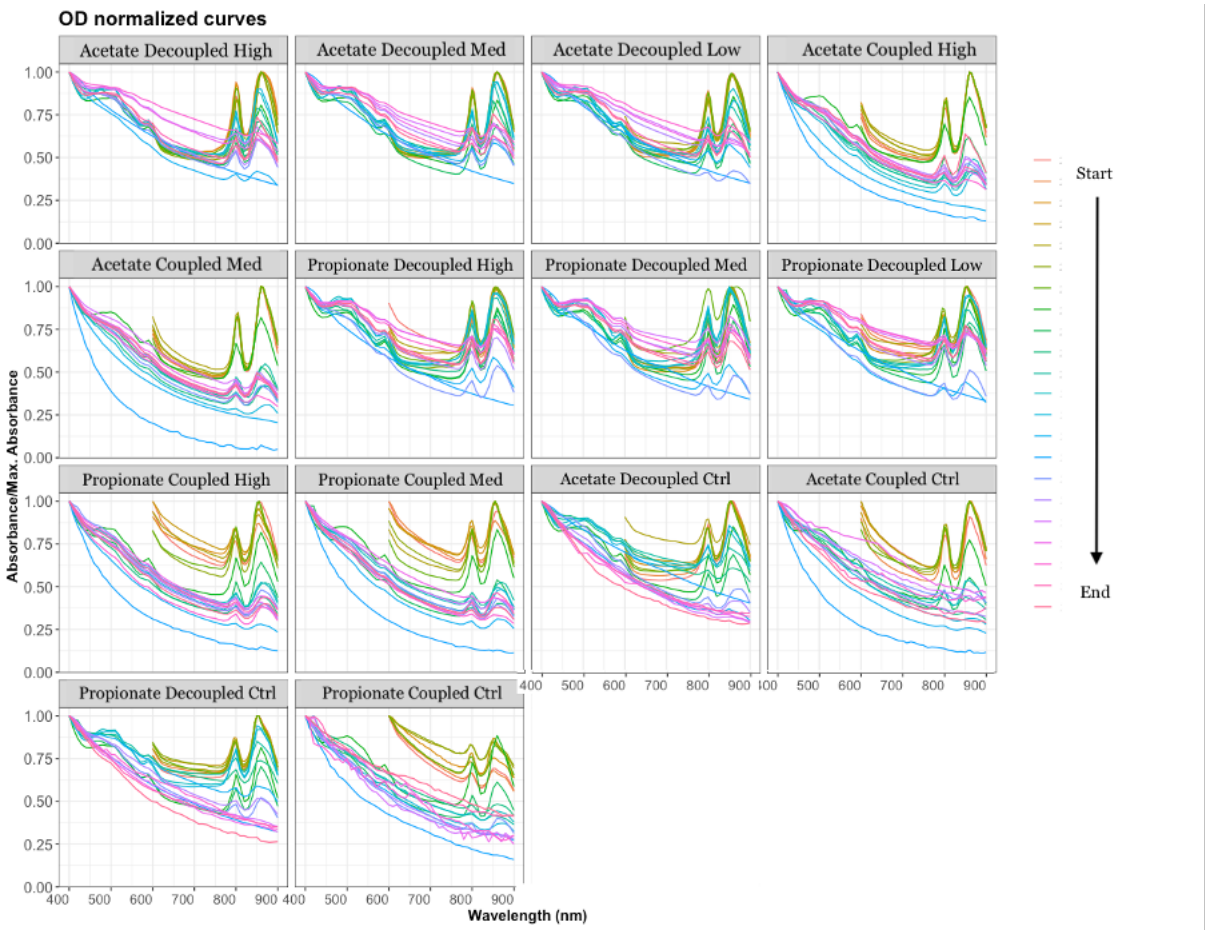

Figure A.4: *Normalised curve showing the presence of BChl a in the reactors. Averages of the normalized values of the duplicates were taken.*

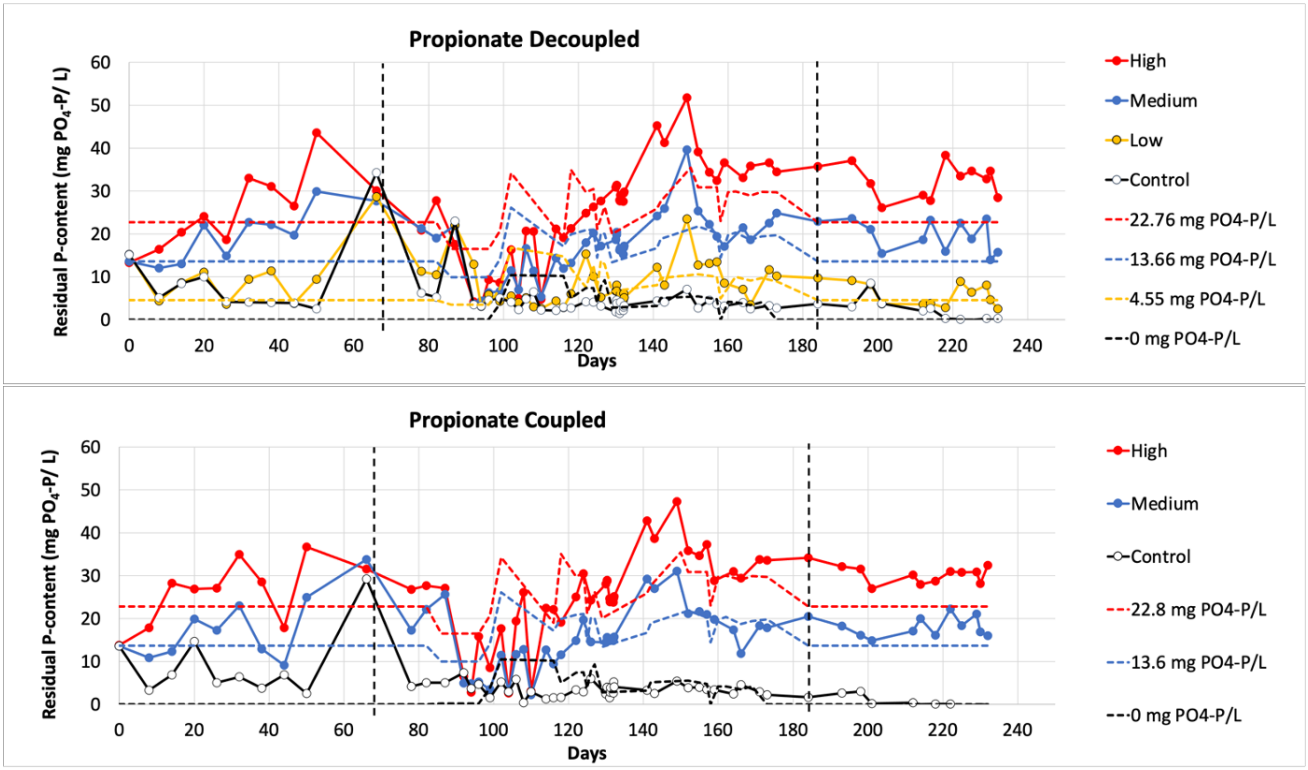

Figure A.5: *Orthophosphate measured in supernatant for propionate-fed reactors in all the phases*

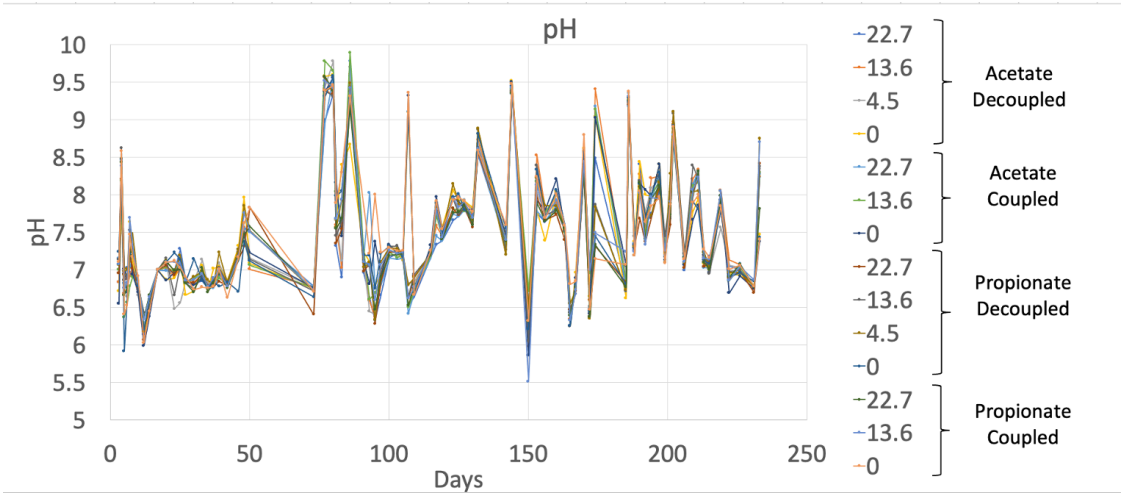

Figure A.6: *pH of all reactors across Phase 1,2,3. The numbers in the legend denote the orthophosphate fed to the reactor in mg* PO_4^{3-}/L.

Appendix B

Orthophosphorus troubleshooting

Test 1: Was the error due to manual operation?

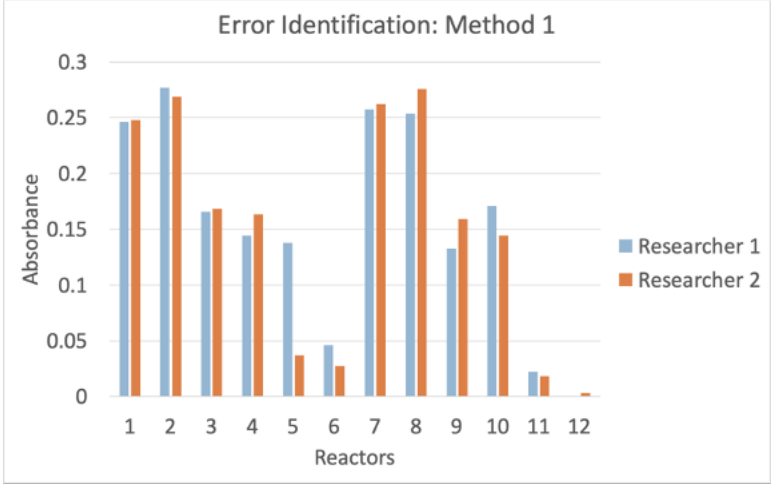

Figure B.1: *P-measurement using the Molybdovanadate (yellow method) was carried out by another independent researcher. The wavelength of the supernatant samples was spectrophotometrically measured at 470 nm. The absorbance data from both researchers was not significantly different ($t(22)=2.07$, $p>0.05$).*

Test 2: Was the error due to the measurement from the supernatant after centrifugation?

Figure B.2: *The supernatant was passed through a 0.22 µm cellulose acetate filter to eliminate any floating bacteria in the supernatant after centrifugation. Measurements of the orthophosphate in supernatant were taken at 470 nm spectrophotometrically using the yellow method before and after filtration. There was no significant difference between the data before and after filtration ($t(46)=2.01$, $p>0.05$).*

Test 3: Was the error due to the colorimetric method chosen?

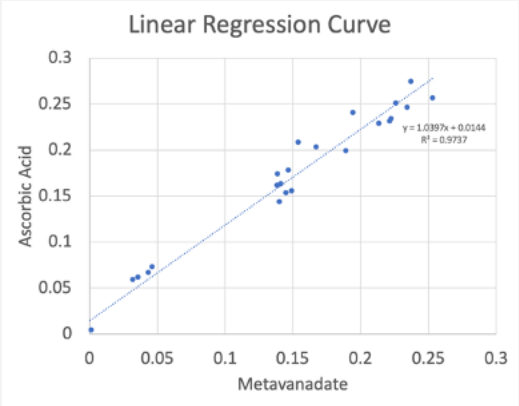

Figure B.3: *A linear regression curve of the absorbance at 470 nm from the samples using the two colorimetric methods - Molybdovanadate (yellow) method and Ascorbic Acid (blue) method is plotted. The standard deviation from the*

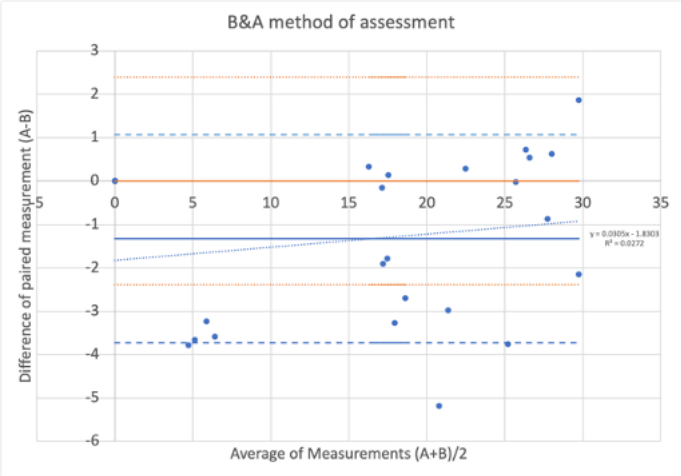

Figure B.4: *A Bland & Altman method of assessment between the Molybdovanadate (yellow) method and Ascorbic Acid (blue) method. However, since the B&A method does not specify the sufficiency of the agreement between the methods, no conclusion could be made.*

Test 4: Was the error in measurement due to reactor setup?

Another set of experiments was conducted with a different reactor setup that used 12 mL deep well plates placed in an airtight box with AnaeroPack™to create an anaerobic environment. The exact procedure as described in Fig. 3.2 was followed. The PNSBs cultured in the system were analyzed using 16s, the results of which are presented below. The reactor setup is called "new reactor" for the sake of simplicity.

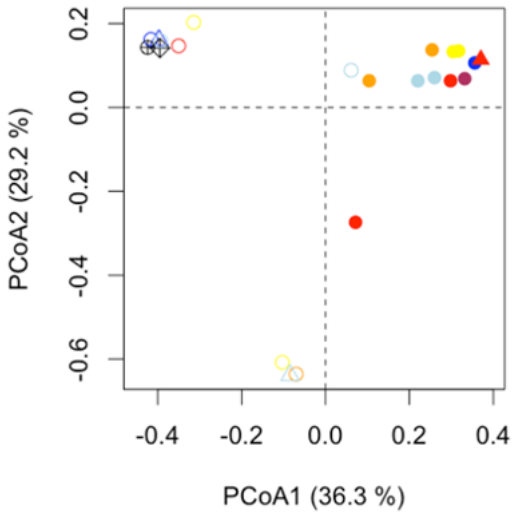

Figure B.5: *PCoA of the bacteria in the reactor are presented here. At the start of the operation, the species of bacteria are not distinct from each other (upper right corner). Although, by the end of the operation, the new population (upper left corner) is different from the initial microbiota, the reactor population is not quite distinct from one another.*

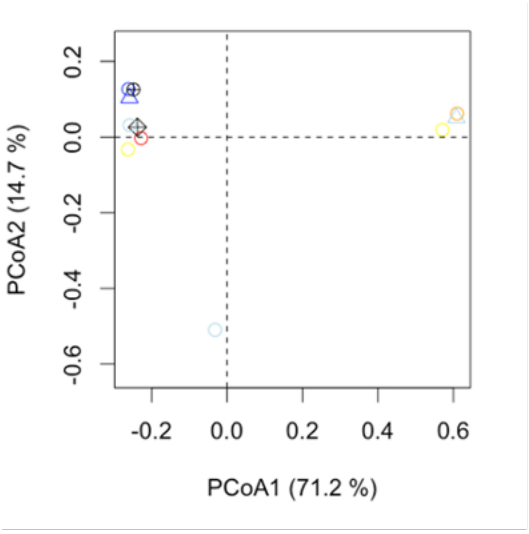

Figure B.6: *When the bacteria at the end of the reactor was analyzed using PCoA, it was observed that there is no significant pattern of population distribution within the different reactors.*

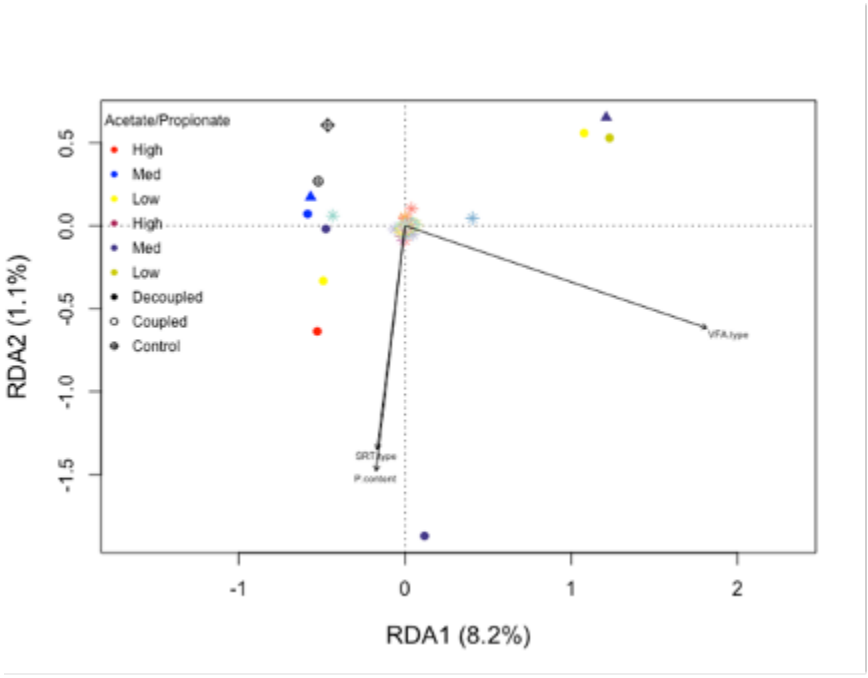

Figure B.7: *On plotting an RDA of the bacteria from different reactors at the end of the operation, the axes of the RDA plot were found to be insignificant denoting no significant pattern in species development.*

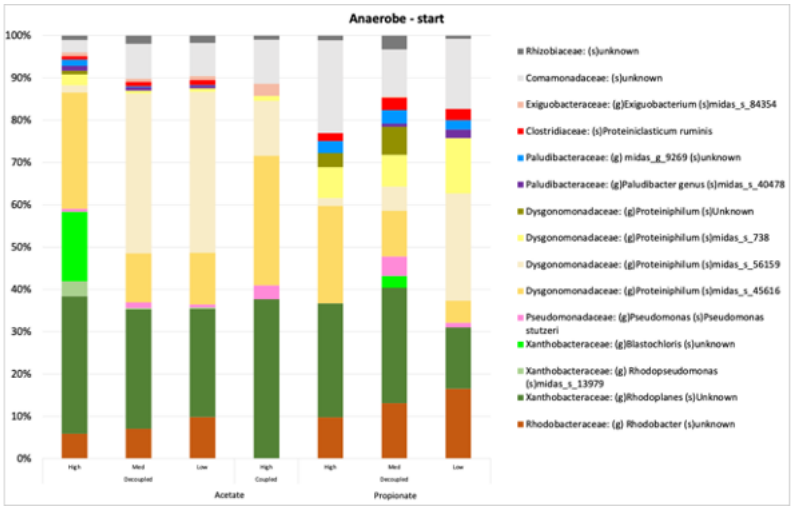

Figure B.8: *The top 10 most abundant species of both acetate and propionate-fed reactors are plotted here. The purple bacteria coexists with fermenters at steady-state reactor operation.*

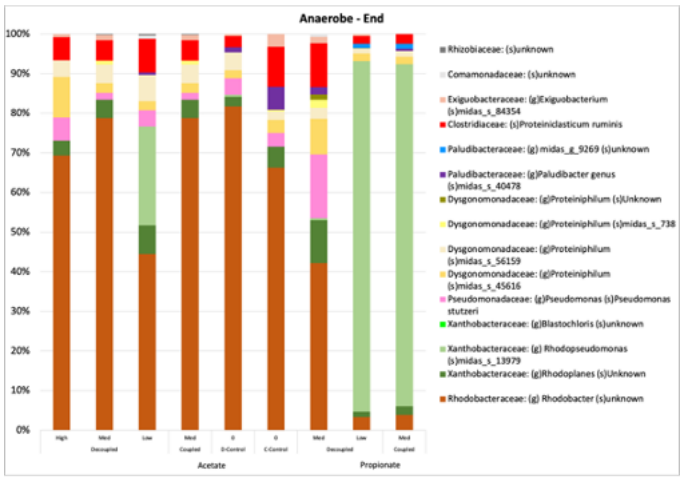

Figure B.9: *By the end of the reactor operation, Rhodobacteraceae and Xanthobacteraceae take over which may signify a better regulation of nutrients by PPBs in the presence of fermenters allowing their abundance when low volumes of bacteria are cultured. (Dow (2021); Efremenko et al. (2023); Zhang et al. (2019))*

Test 4: Was the error due to the supernatant matrix?

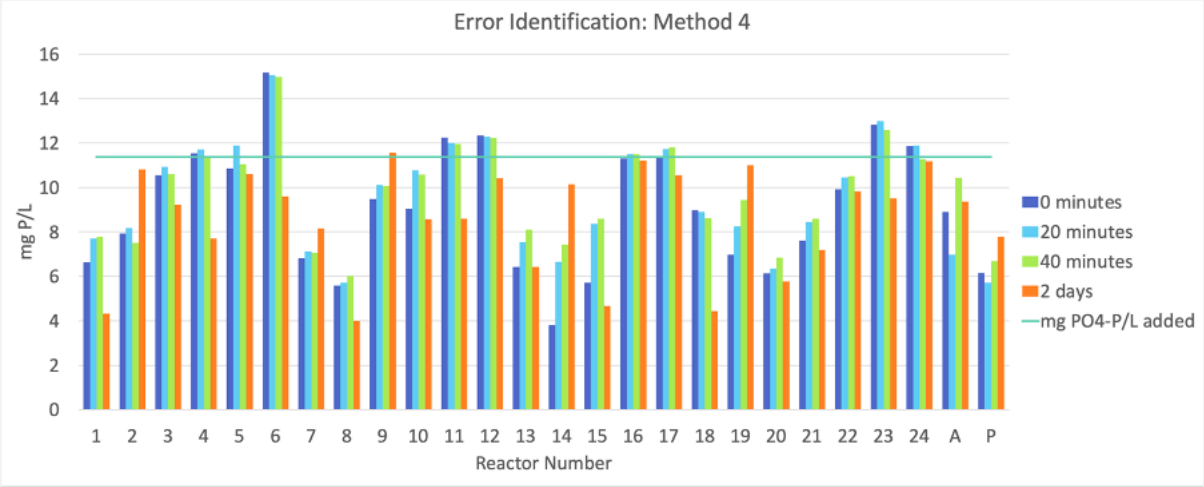

Figure B.10: *The orthophosphate measurement was taken at different time intervals to note any change in P-values in the supernatant over time. It was observed that there was indeed an offset in the P-values indicating the presence of another compound that interacted with* PO_4^{3-}*-P within the supernatant.*

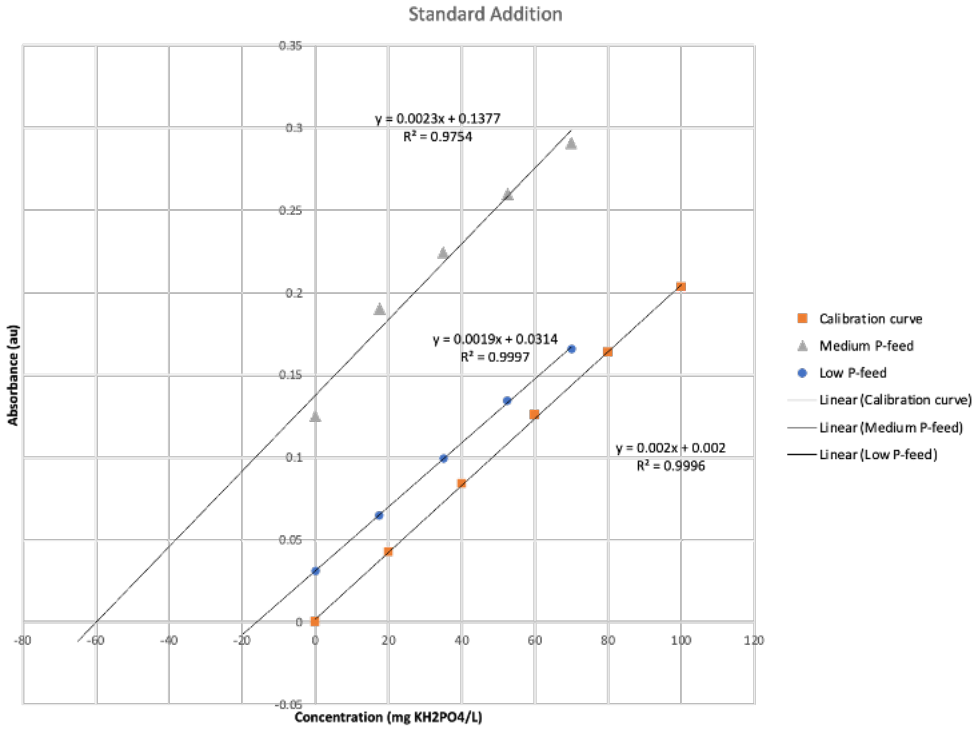

Figure B.11: *To identify the amount of interference that may be taking place while measuring the PO_4^{3-}-P due to the supernatant matrix, an internal standard method of dilution was employed to eliminate the interference. However, another test was conducted using ferric and aluminum oxide ions that precipitated PO_4^{3-}-P chemically (not presented in this document). It was found that the interferent was also precipitated. Thus, the offset in phosphorus measurement from this experiment could not be applied directly to the orthophosphate results obtained in this study.*

Appendix C

Summary of selected genera identified

Table C.1: *Some properties of different fermenters identified in the reactor across phases*

Genus	Characteristics
Acetoanaerobium	"Obligate anaerobe. Chemo-organotrophic. Ferment carbohydrates, producing acetate and sometimes other volatile acids. Ferment yeast extract, producing acetate and several volatile acids. At slower growth rates produce acetate from H_2 and CO_2. May require yeast extract for growth." (Trujillo et al. (2015))
Achloeplasma	Given the ubiquity of this genus in the environment, very little research has been done on its 15 identified species. They are similar to *Mycoplasma* as they lack a cell wall, are very small and have few genes. *Achloeplasma laidlawii* is a well-known process contaminant. Their presence in wastewater is due to their widespread occurrence in respiratory mucosal and urogenital tract. (Williams (April 21, 2021)) They also exhibit cell fusion phenomena. (Vishnyakov (2022))
Erysipelothrix	"*Erysipelothrix* is an aerobic, non–spore-forming, gram-positive bacillus that has been linked to skin infections in meat and fish handlers."(Actor (2012)) "Growth occurs at 15–44°C, with an optimal temperature of 30–37°C, and at a pH range of 6.7–9.2. The organism is a facultative anaerobe, chemoorganotrophic with respiratory metabolism, and weakly fermentative. Acid but no gas produced from glucose and other carbohydrates. Growth is improved by 5–10% carbon dioxide. In addition to lactic acid, small amounts of acetic acid, formic acid, ethyl alcohol, and CO_2 are produced from the fermentation of glucose. Acid without gas is produced within 48 h from glucose, lactose, fructose and galactose." (Stackebrandt et al. (2006))

Exiguobacterium	"The members of the genus display low G+C content and are gram-positive, facultative anaerobes or aerobes with high morphologic, physiologic, and geographic diversity. Cluster analyses of 16S rRNA gene sequence data suggests that *Exiguobacterium* has developed molecular mechanisms and possesses several stress tolerance related genes, confirming its ability to inhabit extreme conditions. Several phosphate-solubilizing *Exiguobacterium* have been isolated and studied through the mechanisms involving acidification, secretion of organic acids, proton extrusion and chelation and exchange reactions. Phosphate solubilization could also be induced by phosphate starvation and release of plant root exudates such as organic ligands."(Pandey (2020)) Species from this genus can degrade polystyrene by forming biofilm (Chauhan et al. (2018); Pandey (2020); Parthasarathy et al. (2022)).
Macellibacteroidetes	"Cells stain Gram-positive but have a Gram-negative type of cell wall. Non-motile, non-spore-forming, mesophilic rods with a fermentative and obligately anaerobic type of metabolism. Growth occurs at 20–45 μC (optimum 35–40 μC) and at pH 5.0–8.5 (optimum pH 6.5–7.5). Does not require NaCl for growth, but tolerates up to 2% NaCl. Yeast extract is required for growth. Catalase-negative. Cellobiose, glucose, lactose, mannose, maltose, peptone, rhamnose, raffinose, sucrose and xylose are used as electron donors, but not arabinose, glycerol, mannitol, Casamino acids, acetate, lactate, pyruvate, H_2/CO_2 or H_2/CO_2 in the presence of acetate. Sodium sulfate, sodium thiosulfate, elemental sulfur, sodium sulfite, sodium nitrate and sodium nitrite are not used as terminal electron acceptors. The main fermentation products from glucose metabolism are lactate, acetate, butyrate and isobutyrate." (Jabari et al. (2012))
Paludibacter	"Nonmotile. Nonsporeforming. Gram-negative. Strictly anaerobic. Chemo-organotrophic. Optimum growth temperature, 30°C. No growth occurs at 37°C. Oxidase and catalase-negative. Nitrate is not reduced. Various sugars are fermented, and acetate and propionate are the major fermentation end products with succinate as a minor product."(Trujillo et al. (2015)) "It could not grow in the presence of oxygen (20%, v/v, in the gas phase) nor after N_2-CO_2 purging only (without adding reducing agents). Growth was observed with the following substrates (20 mM unless specified): arabinose, xylose, fructose, galactose, glucose, mannose, cellobiose, lactose, maltose, sucrose, pectin and starch (1 g l-1). Yeast extract was not required but stimulated the growth. The major end products from glucose fermentation were acetate and propionate in a molar ratio of 4:1."(Qiu et al. (2014))
Proteiniclasticum ruminis	They are strictly anaerobic, proteolytic, grow at 24-46°C, and pH between 5.6 – 8.7. The major fermentation products were acetate, propionate and iso-butyrate from PY medium. (Zhang et al. (2010))
Proteiniphilum	"Nonsporeforming. Gram-stain-negative. Obligately anaerobic. Growth occurs at 20–45°C. Oxidase and catalase-negative. Chemo-organotrophic. Proteolytic. Yeast extract and peptone can be used as energy sources. Nonsaccharolytic. Carbohydrates, alcohols, and organic acids (except pyruvate) are not used. Gelatin is not hydrolyzed. Not resistant to 20% bile. The major fermentation products from peptone-yeast extract (PY) medium are acetic acid and propionic acid. Nitrate is not reduced."(Trujillo et al. (2015)) "The purified rod-shaped bacterial strains utilized pyruvate and produced acetate and propionate from proteinaceous materials, but not glucose or other sugars."(Chen and Dong (2005))

Pseudomonas stutzeri	They do not accumulate PHA but exhibit denitrifying properties with gas release. "The denitrification process carried out by bacteria makes use of N oxides as terminal electron acceptors for cellular bioenergetics under anaerobic, microaerophilic, and occasionally even aerobic conditions."(Lalucat et al. (2006))
Thauera	They are frequently found in wastewater, have versatile metabolism. produce exopolymeric substances, and degrade aromatic compounds.(Liu et al. (2013)) "Species from *Thauera* genus (identified by denaturing gradient gel electrophoresis) were found to be abundant in SBRs operated under ADF conditions using a mixture of acetate, propionate, and lactate and operated at different loading rates. Bacteria from the genera *Thauera* and *Azoarcus* were dominant in an SBR fed with acetate at SRTs of 1 and 10 days." (Reis et al. (2011)) "...the *Thauera* is an important genus with metabolic versatility for the remediation of environmental pollutants in wastewater treatment. They are found to be typical denitrifiers but can also perform P removal. They can also oxidize sulfide/S to form poly-S using CO2 as the electron acceptors, and then poly-S is oxidized to sulfate. Thus *Thauera* can be regarded as one of the key organisms responsible for denitrifying P removal and sulfide oxidation in S-EBPR systems." (Guo et al. (2019))

Appendix D

QIIME2 Codes for 16s Analysis

1. Importing Data

```
      qiime tools import \
--type 'SampleData[PairedEndSequencesWithQuality]' \
--input-path /media/Manifest.txt \
--output-path /media/paired-end-demux.qza \
--input-format PairedEndFastqManifestPhred33

qiime demux summarize \
--i-data /media/paired-end-demux.qza \
--o-visualization /media/paired-end-demux.qzv
```

2. Sequence Quality Control and Feature Table Construction

```
    qiime dada2 denoise-paired \
  --i-demultiplexed-seqs /media/paired-end-demux.qza \
  --p-trim-left-f 0 \
  --p-trim-left-r 3 \
  --p-trunc-len-f 249 \
  --p-trunc-len-r 248 \
  --o-representative-sequences /media/rep-seqs.qza \
  --o-table /media/table.qza \
  --o-denoising-stats /media/stats-dada2.qza \
```

3. Feature Data Summary

```
    qiime feature-table summarize \
--i-table table.qza \
--o-visualization table.qzv \
--m-sample-metadata-file /media/metadata.txt
qiime feature-table tabulate-seqs \
--i-data /media/rep-seqs.qza \
--o-visualization /media/rep-seqs.qzv
```

4. Files for phylogenetic diversity analysis

```
    qiime alignment mafft \
--i-sequences /media/rep-seqs.qza \
--o-alignment /media/aligned-rep-seqs.qza

    qiime alignment mask \
--i-alignment /media/aligned-rep-seqs.qza \
--o-masked-alignment /media/maksed-aligned-rep-seqs.qza

    qiime phylogeny fasttree \
--i-alignment /media/maksed-aligned-rep-seqs.qza \
--o-tree /media/unrooted-tree.qza

    qiime phylogeny midpoint-root \
--i-tree /media/unrooted-tree.qza \
--o-rooted-tree /media/rooted-tree.qza
```

5. Alpha Diversity Analysis

```
    qiime diversity alpha-rarefaction \
--i-table /media/table.qza \
--i-phylogeny /media/rooted-tree.qza \
--p-max-depth 31641 \
--m-metadata-file /media/metadata.txt \
--o-visualization /media/alpha-rarefaction.qzv
```

6. Beta Diversity Analysis

```
   qiime diversity core-metrics-phylogenetic \
 --i-phylogeny /media/rooted-tree.qza \
 --i-table /media/table.qza \
 --p-sampling-depth 18108 \
 --m-metadata-file /media/metadata.txt \
 --output-dir core-metrics-results
```

7. Taxonomic Analysis

```
   qiime feature-classifier classify-sklearn \
 --i-classifier /media/MIDASClassifier4.8.1.qza \
 --i-reads /media/rep-seqs.qza \
 --o-classification /media/taxonomy.qza

   qiime metadata tabulate \
--m-input-file /media/taxonomy.qza \
--o-visualization /media/taxonomy.qzv

   qiime taxa barplot \
--i-table /media/table.qza \
--i-taxonomy /media/taxonomy.qza \
--m-metadata-file /media/metadata.txt \
--o-visualization /media/taxa-bar-plots.qzv
```

Appendix E

LP2 optimization

E.1 Objective

The experiment by Kettner and Griehl (2020) utilizing lipidgreen2 (LP2) for staining PHA was improvised. The objective of this experiment was to develop a protocol for quantitative measurement of PHA in a continuously operating reactor. It involved optimizing the wavelengths and volumes of LP2 at which a usable calibration curve could be obtained by modifying the protocol by Kettner and Griehl (2020).

E.2 Methodology

To create a calibration curve, 1, 1.5, and 2 mL of *Cupriviadus necator* DSM541 strain were washed and suspended in PBS and HEPES in two different sets of centrifuge tubes. Different volumes (20,

50, and 100 μL) of 50μM LP2 were used for staining the cell suspension. The fluorescence was measured at 440, 450, and 460 nm excitation wavelengths and 490, 500, 510, and 520 nm emission wavelengths.

E.3 Result

A volume of 100 μL, 50 μM LP2 was ideal for staining the cells. The bacterial cells must be suspended in PBS and the fluorescence is to be measured at 450 nm excitation and 520 nm emission wavelengths. The calibration curve obtained at the above conditions is presented in Fig. E.1.

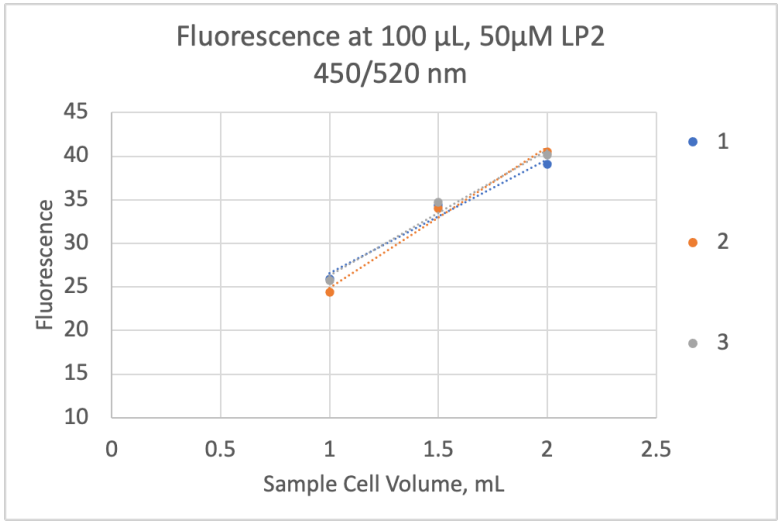

Figure E.1: *A straight calibration curve was obtained when using LP2 stain as a quantitative tool for measuring PHA within Cupriviadus necator DSM541. The cells were suspended in PBS and stained with 100 μL of μM LP2 in 2 mL aliquots. The fluorescence was measured at 450 nm excitation and 520 nm emission wavelength. The numbers in the legend indicate the triplicate measurements taken.*

References

Actor, J.K., 2012. 12 - Clinical Bacteriology. W.B. Saunders, Philadelphia. pp. 105–120. doi:https://doi.org/10.1016/B978-0-323-07447-6.00012-0.

Chauhan, D., Agrawal, G., Deshmukh, S., Roy, S.S., Priyadarshini, R., 2018. Biofilm formation by exiguobacterium sp. dr11 and dr14 alter polystyrene surface properties and initiate biodegradation. RSC Advances 8, 37590–37599. doi:10.1039/C8RA06448B.

Chen, S., Dong, X., 2005. Proteiniphilum acetatigenes gen. nov., sp. nov., from a uasb reactor treating brewery wastewater. International Journal of Systematic and Evolutionary Microbiology 55, 2257–2261. doi:https://doi.org/10.1099/ijs.0.63807-0.

Dow, L., 2021. How do quorum-sensing signals mediate algae-bacteria interactions? Microorganisms 9. doi:10.3390/microorganisms9071391.

Efremenko, E., Senko, O., Stepanov, N., Aslanli, A., Maslova, O., Lyagin, I., 2023. Quorum sensing as a trigger that improves characteristics of microbial biocatalysts. Microorganisms 11, 1395.

Guo, G., Ekama, G.A., Wang, Y., Dai, J., Biswal, B.K., Chen, G., Wu, D., 2019. Advances in sulfur conversion-associated enhanced biological phosphorus removal in sulfate-rich wastewater treatment: A review. Bioresource Technology 285, 121303. doi:https://doi.org/10.1016/j.biortech.2019.03.142.

Jabari, L., Gannoun, H., Cayol, J.L., Hedi, A., Sakamoto, M., Falsen, E., Ohkuma, M., Hamdi, M., Fauque, G., Ollivier, B., Fardeau, M.L., 2012. Macellibacteroides fermentans gen. nov., sp. nov.,

a member of the family porphyromonadaceae isolated from an upflow anaerobic filter treating abattoir wastewaters. International Journal of Systematic and Evolutionary Microbiology 62, 2522–2527. doi:https://doi.org/10.1099/ijs.0.032508-0.

Kettner, A., Griehl, C., 2020. The use of lipidgreen2 for visualization and quantification of intracellular poly(3-hydroxybutyrate) in cupriavidus necator. Biochemistry and Biophysics Reports 24, 100819. doi:https://doi.org/10.1016/j.bbrep.2020.100819.

Lalucat, J., Bennasar, A., Bosch, R., García-Valdés, E., Palleroni, N.J., 2006. Biology of pseudomonas stutzeri. Microbiol Mol Biol Rev 70, 510–47. doi:10.1128/mmbr.00047-05.

Liu, B., Frostegård, , Shapleigh, J.P., 2013. Draft genome sequences of five strains in the genus ¡i¿thauera¡/i¿. Genome Announcements 1, 10.1128/genomea.00052–12. URL: https://journals.asm.org/doi/abs/10.1128/genomea.00052-12, doi:doi:10.1128/genomea.00052-12.

Pandey, N., 2020. Chapter 10 - Exiguobacterium. Academic Press. pp. 169–183. doi:https://doi.org/10.1016/B978-0-12-823414-3.00010-1.

Parthasarathy, A., Miranda, R.R., Eddingsaas, N.C., Chu, J., Freezman, I.M., Tyler, A.C., Hudson, A.O., 2022. Polystyrene degradation by exiguobacterium sp. rit 594: Preliminary evidence for a pathway containing an atypical oxygenase. Microorganisms 10. doi:10.3390/microorganisms10081619.

Qiu, Y.L., Kuang, X.Z., Shi, X.S., Yuan, X.Z., Guo, R.B., 2014. Paludibacter jiangxiensis sp. nov.,

a strictly anaerobic, propionate-producing bacterium isolated from rice paddy field. Archives of Microbiology 196, 149–155. doi:10.1007/s00203-013-0951-1.

Reis, M., Albuquerque, M., Villano, M., Majone, M., 2011. 6.51 - Mixed Culture Processes for Polyhydroxyalkanoate Production from Agro-Industrial Surplus/Wastes as Feedstocks. Academic Press, Burlington. pp. 669–683. doi:https://doi.org/10.1016/B978-0-08-088504-9.00464-5.

Stackebrandt, E., Reboli, A.C., Farrar, W.E., 2006. The Genus Erysipelothrix. Springer US, New York, NY. pp. 492–510. URL: https://doi.org/10.1007/0-387-30744-3_13, doi:10.1007/0-387-30744-3_13.

Trujillo, M., Dedysh, S., DeVos, P., Hedlund, B., Kämpfer, P., Rainey, F., Whitman, W., 2015. Proteiniphilum. pp. 1–2. doi:https://doi.org/10.1002/9781118960608.gbm00247.

Vishnyakov, I.E., 2022. Cell-in-cell phenomena in wall-less bacteria: Is it possible? International Journal of Molecular Sciences 23, 4345. URL: https://www.mdpi.com/1422-0067/23/8/4345.

Williams, K.L., April 21, 2021. *Acholeplasma laidlawii*: Potential Process Contaminant of Cell Culture Media. Technical Report. Biomérieux. URL: https://www.biomerieux.com/nl/en/resource-hub/knowledge/scientific-library/pharma-microorganisms-library/acholeplasma-laidlawii-scientific-library.html.

Zhang, K., Song, L., Dong, X., 2010. Proteiniclasticum ruminis gen. nov., sp. nov., a strictly anaerobic proteolytic bacterium isolated from yak rumen. International Journal of

Systematic and Evolutionary Microbiology 60, 2221–2225. doi:https://doi.org/10.1099/ijs.0.011759-0.

Zhang, Z., Yu, Z., Wang, Z., Ma, K., Xu, X., Alvarezc, P.J.J., Zhu, L., 2019. Understanding of aerobic sludge granulation enhanced by sludge retention time in the aspect of quorum sensing. Bioresource Technology 272, 226–234. doi:https://doi.org/10.1016/j.biortech.2018.10.027.